



National Library of Canada

Cataloguing Branch  
Canadian Theses Division

Ottawa, Canada  
K1A 0N4

Bibliothèque nationale du Canada

Direction du catalogage  
Division des thèses canadiennes

## NOTICE

The quality of this microfiche is heavily dependent upon the quality of the original thesis submitted for microfilming. Every effort has been made to ensure the highest quality of reproduction possible.

If pages are missing, contact the university which granted the degree.

Some pages may have indistinct print especially if the original pages were typed with a poor typewriter ribbon or if the university sent us a poor photocopy.

Previously copyrighted materials (journal articles, published tests, etc.) are not filmed.

Reproduction in full or in part of this film is governed by the Canadian Copyright Act, R.S.C. 1970, c. C-30. Please read the authorization forms which accompany this thesis.

**THIS DISSERTATION  
HAS BEEN MICROFILMED  
EXACTLY AS RECEIVED**

## AVIS

La qualité de cette microfiche dépend grandement de la qualité de la thèse soumise au microfilmage. Nous avons tout fait pour assurer une qualité supérieure de reproduction.

S'il manque des pages, veuillez communiquer avec l'université qui a conféré le grade.

La qualité d'impression de certaines pages peut laisser à désirer, surtout si les pages originales ont été dactylographiées à l'aide d'un ruban usé ou si l'université nous a fait parvenir une photocopie de mauvaise qualité.

Les documents qui font déjà l'objet d'un droit d'auteur (articles de revue, examens publiés, etc.) ne sont pas microfilmés.

La reproduction, même partielle, de ce microfilm est soumise à la Loi canadienne sur le droit d'auteur, SRC 1970, c. C-30. Veuillez prendre connaissance des formules d'autorisation qui accompagnent cette thèse.

**LA THÈSE A ÉTÉ  
MICROFILMÉE TELLE QUE  
NOUS L'AVONS REÇUE**

DIGITAL-FILTER STRUCTURES BASED ON GENERALIZED-IMMITTANCE CONVERTERS,  
AND COMPARISON WITH OTHER STRUCTURES

M.G. REZK

A Thesis

in

The Faculty

of

Engineering

Presented in Partial Fulfillment of the Requirement of  
the degree of Doctor of Engineering at

Concordia University

Montreal, Quebec, Canada

August, 1978

© M.G. Rezk

ABSTRACT

DIGITAL-FILTER STRUCTURES BASED ON GENERALIZED-IMMITTANCE CONVERTERS,  
AND COMPARISON WITH OTHER STRUCTURES

Mohamed G. Rezk, D.Eng.  
Concordia University, 1978...

By using the wave characterization, a digital realization of the generalized-immittance converter (GIC) is first derived. Then, five universal second-order digital-filter sections are developed which can be used as building blocks in a cascade GIC synthesis. The synthesis is illustrated by designing four digital filters, namely, a Butterworth lowpass filter, an elliptic bandstop filter, an elliptic bandpass filter, and a delay equalizer.

The computational efficiency of digital-filter structures based on the GIC synthesis are compared with corresponding cascade canonic and wave digital-filter structures. The results show that the GIC structures are more efficient than the corresponding wave structures and approximately of the same efficiency as the cascade canonic structures. In addition, the number of unit-delays used in the GIC structures is minimal.

The effects of product quantization in various GIC structures are studied and compared with those in corresponding cascade canonic and wave structures. It is found that, the GIC synthesis yields lowpass and bandstop filters, and also delay equalizers with improved inband signal-to-noise ratio relative to that in the corresponding cascade canonic and wave structures.

The required coefficient wordlength for various digital filter is obtained first by using an exact method, and then by using a statistical method. The results show that GIC structures give better results than corresponding cascade canonic and wave structures, in the case of lowpass and bandpass filters.

ACKNOWLEDGEMENTS

The author wishes to express his gratitude to Professor A. Antoniou for suggesting the problem and for his guidance and assistance throughout the course of this investigation, and for his advice during the preparation of the manuscript. Thanks are due to Dr. R.A. El-Attar for obtaining the approximation for the digital equalizer described in Section. 2.4.

Thanks are also due to Miss J. Anderson for typing the thesis.

This work was supported by the National Research Council of Canada under Grant A-7770, awarded to Professor A. Antoniou.

TO MY PARENTS  
AND  
TO MY WIFE AIDA

TABLE OF CONTENTS

	Page
LIST OF TABLES . . . . .	ix
LIST OF FIGURES . . . . .	xi
LIST OF ABBREVIATIONS AND SYMBOLS . . . . .	xiv
1. INTRODUCTION . . . . .	1
1.1 General . . . . .	1
1.2 Digital Filter Realization . . . . .	4
1.2.1 Direct Realization . . . . .	6
1.2.2 Direct Canonic Realization . . . . .	8
1.2.3 Cascade Realization . . . . .	11
1.2.4 Parallel Realization . . . . .	14
1.2.5 Wave Realization . . . . .	14
1.3 Digital Filter Imperfections . . . . .	31
1.4 Comparison of Various Digital Filter Structures . . . . .	34
1.5 Scope of the Thesis . . . . .	35
2. A WAVE DIGITAL FILTER SYNTHESIS BASED ON GIC'S . . . . .	37
2.1 Introduction . . . . .	37
2.2 General Second-Order Section . . . . .	37
2.2.1 The Current-Conversion GIC . . . . .	38
2.2.2 Analog R-GIC Configuration . . . . .	38
2.2.3 Digital R-GIC Configuration . . . . .	41

2.3	Realization of any Transfer Function Using the GIC Synthesis . . . . .	45
2.4	Design Examples . . . . .	50
2.5	General Comparison . . . . .	67
2.5.1	Number of Arithmetic Operation . . . . .	67
2.5.2	Processing Speed . . . . .	76
2.5.3	Parallelism . . . . .	78
2.6	Conclusions . . . . .	79
3.	PRODUCT QUANTIZATION . . . . .	83
3.1	Introduction . . . . .	83
3.2	Signal Scaling . . . . .	83
3.3	Product Quantization Errors . . . . .	97
3.4	Comparison . . . . .	110
3.5	Conclusions . . . . .	111
4.	COEFFICIENT QUANTIZATION . . . . .	121
4.1	Introduction . . . . .	121
4.2	Sensitivity Analysis . . . . .	121
4.3	Exact Wordlength . . . . .	127
4.4	Statistical Wordlength . . . . .	128
4.5	Comparison . . . . .	134
4.6	Conclusions . . . . .	150
5.	CONCLUSIONS . . . . .	151
5.1	Summary . . . . .	151
5.2	Areas for Future Research . . . . .	152
	REFERENCES . . . . .	154



LIST OF TABLES

Table 1.1	Digital-Filter Elements . . . . .
Table 1.2	Realization of Impedances . . . . .
Table 1.3	Realization of Voltage Sources . . . . .
Table 2.1	Lowpass Filter Parameters . . . . .
Table 2.2	Bandstop Filter Parameters . . . . .
Table 2.3	Bandpass Filter Parameters . . . . .
Table 2.4	Delay Equalizer Parameters . . . . .
Table 2.5	Lowpass Filter Parameters (GIC Synthesis) . . . . .
Table 2.6	Bandstop Filter Parameters (GIC Synthesis) . . . . .
Table 2.7	Bandpass Filter Parameters (GIC Synthesis) . . . . .
Table 2.8	Delay Equalizer Parameters (GIC Synthesis) . . . . .
Table 2.9	Lowpass Filter Parameters (Cascade Canonic Synthesis) . . . . .
Table 2.10	Bandstop Filter Parameters (Cascade Canonic Synthesis) . . . . .
Table 2.11	Bandpass Filter Parameters (Cascade Canonic Synthesis) . . . . .
Table 2.12	Delay Equalizer Parameters (Cascade Canonic Synthesis) . . . . .
Table 2.13	Multiplier Values of the Bandstop Filter (Wave Synthesis) . . . . .
Table 2.14	Multiplier Values of the Bandpass Filter (Wave Synthesis) . . . . .

Table 2.15	Arithmetic Operations . . . . .
Table 3.1	Polynomials in GIC Sections . . . . .
Table 3.2	Lowpass Filter Parameters after Scaling (GIC and Cascade Canonic Synthesis) . . . . .
Table 3.3	Bandstop Filter Parameters after Scaling (GIC and Cascade Canonic Synthesis) . . . . .
Table 3.4	Bandpass Filter Parameters after Scaling (GIC and Cascade Canonic Synthesis) . . . . .
Table 3.5	Delay Equalizer Parameters after Scaling (GIC and Cascade Canonic Synthesis) . . . . .

LIST OF FIGURES

- Fig. 1.1 Processing of Continuous-Time Signals by using a Digital Filter . . . . .
- Fig. 1.2 Block Diagram Representation of a Digital Filter . . . . .
- Fig. 1.3 Digital Realization of Eqn. 1.3b . . . . .
- Fig. 1.4 Direct Realization . . . . .
- Fig. 1.5 Direct Realization of Eqn. 1.4a . . . . .
- Fig. 1.6 Direct Canonic Realization . . . . .
- Fig. 1.7 Cascade Realization . . . . .
- Fig. 1.8 Parallel Realization . . . . .
- Fig. 1.9 Wave Characterization of n-port Network . . . . .
- Fig. 1.10 Wave Characterization of an Impedance . . . . .
- Fig. 1.11 Wave Characterization of a Voltage Source . . . . .
- Fig. 1.12 Wave Characterization of 3-port Wire Interconnection . . . . .
- Fig. 1.13 Adaptors . . . . .
- Fig. 1.14 Number Representation . . . . .
- Fig. 2.1 CGIC Wave Representation . . . . .
- Fig. 2.2 General Second-Order R-GIC Analog Configuration . . . . .
- Fig. 2.3 Digital Realization of the CGIC with  $h(s)=s$  . . . . .
- Fig. 2.4 General Second-Order Digital GIC Section . . . . .
- Fig. 2.5 Universal Second-Order Digital GIC Sections . . . . .
- Fig. 2.6 Canonic Second-Order Sections . . . . .
- Fig. 2.7 Block Diagram Representations of the Lowpass Filter, Bandstop Filter, Bandpass Filter and the Delay Equalizer . . . . .

Fig. 2.8	Butterworth 6th-Order Lowpass Wave Digital Filter . . . . .
Fig. 2.9	Elliptic 6th-Order Bandstop Wave Digital Filter . . . . .
Fig. 2.10	Elliptic 6th-Order Bandpass Wave Digital Filter . . . . .
Fig. 2.11	Degree of Parallelism in the Lowpass Filter, Bandstop Filter, Bandpass Filter and the Delay Equalizer . . . . .
Fig. 3.1	Scaling of a Digital Filter . . . . .
Fig. 3.2	Canonic Second-Order Section . . . . .
Fig. 3.3	Signal Scaling of GIC Structure . . . . .
Fig. 3.4	Signal Scaling in Wave Digital-Filter Structure . . . . .
Fig. 3.5	S1-Type Adaptor after Scaling . . . . .
Fig. 3.6	P1-Type Adaptor after Scaling . . . . .
Fig. 3.7	S2-Type Adaptor after Scaling . . . . .
Fig. 3.8	P2-Type Adaptor after Scaling . . . . .
Fig. 3.9	Multiplier Noise Model . . . . .
Fig. 3.10	Probability-Density Function of the Quantization Noise in Fixed-Point Arithmetic . . . . .
Fig. 3.11	Quantization-Noise Model for GIC Sections . . . . .
Fig. 3.12	PSD Versus Frequency (Butterworth Lowpass Filter) . . . . .
Fig. 3.13	PSD Versus Frequency (Elliptic Bandstop Filter) . . . . .
Fig. 3.14	PSD Versus Frequency (Elliptic Bandpass Filter) . . . . .
Fig. 3.15	PSD Versus Frequency (Delay Equalizer) . . . . .
Fig. 4.1	Digital-Network Model for Sensitivity Analysis . . . . .

Fig. 4.2 Second-Order Canonic Lowpass Section Model for Sensitivity Analysis . . . . .

Fig. 4.3 Lowpass GIC Second-Order Section Model for Sensitivity Analysis . . . . .

Fig. 4.4 Amplitude Response of a Digital Filter . . . . .

Fig. 4.5  $|\Delta M|_{\max}$  Versus Wordlength (Butterworth Lowpass Filter) . . . . .

Fig. 4.6 The Average of  $|\Delta M|$  Versus Wordlength (Butterworth Lowpass Filter) . . . . .

Fig. 4.7 Standard Deviation of  $\Delta M$  Versus Wordlength (Butterworth Lowpass Filter) . . . . .

Fig. 4.8  $|\Delta M|_{\max}$  Versus Wordlength (Elliptic Bandstop Filter) . . . . .

Fig. 4.9 The Average of  $|\Delta M|$  Versus Wordlength (Elliptic Bandstop Filter) . . . . .

Fig. 4.10 Standard Deviation of  $\Delta M$  Versus Wordlength (Elliptic Bandstop Filter) . . . . .

Fig. 4.11  $|\Delta M|_{\max}$  Versus Wordlength (Elliptic Bandpass Filter) . . . . .

Fig. 4.12 The Average of  $|\Delta M|^2$  Versus Wordlength (Elliptic Bandpass Filter) . . . . .

Fig. 4.13 Standard Deviation of  $\Delta M$  Versus Wordlength (Elliptic Bandpass Filter) . . . . .

Fig. 4.14  $W(\omega)$  Versus Frequency (Butterworth Lowpass Filter) . . . . .

Fig. 4.15  $W(\omega)$  Versus Frequency (Elliptic Bandstop Filter) . . . . .

Fig. 4.16  $W(\omega)$  Versus Frequency (Elliptic Bandpass Filter) . . . . .

Fig. 4.17  $W(\omega)$  Versus Frequency (Delay Equalizer) . . . . .

LIST OF ABBREVIATIONS AND SYMBOLS

AP	Allpass
BP	Bandpass
CGIC	Current Conversion Generalized-Immittance Converter
GIC	Generalized-Immittance Converter
HP	Highpass
$h(s)$	Conversion Function of the CGIC
LP	Lowpass
N	Notch
PSD	Power Spectral Density
$s$	Complex Frequency Variable in the Analog Domain
$S_e^x$	Sensitivity of the Function $x$ with respect to Parameter $e$
T	Sampling Period
$z$	Complex Frequency Variable in the Digital Domain

CHAPTER 1

INTRODUCTION

1.1 GENERAL

A digital filter is a digital system which will transform a sequence of numbers representing a given signal into a second sequence of numbers, according to some rule of correspondence. Digital filters can perform many of the tasks that can be performed by analog filters such as differentiation, integration, resolution of signals into their components, spectrum shaping and so on.

A digital filter can be represented by a discrete-time transfer function or by a network. The discrete-time transfer function, designated by  $H(z)$ , is often obtained by applying the bilinear transformation

$$s = \frac{2}{T} \frac{(z-1)}{(z+1)}$$

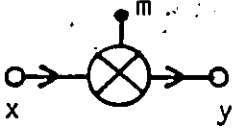
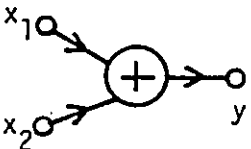

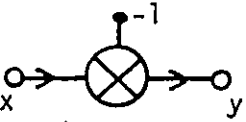
to a continuous-time transfer function  $H(s)$ , that is

$$H_D(z) = H(s) \Big|_{s = \frac{2}{T} \frac{(z-1)}{(z+1)}} \tag{1.1}$$

where  $T$  is a constant. A digital-filter network is an interconnection of multipliers, adders and unit delays. The symbolic representation and characterization of these elements are summarized in Table 1.1.

The implementation of a digital filter can assume two forms namely, software, and hardware. Software implementation involves the simulation of the filter network on a general-purpose digital computer.

TABLE 1.1 DIGITAL-FILTER ELEMENTS

ELEMENT	SYMBOL	FUNCTION
MULTIPLIER		$y = mx$
ADDER		$y = x_1 + x_2$
UNIT-DELAY		$y(n) = x(n-1)$
INVERTER		$y = -x$



Hardware implementation, on the other hand, involves the conversion of the filter network into a dedicated piece of hardware.

Software digital filters are computer programs which can be used to manipulate sequences of numbers. Therefore, they first appeared in the late forties along with the first digital computer, although the term 'digital filter' was not used until the mid-sixties. In the early stages of digital computers, many of the classical numerical analysis formulas of Newton, Gauss and others were used to carry out mathematical operations such as interpolation, differentiation, and integration of functions represented by sequences of numbers. Since these operations entail spectrum manipulation of a signal, the programs or subroutines which carry out these operations were essentially digital filters. With the tremendous development in the field of digital computers in subsequent years, very complicated algorithms and programs were developed to perform a variety of filtering tasks in many applications, such as spectrum analysis, data smoothing, and pattern recognition, etc. As a result, digital filters have a variety of applications in the areas of seismic exploration, sonar, radar, analysis of biomedical signals, speech communications, and so on.

A continuous-time signal can be transformed into a sequence of numbers by utilizing an analog-to-digital (A/D) converter. The sequence of numbers so generated can then be transformed according to some computational algorithm into a second sequence of numbers. Finally, the transformed sequence of numbers can be used to regenerate a corresponding continuous-time signal by utilizing a digital-to-analog (D/A) converter. Therefore, by utilizing an A/D converter and a D/A

converter as illustrated in Fig. 1.1, a digital filter can be used to process continuous-time signals.

The performance of hardware digital filter, unlike that of analog filters, is free of drift and the size of digital components does not depend on the frequency of operation. Consequently, the use of digital filters will guarantee high numerical accuracy and small size. New large-scale integration techniques (LSI) have produced low-priced digital components such as read-only-memories (ROM) and microprocessors, which provide enormous flexibility in the design of digital hardware. In addition, the possibility of time-sharing one and the same digital system can result in low hardware costs. Because of these reasons, hardware digital filters have achieved wide usage in recent years, in many applications such as wave analyzers, frequency synthesizers, and communication systems [1]-[10].

## 1.2 DIGITAL FILTER REALIZATION

The embodiment of a discrete-time transfer function into a network is said to be a realization of the digital filters. There are two broad classes of realizations, namely nonrecursive and recursive. In a nonrecursive realization, the filter network has only feedforward paths whereas in a recursive realization the filter network has feedforward as well as feedback paths. This thesis is concerned with recursive digital filters. There are five types of recursive realizations in common use as follows:

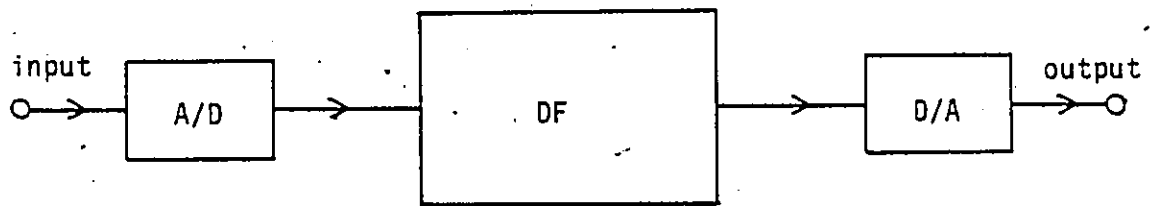


FIG. 1.1 Processing of Continuous-time Signals by using a Digital Filter

- 1) Direct
- 2) Direct Canonic
- 3) Cascade
- 4) Parallel
- 5) Wave

In the first four methods, the discrete-time transfer function  $H(z)$  is realized directly [9]-[11]. In the last method, namely the wave method [12]-[16], the desired transfer function is realized indirectly by transforming a suitable analog LC filter into a corresponding digital network. The above realizations are described in the following sections.

### 1.2.1 Direct Realization

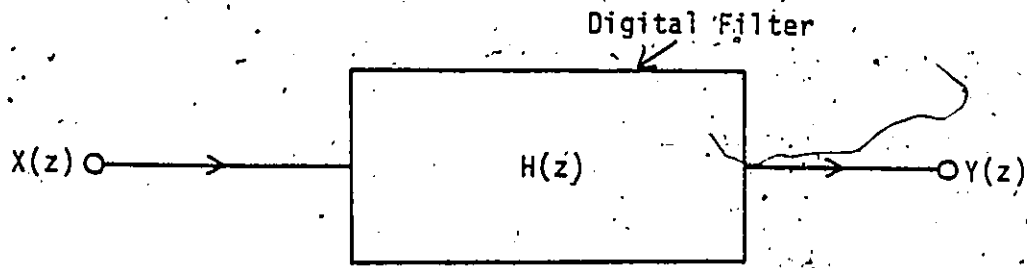
Consider a transfer function

$$H(z) = \frac{\sum_{i=0}^N a_i z^{-i}}{1 + \sum_{i=1}^N b_i z^{-i}} \quad (1.2)$$

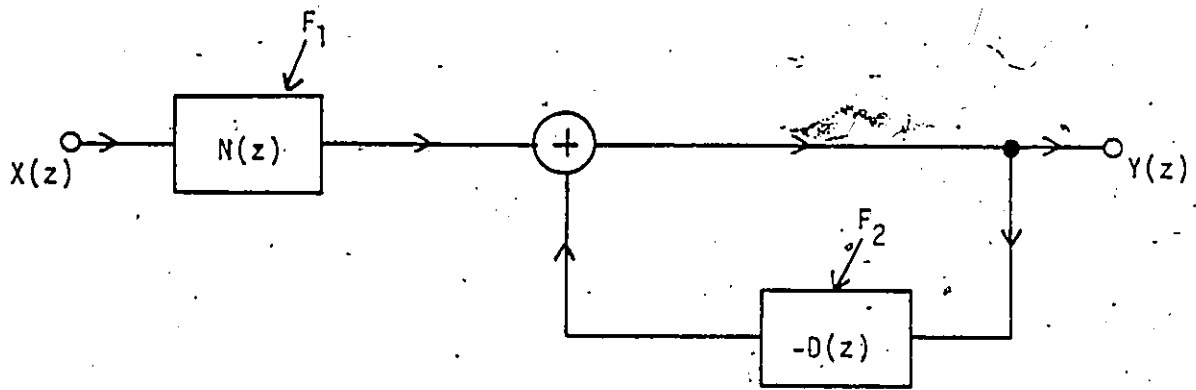
and assume that it characterizes the digital filter of Fig. 1.2a.  $X(z)$  and  $Y(z)$  are the  $z$  transforms of the input and output of digital filter, respectively. We can write

$$H(z) = \frac{Y(z)}{X(z)} = \frac{N(z)}{1+D'(z)} \quad (1.3a)$$

where



(a)



(b)

FIG. 1.2 Block Diagram Representation of a Digital Filter

(a) Realization of Eqn. 1.2

(b) Realization of Eqn. 1.3c

$$\left. \begin{aligned} N(z) &= \sum_{i=0}^N a_i z^{-i} \\ D'(z) &= \sum_{i=1}^N b_i z^{-i} \end{aligned} \right\} \quad (1.3b)$$

From Eqn. 1.3a we have

$$Y(z) = N(z)X(z) - Y(z)D'(z) \quad (1.3c)$$

and hence the digital filter of Fig. 1.2a can be represented by the block diagram of Fig. 1.2b. In this way, the digital filter can be decomposed into two simpler filters, namely filter  $F_1$  and  $F_2$  as shown in Fig. 1.2b. Filter  $F_1$  has a transfer function  $N(z)$ , whereas filter  $F_2$  has a transfer function  $-D'(z)$ . These transfer functions can be realized independently as shown in Figs. 1.3a and 1.3b and hence the realization of  $H(z)$  can be readily completed as shown in Fig. 1.4.

### 1.2.2 Direct Canonic Realization

The direct canonic realization is similar to the preceding realization except that a minimum number of unit-delays is used. We can rewrite Eqn. 1.2 as

$$\frac{Y(z)}{X(z)} = H(z) = H_1(z) \cdot H_2(z) = \frac{V(z)}{X(z)} \cdot \frac{Y(z)}{V(z)} \quad (1.4a)$$

where

$$H_1(z) = \frac{1}{1 + \sum_{i=1}^N b_i z^{-i}} = \frac{1}{1 + D'(z)}$$

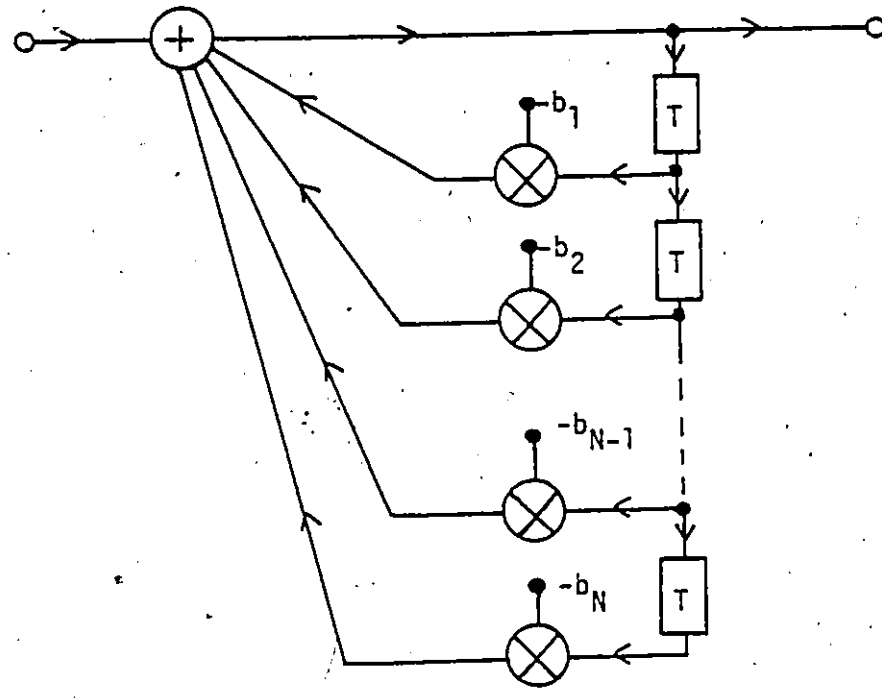
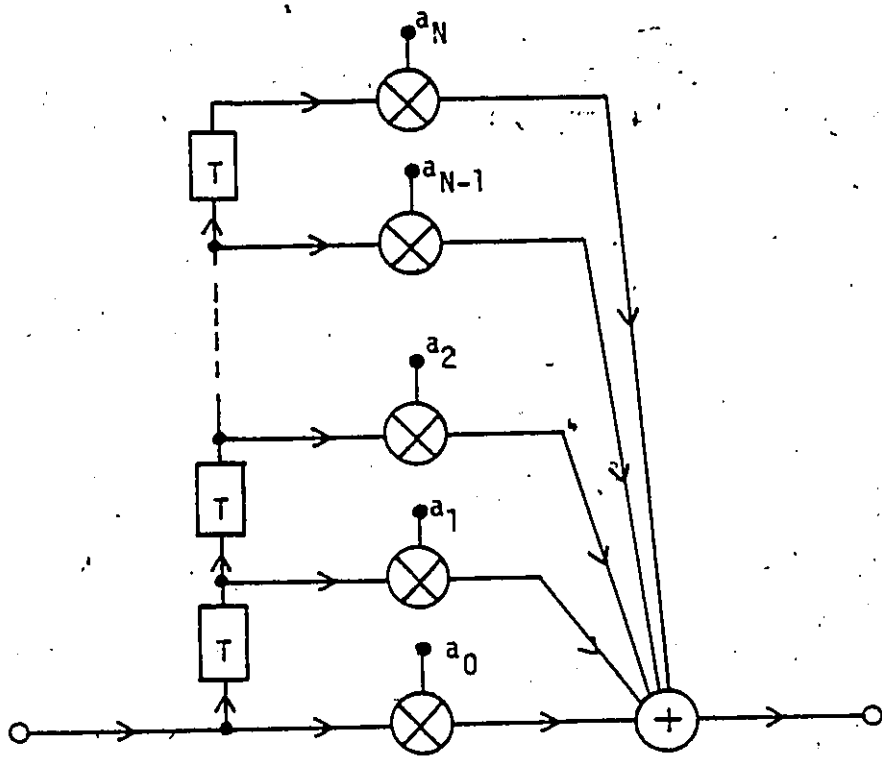


FIG. 1.3. Digital Realization of Eqn. 1.3b  
(a) Realization of  $N(z)$   
(b) Realization of  $D'(z)$

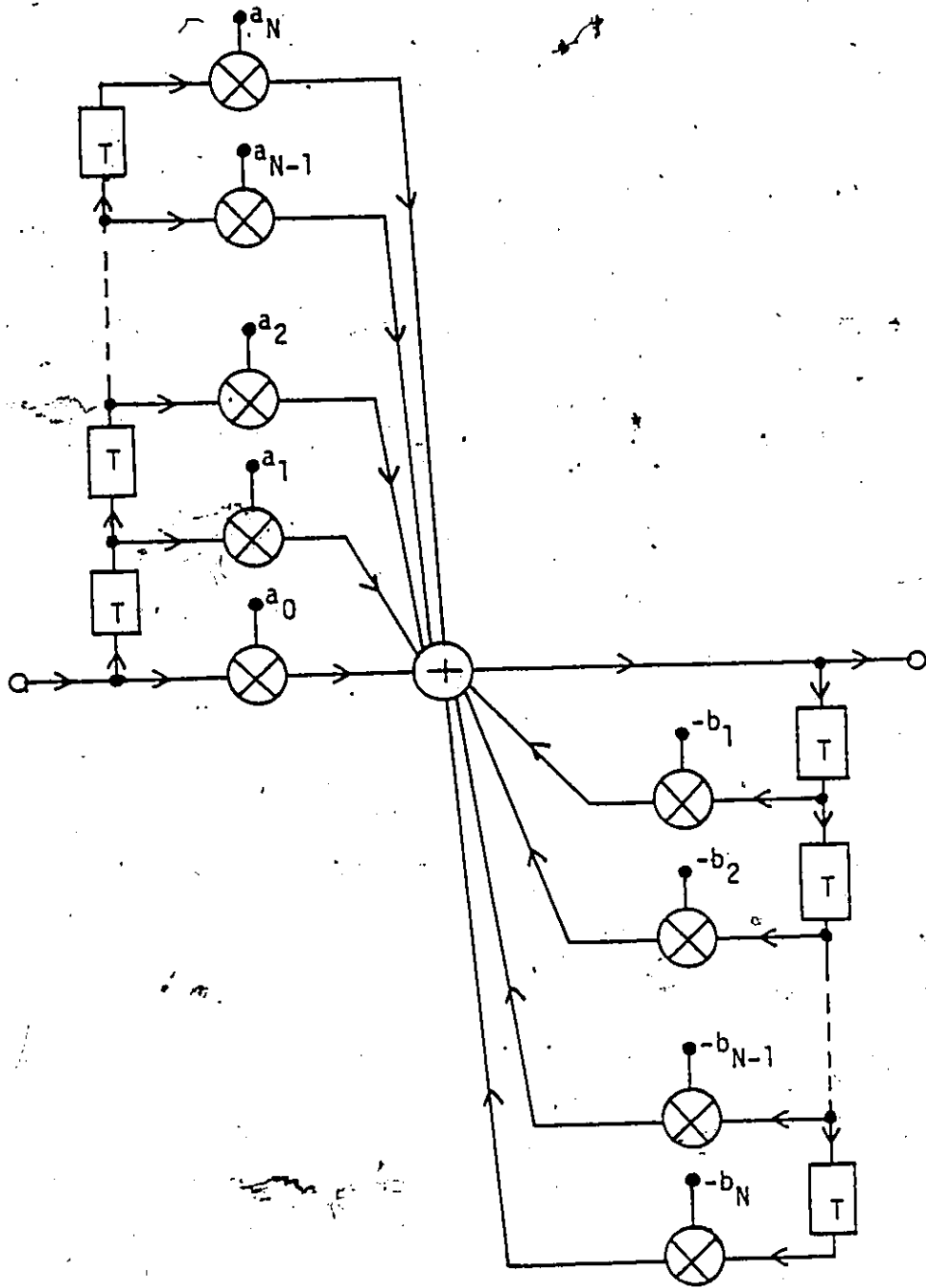


FIG. 1.4 Direct Realization



and

$$H_2(z) = \sum_{i=0}^N a_i z^{-i} = N(z)$$

Hence we may assign

$$\left. \begin{aligned} \frac{V(z)}{X(z)} &= H_1(z) = \frac{1}{1+D^1(z)} \\ \frac{Y(z)}{V(z)} &= H_2(z) = N(z) \end{aligned} \right\} \quad (1.4b)$$

In this way  $H(z)$  can be realized by using two cascade filters, as shown in Fig. 1.5a.  $H_1(z)$  and  $H_2(z)$  can be realized by using the method of the previous section. The complete realization is shown in Fig. 1.5b. Evidently, the signals at nodes,  $A_1, A_2, \dots, A_k$  are the same as at  $A'_1, A'_2, \dots, A'_k$ , respectively, and so the delays in branch  $A_1-A_k$  can be deleted, as depicted in Fig. 1.6.

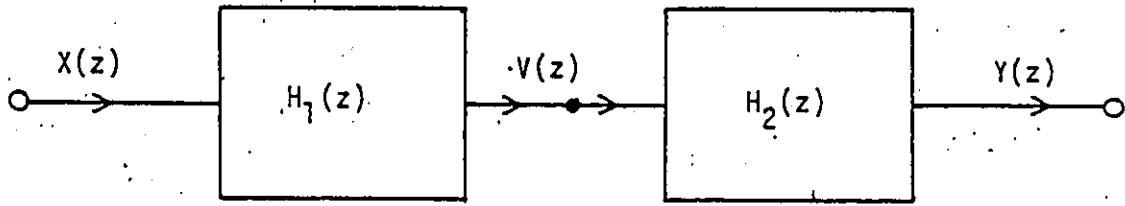
### 1.2.3 Cascade Realization

In this realization the given transfer function is factorized into first- and/or second-order transfer functions. In other words, Eqn. 1.2 is written as

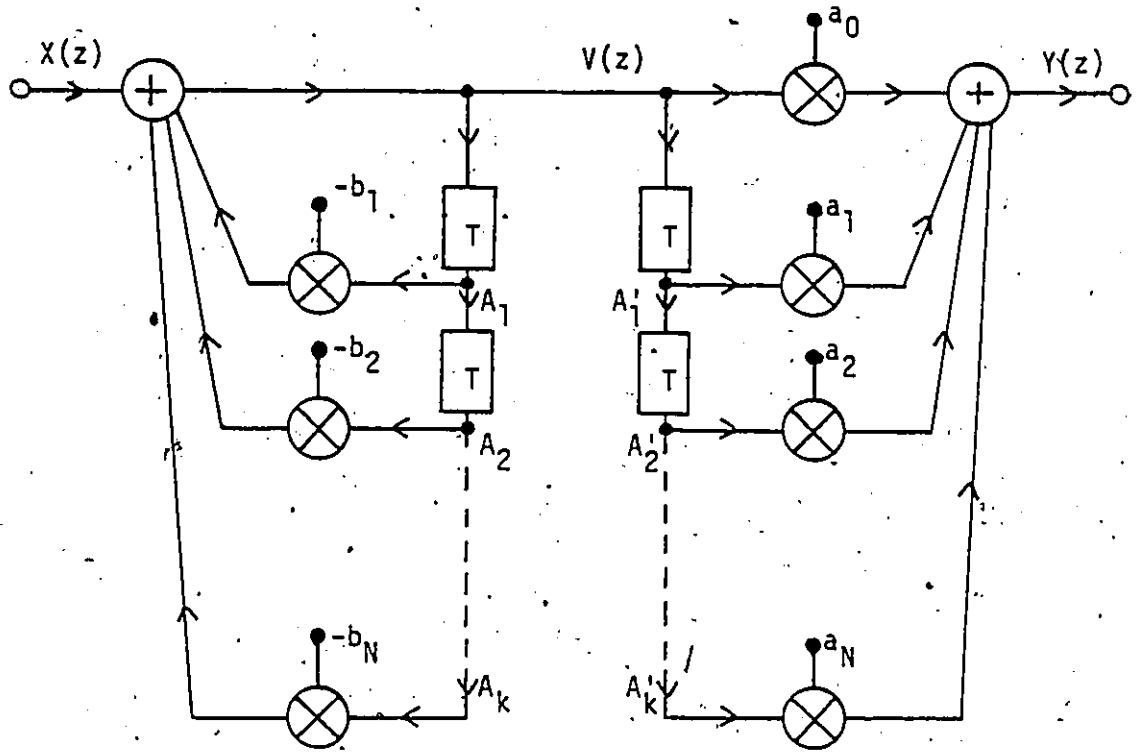
$$H(z) = \prod_{i=1}^L H_i(z)$$

where  $H_i(z)$  is a second-order transfer function of the form

$$H_i(z) = \frac{a_{0i} + a_{1i}z^{-1} + a_{2i}z^{-2}}{1 + b_{1i}z^{-1} + b_{2i}z^{-2}}$$



(a)



(b)

FIG. 1.5 Direct Realization of Eqn. 1.4a

(a) Realization of Eqn. 1.4a as building blocks

(b) Realization of Eqn. 1.4b.

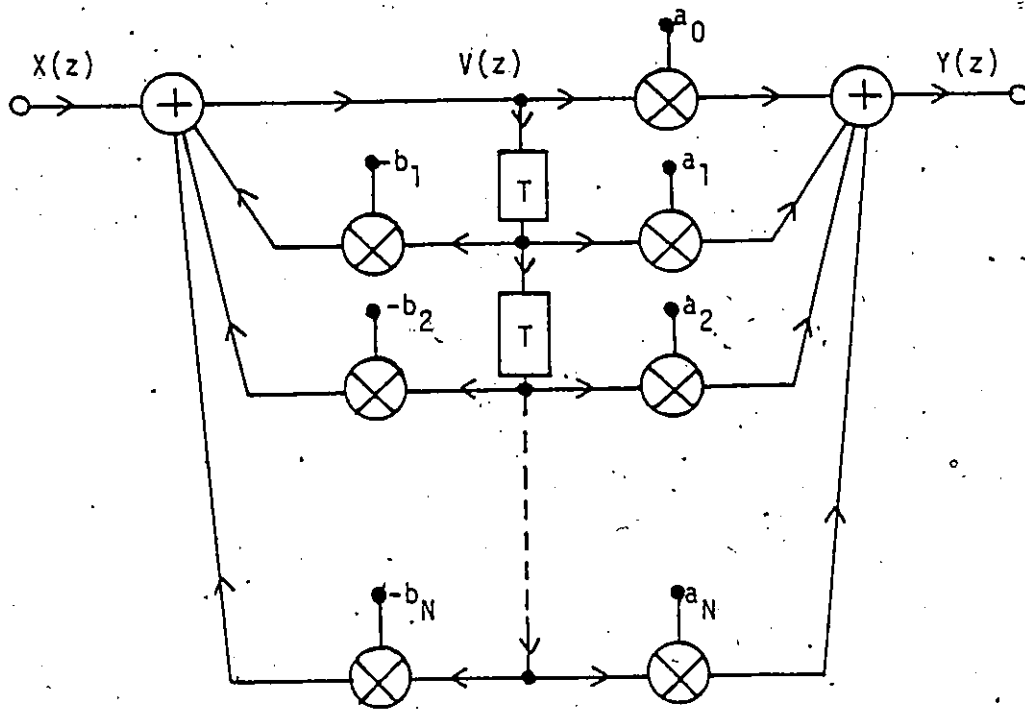


FIG. 1.6 Direct Canonic Realization

The individual sections can be realized by employing either the Direct or Direct Canonic realization. By cascading the individual networks obtained, the realization can be completed as shown in Fig. 1.7.

#### 1.2.4 Parallel Realization

The transfer function given in Eqn. 1.2 can be expanded into partial fractions as

$$H(z) = \sum_{i=1}^L H_i(z)$$

where each  $H_i(z)$  is a second-order transfer function of the form

$$H_i(z) = \frac{a_{0i} + a_{1i}z^{-1}}{1 + b_{1i}z^{-1} + b_{2i}z^{-2}}$$

As in the cascade realization, each individual transfer function is realized by using either the Direct or Direct Canonic realization. By connecting the individual networks obtained in parallel, the realization can be completed as shown in Fig. 1.8.

#### 1.2.5 Wave Realization

In this approach, the realization is accomplished by using the following two general steps:

- 1) An LC filter satisfying appropriate specifications is designed.
- 2) The analog elements of the LC filter obtained in step 1 are replaced one-for-one by corresponding digital realizations.

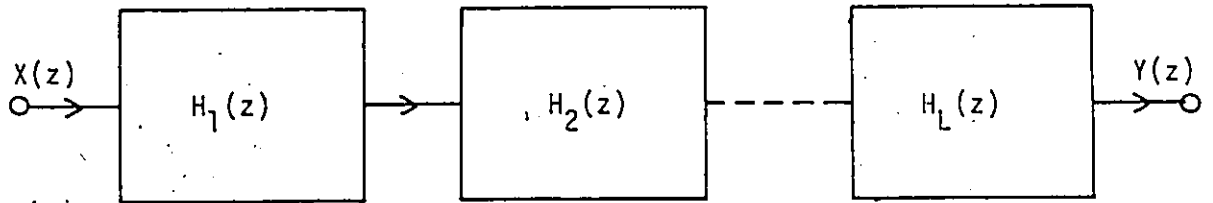


FIG. 1.7 Cascade Realization

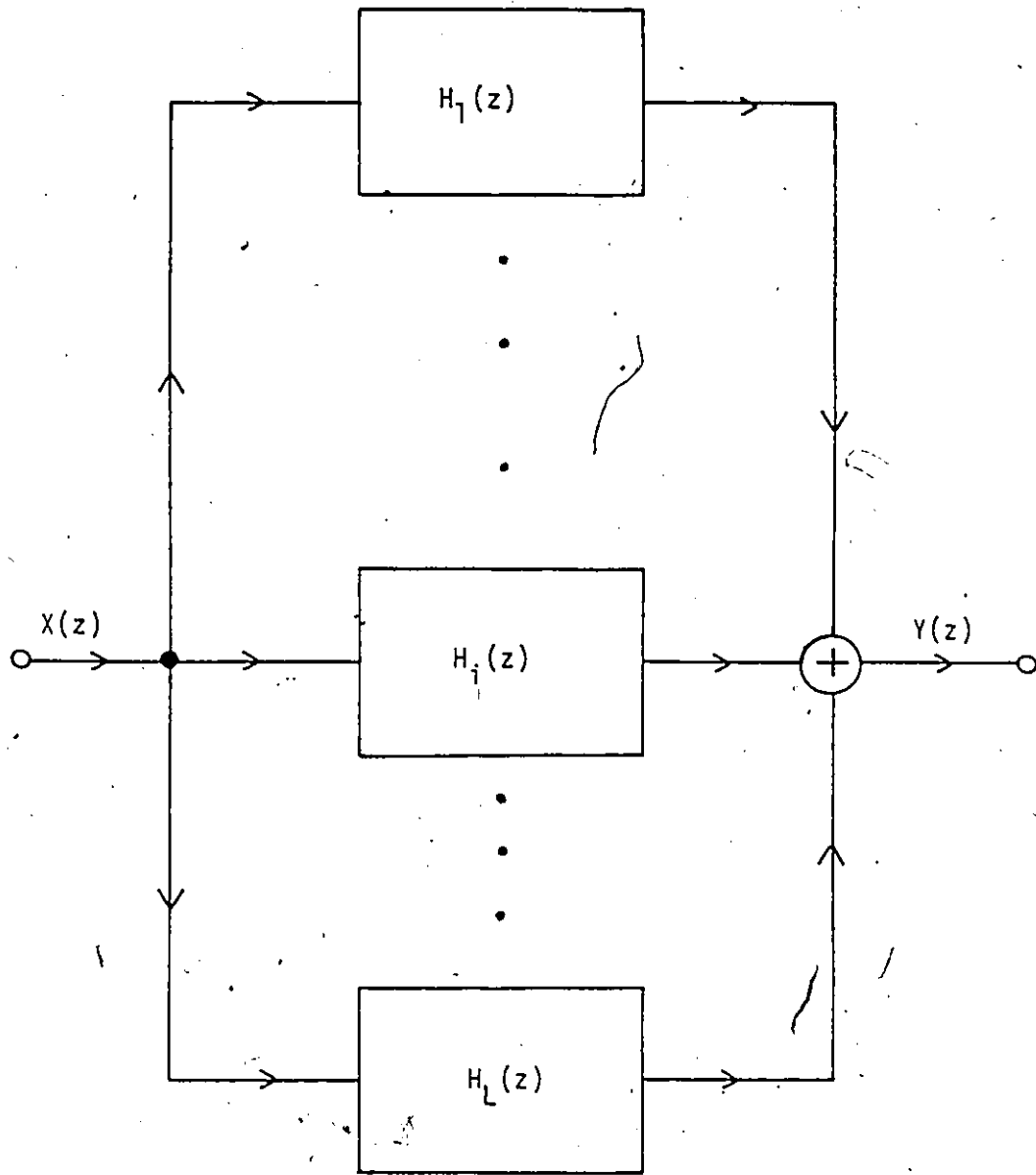


FIG. 1.8. Parallel Realization

Digital realizations for conventional analog elements have been proposed by Fettweis [12]-[14], and Sedlmeyer and Fettweis [15], [16]. Such realizations can be obtained by using the wave characterization.

An analog n-port network of the type shown in Fig. 1.9 can be characterized by the relations

$$\left. \begin{aligned} A_k &= V_k + I_k R_k \\ B_k &= V_k - I_k R_k \end{aligned} \right\} \quad (1.5)$$

where  $k = 1, 2, \dots, n$ . The quantities  $A_k$  and  $B_k$  are referred to as the incident and reflected wave quantities while  $R_k$  is referred to as the port resistance. In an interconnection of n-ports, two interconnected ports must be assigned the same resistance so as to maintain continuity in the wave flow. Otherwise  $R_k$  can be chosen arbitrarily.

The impedances shown in Fig. 1.10 can be represented by the equation

$$Z(s) = s^\lambda R_x$$

where  $R_x$  is a positive constant and  $\lambda = -1$  for a capacitance,  $\lambda = 0$  for a resistance, and  $\lambda = 1$  for an inductance. According to Eqn. 1.5, each of these impedances can be represented by

$$\begin{aligned} A_1 &= V_1 + I_1 R \\ B_1 &= V_1 - I_1 R \\ V_1 &= I_1 Z(s) \end{aligned} \quad (1.6)$$

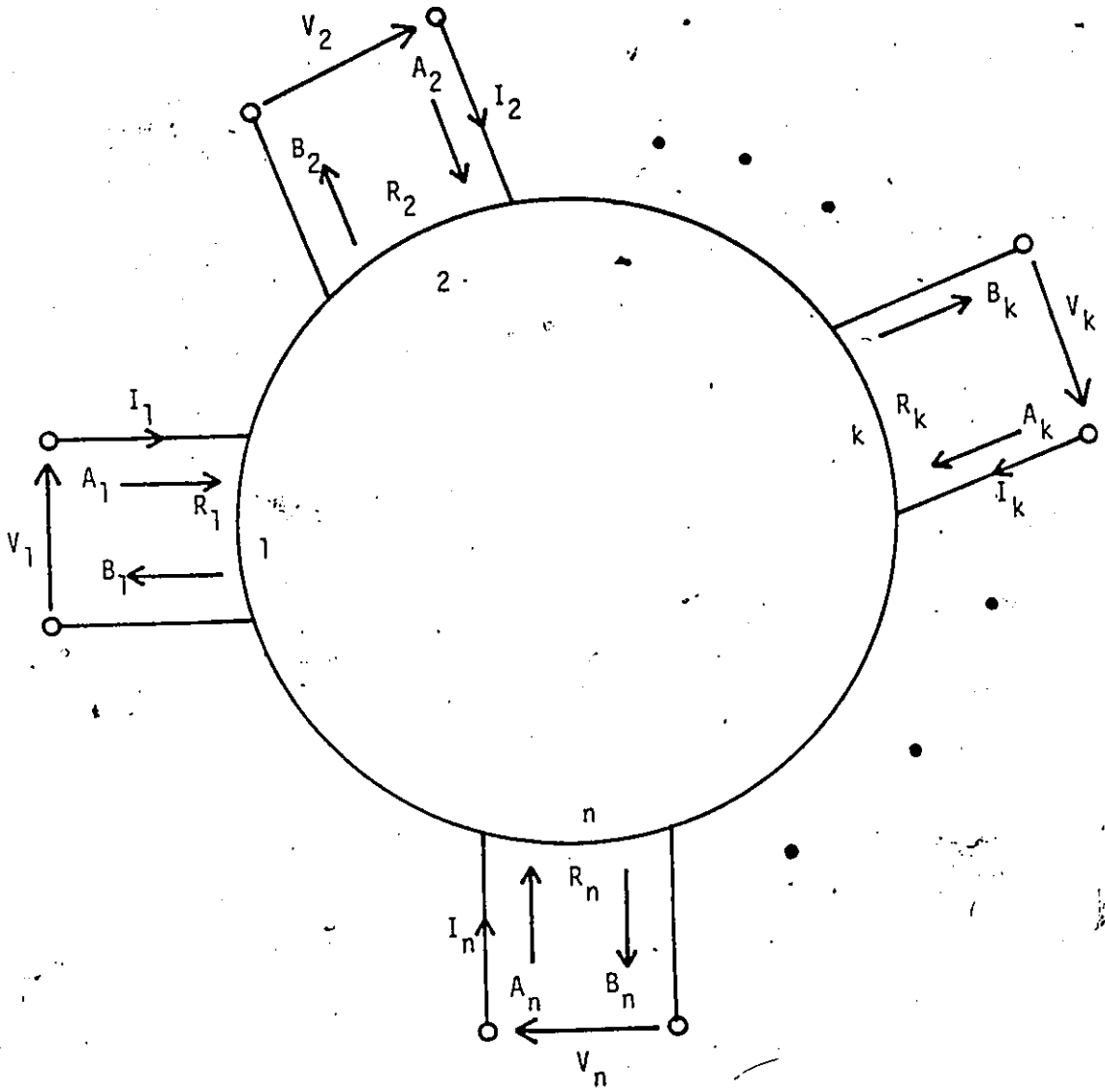


FIG. 1.9 Wave Characterization of n-port Network



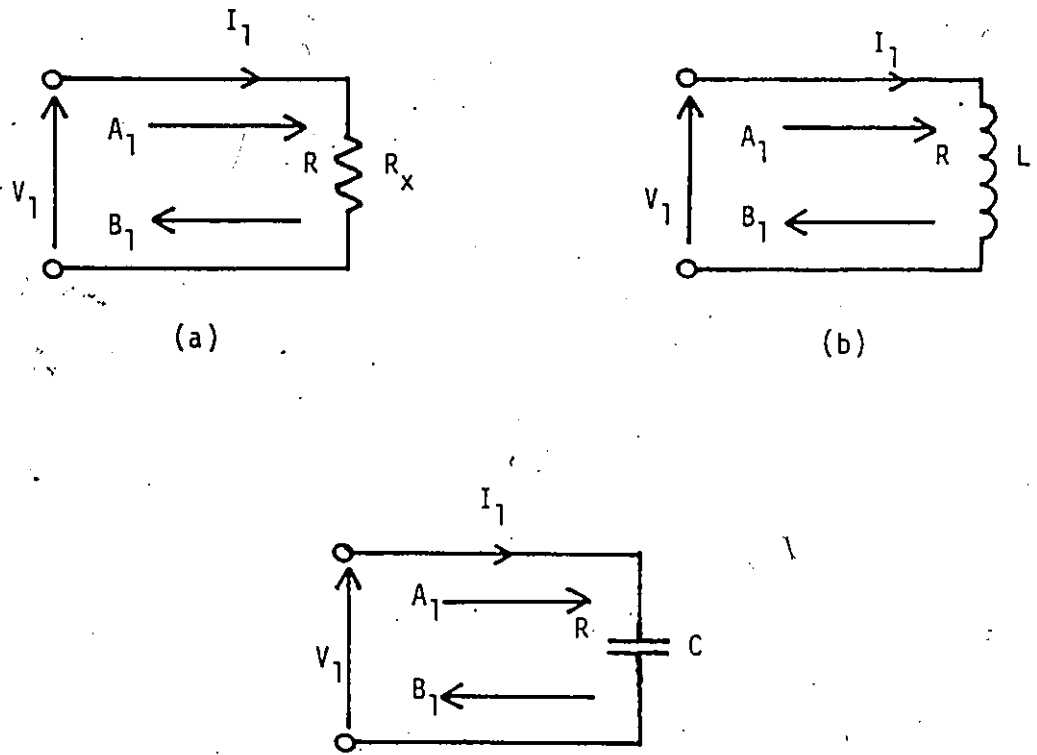


FIG. 1.10 Wave Characterization of an Impedance

- (a) Resistance
- (b) Inductance
- (c) Capacitance

and if we choose

$$R = \left(\frac{2}{T}\right)^\lambda R_x$$

then

$$\left. \begin{aligned} A_1 &= V_1 + I_1 \left(\frac{2}{T}\right)^\lambda R_x \\ B_1 &= V_1 - I_1 \left(\frac{2}{T}\right)^\lambda R_x \end{aligned} \right\} \quad (1.7)$$

By using the bilinear transformation

$$s = \frac{2}{T} \frac{(z-1)}{(z+1)}$$

Eqn. 1.6 can be written as

$$V_1 = I_1 \left(\frac{2}{T}\right)^\lambda R_x \left(\frac{z-1}{z+1}\right)^\lambda$$

By eliminating  $V_1$  in Eqn. 1.7, we have

$$A_1 = I_1 \left(\frac{2}{T}\right)^\lambda R_x \left[ \left(\frac{z-1}{z+1}\right)^\lambda + 1 \right]$$

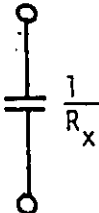
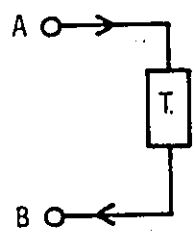
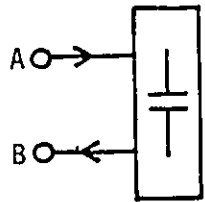
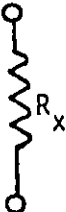


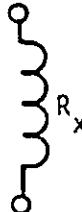
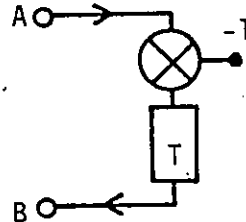
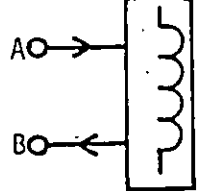
$$B_1 = I_1 \left(\frac{2}{T}\right)^\lambda R_x \left[ \left(\frac{z-1}{z+1}\right)^\lambda - 1 \right]$$

or

$$B_1 = \left[ \frac{(z-1)^\lambda - (z+1)^\lambda}{(z-1)^\lambda + (z+1)^\lambda} \right] A_1$$

Now by letting  $\lambda = -1, 0$  or  $1$ , digital realizations for a capacitance, resistance or inductance can be obtained as shown in Table 1.2. By using the same procedure for the voltage sources shown

TABLE 1.2 REALIZATION OF IMPEDANCES

$\lambda$	ELEMENT	R	$f(z)$	REALIZATION	SYMBOL
-1	 $\frac{1}{R_x}$	$\frac{T}{2C}$	$\frac{1}{z}$		
0	 $R_x$	R	0		
1	 $R_x$	$\frac{2L}{T}$	$-\frac{1}{z}$		

in Fig. 1.11, the wave digital realizations shown in Table 1.3 can be readily derived.

The digital realization of the 3-port series and the 3-port parallel wire interconnections shown in Fig. 1.12a and 1.12b can be obtained as shown in Fig. 1.13a and 1.13b [12]-[17] by using the above approach. These realizations are referred to as adaptors. The series adaptor can be referred to as type S2 (series, 2-multiplier) adaptor, while the parallel adaptor can be referred to as type P2 (parallel, 2-multiplier) adaptor. The multiplier constants for a type S2 adaptor are given by

$$m_{s1} = \frac{2R_1}{R_1 + R_2 + R_3} \quad (1.8)$$

$$m_{s2} = \frac{2R_2}{R_1 + R_2 + R_3} \quad (1.9)$$

On the other hand, the multiplier constants for a type P2 adaptor are given by

$$m_{p1} = \frac{2G_1}{G_1 + G_2 + G_3} \quad (1.10)$$

$$m_{p2} = \frac{2G_2}{G_1 + G_2 + G_3} \quad (1.11)$$

Two special cases of these adaptors are of particular interest, namely, the type S1 adaptor of Fig. 1.13c and the type P1 adaptor of Fig. 1.13d. These can be derived from the 2-multiplier adaptors by assigning  $m_{s2} = 1$  or  $R_1 + R_3 = R_2$  in the first case and  $m_{p2} = 1$  or  $G_1 + G_3 = G_2$

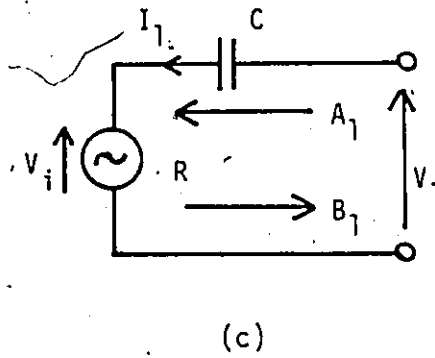
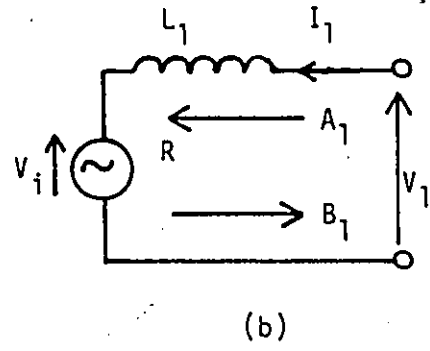
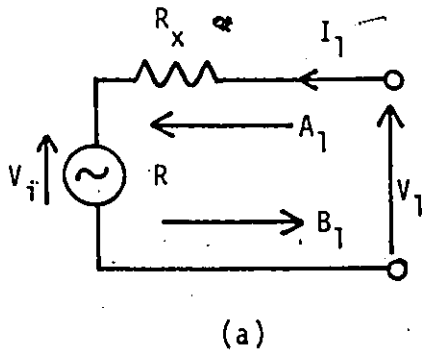
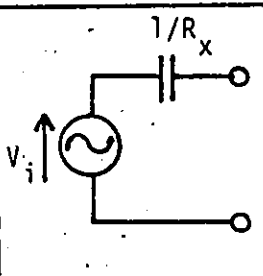
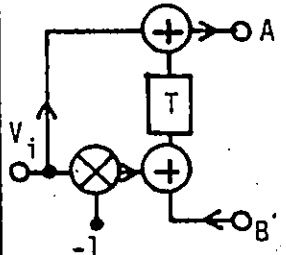
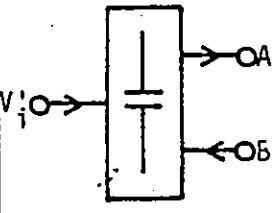
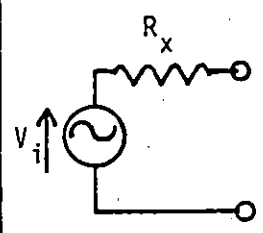
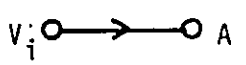
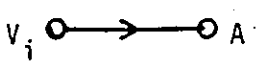
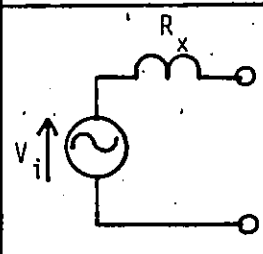
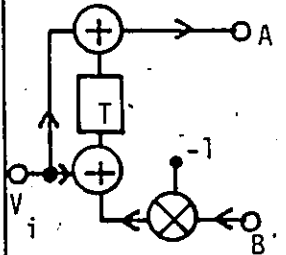
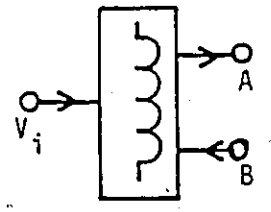
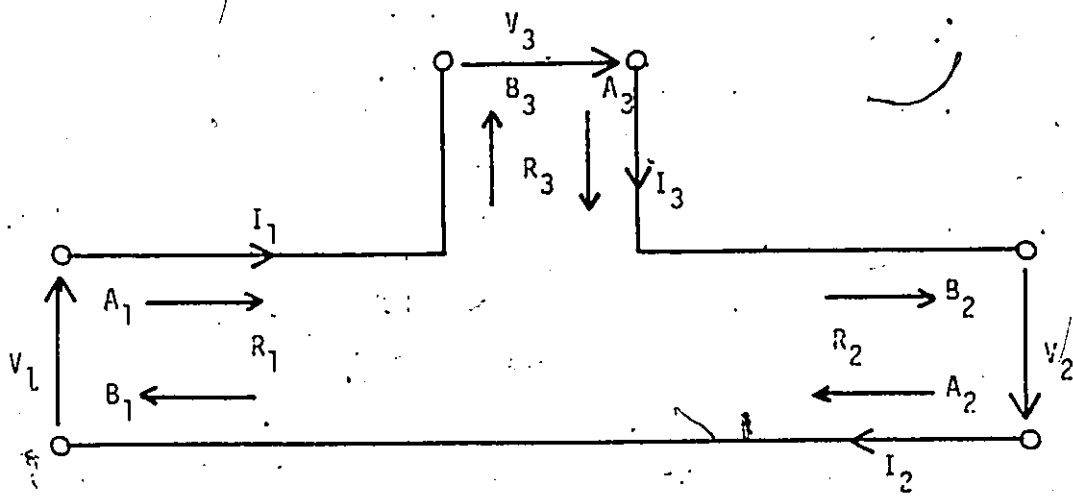


FIG. 1.11 Wave Characterization of a Voltage Source

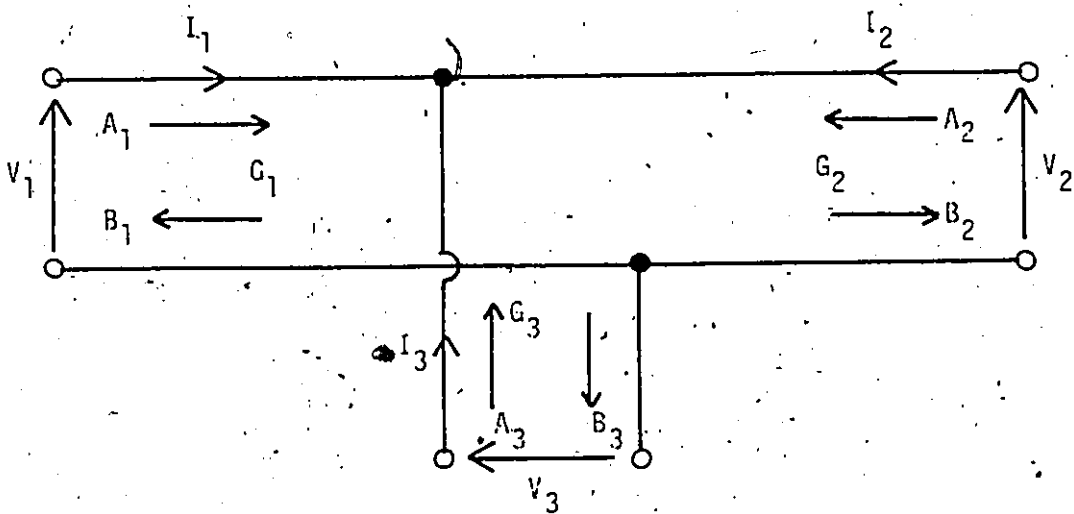
- (a) Voltage Source with Internal Resistance
- (b) Voltage Source with Internal Inductance
- (c) Voltage Source with Internal Capacitance

TABLE 1.3 REALIZATION OF VOLTAGE SOURCES

$\lambda$	VOLTAGE SOURCE	R	REALIZATION	SYMBOL
-1		$\frac{T}{2C}$		
0		R		
1		$\frac{2L}{T}$		



(a)



(b)

FIG. 1.12 Wave Characterization of 3-port Wire Interconnection

(a) Series Interconnection

(b) Parallel Interconnection

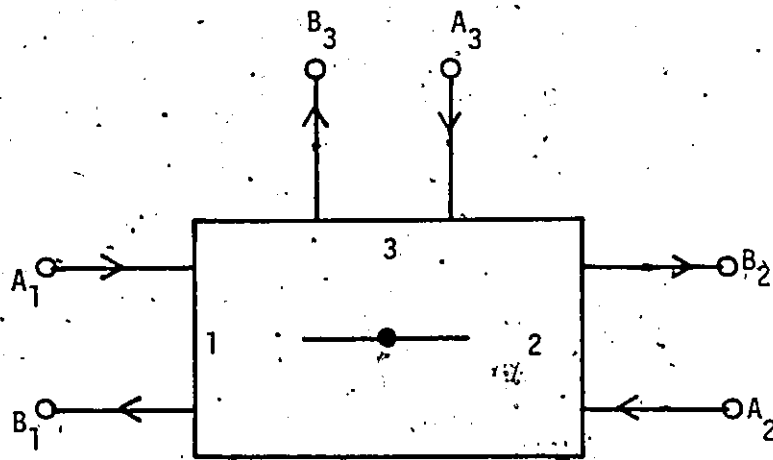
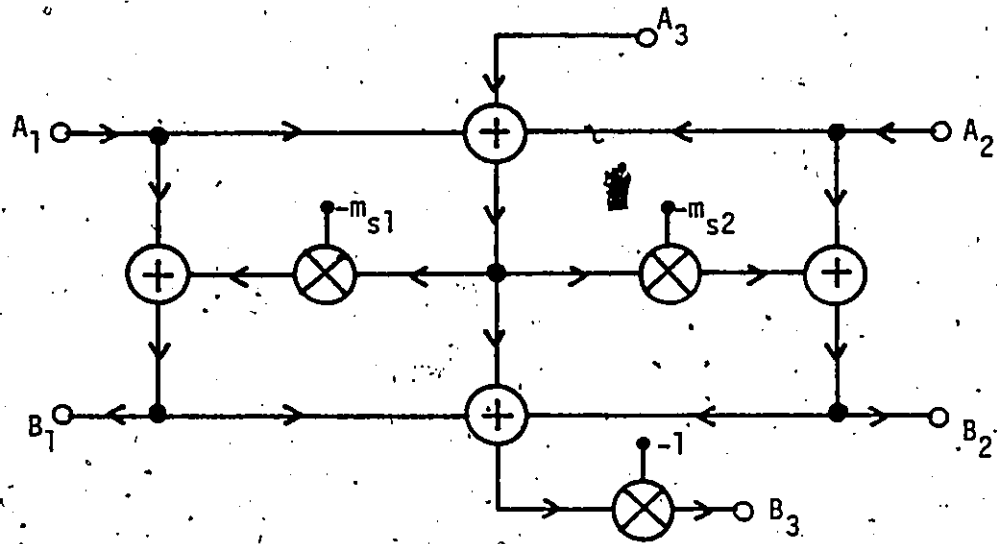


FIG. 1.13 Adaptors

(a) S2-Type Series Adaptor



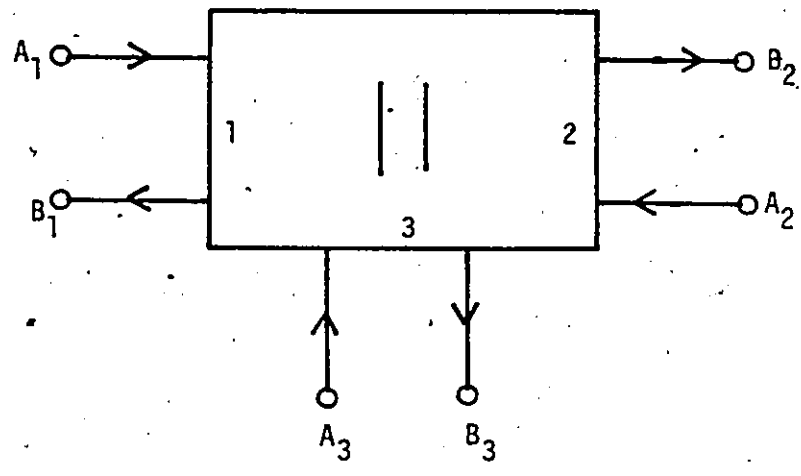
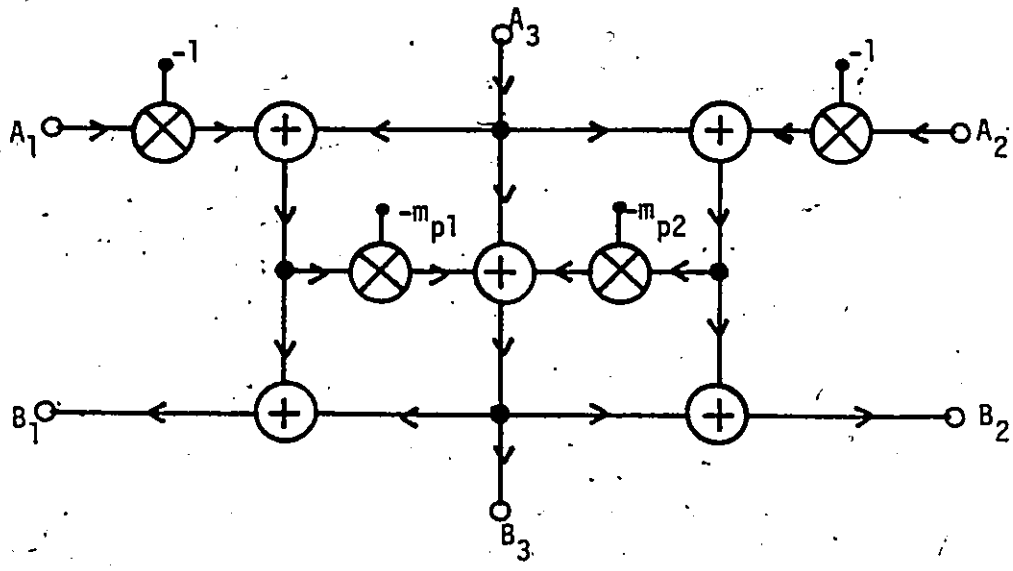


FIG. 1.13 Adaptors

(b) P2-Type Parallel Adaptor

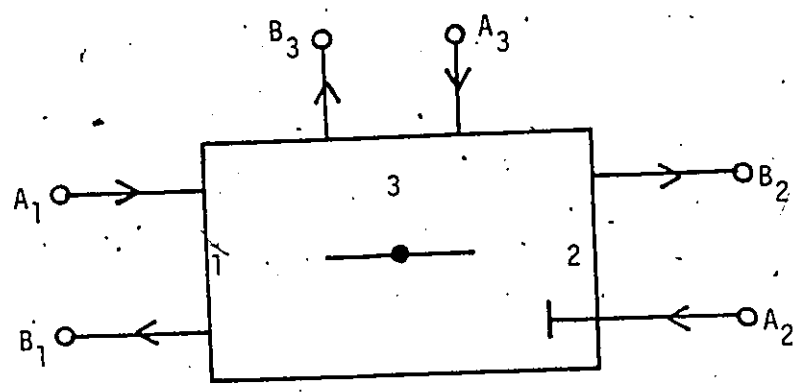
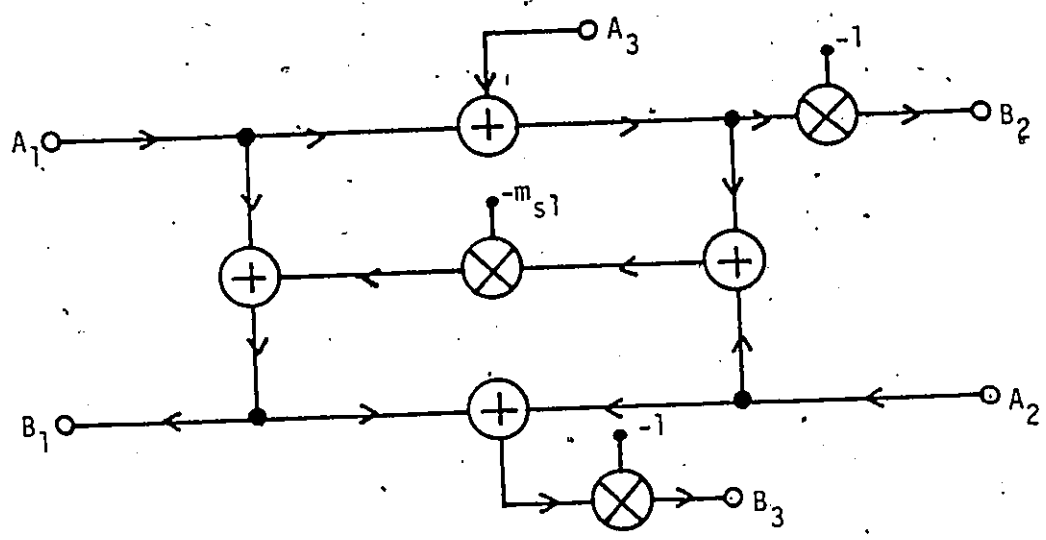


FIG. 1.13 Adaptors

(c) S1-Type Series Adaptor



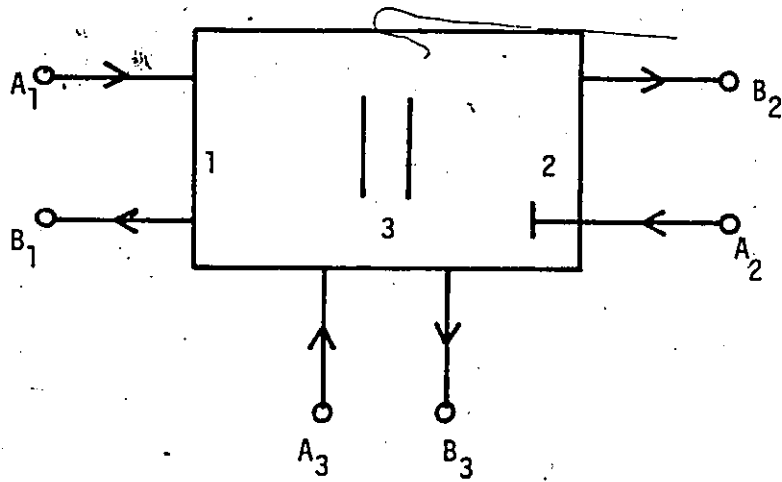
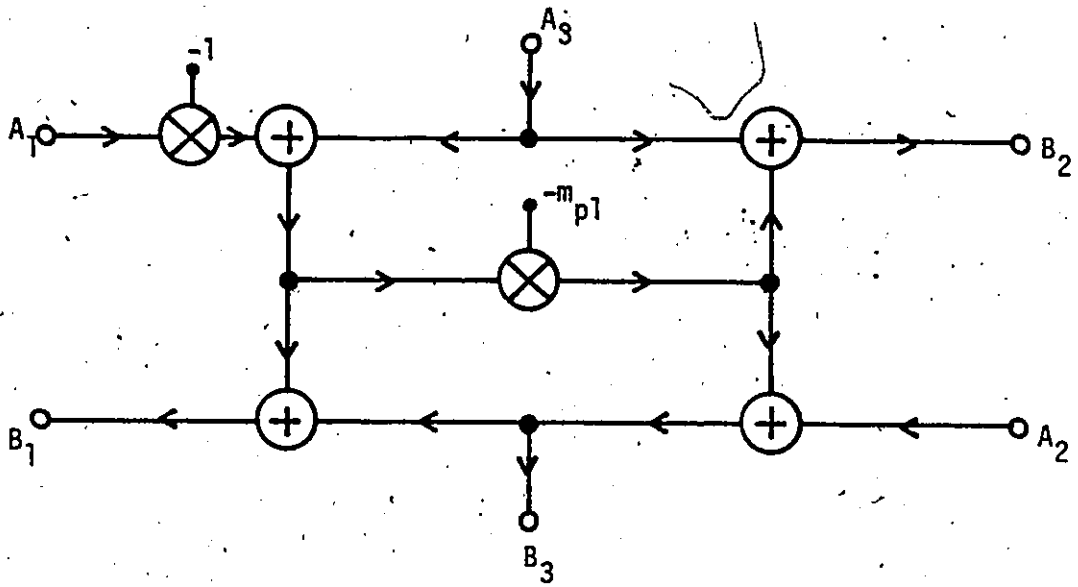


FIG. 1.13 Adaptors

(d) PI-Type Parallel Adaptor

in the second case.

Direct connection between any two adaptor ports will yield a delay-free loop unless one of the ports is a port 2 of adaptor S1 or P1. As was demonstrated by Fettweis [15], delay-free loops lead to unrealizability. Therefore, it is necessary to ensure that every direct connection between adaptor ports involves a port 2 of either an S1 or P1 adaptor.

With digital realizations available for the various analog elements, given an LC filter a corresponding wave digital filter can be obtained by using the following procedure:

- 1) Identify the various series and parallel wire interconnections in the LC filter. Then number the ports such that each and every direct connection between wire interconnection ports involves a port 2.
- 2) Assign port resistances to the wire interconnection ports. For a port terminated by an impedance  $s^\lambda R_x$  ( $\lambda = -1, 0, \text{ or } 1$ ) or by a voltage source with an internal impedance  $s^\lambda R_x$ , assign a port resistance  $(\frac{2}{T})^\lambda R_x$ . Then choose the unspecified port resistances to give as far as possible type S1 and P1 adaptors, ensuring that a common resistance is assigned to any two interconnected ports.
- 3) Calculate the multiplier constants for the various adaptors, using Eqns. 1.8 - 1.11.

- 4) Replace each analog element in the LC filter by its digital realization.

An alternative approach to the synthesis of wave digital filters, was proposed independently by Constantinides [18], [20], [23], and Swamy and Thyagarajan [19], [21], [22]. In this approach the need for adaptors is eliminated.

### 1.3 DIGITAL FILTER IMPERFECTIONS

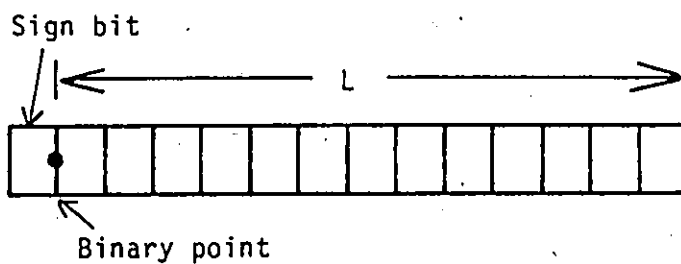
Two common types of arithmetic are used in the implementation of digital filters, namely fixed-point and floating-point. In a fixed-point arithmetic signed numbers are stored in registers such as that illustrated in Fig. 1.14a. Normally, numbers are assumed to be fractional and hence the binary point is fixed just to the right of the first bit location. The first bit is used to represent the sign of the number. The number of significant bits to the right of the binary point, namely  $L$ , is referred to as the wordlength. For a floating-point arithmetic, numbers are assumed to be of the form

$$x = Ae^b$$

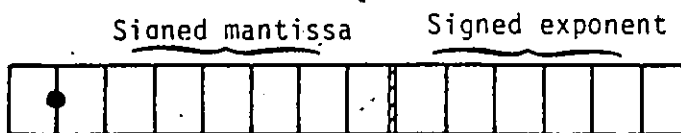
where

$$\frac{1}{2} \leq A < 1$$

$A$  and  $b$  are said to be the mantissa and exponent, respectively. A floating-point number is stored by using two registers, as depicted in Fig. 1.14b.



(a)



(b)

FIG. 1.14 Number Representation

(a) Fixed-Point Arithmetic

(b) Floating-Point Arithmetic

In the implementation of either software or hardware digital filters, a finite wordlength must be employed. Consequently, coefficients and signal values must be quantized. Therefore, once the wordlength  $L$  is assigned, any number consisting of  $b$  bits (excluding the sign bit) where  $b > L$  must be quantized. Number quantization can be accomplished in two ways, as follows:

- a) By truncating all bits that cannot be accommodated in the register. Truncation can be effected by simply disregarding all bits to the right of the  $L$ th bit.
- b) By rounding the number to the nearest machine representable number. Rounding can be effected, by adding 1 at position  $L+1$  and then truncating the number to  $L$  bits.

Quantization in digital filters gives rise to three sources of arithmetic errors, as follows:

- 1) Product quantization errors
- 2) Coefficient quantization errors
- 3) Input quantization errors.

The effect of each of these errors on the filter performance will be briefly discussed in the following sections.

#### Product Quantization

The product resulting from the multiplication of a signal represented by  $N$  digits and a multiplier coefficient represented by  $M$  digits, will have as many as  $N+M$  digits. Since a uniform register

length must in practice be used throughout the filter, the result of each multiplication must be quantized before processing can continue. Hence, quantization errors will arise at the outputs of multipliers. The effect of this quantization is to inject a noise component at the output of the filter.

#### Coefficient Quantization

The transfer function coefficients are normally evaluated to a high degree of accuracy when the required transfer function is derived. If these coefficients are quantized the zero and pole positions will change, and as a result the frequency response of the filter will change. In fact, in very selective filters coefficient quantization can actually cause filter instability.

#### Input Quantization

Input quantization errors arise when digital filters are used to process continuous-time signals. These are the errors inherent in the analog-to-digital conversion. Input quantization like product quantization gives rise to output noise.

### 1.4 COMPARISON OF VARIOUS DIGITAL FILTER STRUCTURES

There are three principal criteria for evaluating and choosing a digital filter structure. These are the sensitivity of the structure to coefficient quantization, the output noise level due to product quantization, and the structure computational efficiency in terms of the number of arithmetic operations. By using these criteria a brief comparison between direct, cascade, parallel, and wave structures can be



made, as follows:

- 1) Direct structures are very sensitive to coefficient quantization [24], [25], and also generate a high level of product-quantization noise [25], [26].
- 2) For the case of fixed-point arithmetic, the sensitivity properties of the cascade, parallel, and wave structures are similar [24], [26]. On the other hand, for floating-point arithmetic, wave structures are superior to the cascade ones [27], [28].
- 3) Wave structures require a higher number of arithmetic operations as compared to cascade or parallel structures [29], while the cascade structures are the most economical [24].

There are some other factors in addition to the above in the choice of structure, like for instance limit-cycle effects, hardware-cost, etc. Parallel structures are not considered in this thesis.

### 1.5 SCOPE OF THE THESIS

This thesis is concerned with the effects of coefficient and product quantization in a class of wave digital filters based on the generalized-immittance converter (GIC). The specific topics discussed may be summarized as follows:

In Chapter 2, a digital realization of the generalized-immittance converter is first derived, by using the wave characterization. Next, five universal digital-filter second-order sections, namely, a

lowpass, a highpass, a bandpass, a notch, and an allpass section are developed. These are then used as building blocks in a cascade digital-filter synthesis which we shall refer to as the GIC synthesis. The synthesis is illustrated by designing four digital filters, namely, a Butterworth lowpass filter, an elliptic bandstop filter, an elliptic bandpass filter, and a delay equalizer. All these filters are also designed by using the cascade canonic synthesis of Section 1.2.3. In addition, the first three of these filters, are also designed by using the wave synthesis of Section 1.2.5. The three synthesis are compared on the basis of the number of arithmetic operations, the speed of processing a signal, and the degree of parallelism.

Chapter 3 deals with signal scaling and with the effects of product quantization. A signal scaling technique due to Jackson is described which can be used to optimize the signal-to-noise ratio. This is then applied to the various digital filters designed in Chapter 2. The effect of product quantization in these filters is then studied. Chapter 3 concludes with a comparison between the GIC synthesis and the cascade canonic and wave syntheses.

Next in Chapter 4, a sensitivity analysis for digital filter is described. Then, a procedure for evaluating the exact wordlength is presented. Subsequently, a statistical approach due to Crochiere is discussed, which can be used to estimate the required wordlength. By using these procedures, coefficient wordlengths are obtained for the digital filters designed in Chapter 2. Finally, a comparison of GIC, cascade canonic and wave syntheses is made on the bases of sensitivity and wordlength.

The highpass filter is not considered any further in the thesis because it is the image of the lowpass filter.

## CHAPTER 2

### A WAVE DIGITAL FILTER SYNTHESIS BASED ON GIC'S

#### 2.1 INTRODUCTION

In Chapter 1, two general types of digital-filter synthesis procedures have been described, namely, direct and indirect procedures. This Chapter describes an alternative indirect cascade synthesis procedure [30]. The basis of the synthesis is an analog configuration comprising of resistors and generalized-immittance converters (GIC's).

By using the wave characterization, a digital realization of the generalized-immittance converter is first derived in Section 2.2. Then, a set of universal digital-filter second-order sections is obtained. This set consists of five universal sections, namely, a lowpass, a highpass, a bandpass, a notch, and an allpass section.

The synthesis is illustrated by designing, a Butterworth lowpass filter, an elliptic bandpass filter, an elliptic bandstop filter, and a delay equalizer. The GIC synthesis is subsequently compared with the cascade canonic synthesis as well as the wave synthesis of Sedımeıyer and Fettweis (see Section 1.2.5) on the basis of the number of arithmetic operations, the speed of processing a signal, and the degree of parallelism.

#### 2.2 GENERAL SECOND-ORDER SECTION

In this section, a brief review of the current-conversion GIC and the basic analog R-GIC configuration are given. We start with the

concept of the GIC.

### 2.2.1 The Current-Conversion GIC

The GIC is a 2-port network in which the input admittance  $Y_i$  is related to the load admittance  $Y_L$  by the relation

$$Y_i = h(s) Y_L$$

Function  $h(s)$  is said to be the admittance conversion function of the device. Two types of GIC can be identified, namely, the current-conversion GIC (CGIC) and the voltage conversion GIC (VGIC). The CGIC is characterized by the relations

$$V_1 = V_2, \quad I_1 = -h(s)I_2 \quad (2.1)$$

The VGIC on the other hand, is characterized by the relations

$$I_1 = -I_2, \quad V_1 = h(s)V_2$$

The CGIC is usually represented by the symbol of Fig. 2.1a. This has been used extensively in the past in the synthesis of analog filters [31]-[36]. The intention in this thesis is to use the CGIC in the synthesis of digital filters.

### 2.2.2 Analog R-GIC Configuration

Consider the configuration of Fig. 2.2 where each CGIC has a conversion function  $h(s) = s$ . By analyzing this circuit we can show that

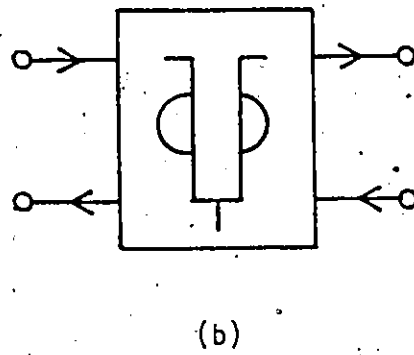
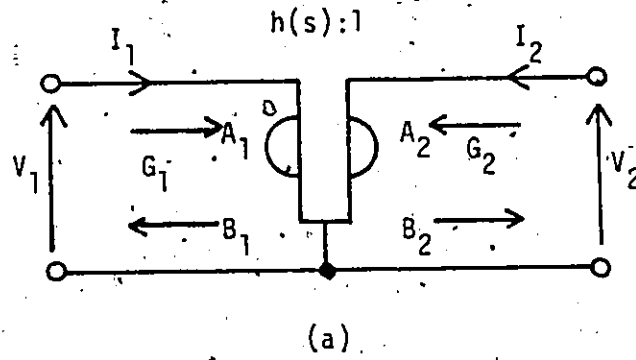


FIG. 2.1 CGIC Wave Representation

(a) Wave Characterization of the CGIC

(b) Wave Digital Representation of the CGIC

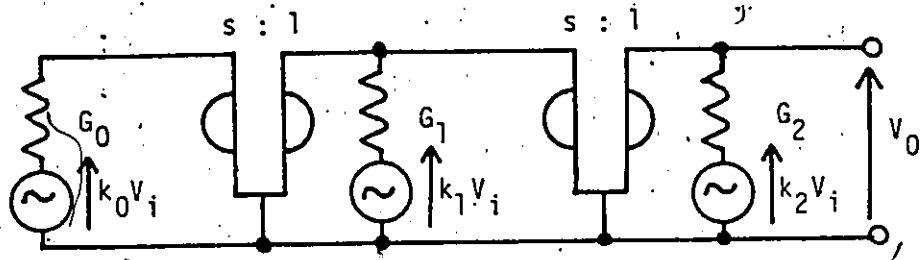


FIG. 2.2 General Second-Order R-GIC Analog Configuration

$$\frac{V_o}{V_i} = \frac{k_0 G_0 + k_1 G_1 s + k_2 G_2 s^2}{G_0 + G_1 s + G_2 s^2}$$

Hence if  $G_r = b_r$ ,  $k_r = a_r/b_r$  for  $r = 0,1,2$  the network of Fig. 2.2 realizes the transfer function

$$H(s) = \frac{a_0 + a_1 s + a_2 s^2}{b_0 + b_1 s + b_2 s^2}$$

Any stable transfer function can be realized by cascading a number of network sections such as that in Fig. 2.2.

### 2.2.3 Digital R-GIC Configuration

As was shown in Section 1.2 digital realization can be derived for conductances, voltage sources and wire interconnection (see Figs. 1.13a-1.13d, and Tables 1.2-1.3). The same technique can be extended to the CGIC of Fig. 2.1a. The CGIC can be represented by the relations

$$\left. \begin{aligned} -A_k &= V_k + I_k/G_k \\ B_k &= V_k - I_k/G_k \end{aligned} \right\} \quad (2.2)$$

where  $A_k$  and  $B_k$  are the incident and reflected wave quantities respectively, while  $G_k$  is the port conductance assigned to the  $k$ th port ( $k = 1$  or  $2$ ). By transforming variables  $A_k$ ,  $B_k$ ,  $V_k$  and  $I_k$  employing the bilinear transformation

$$s \rightarrow \frac{2}{T} \frac{z-1}{z+1} \quad (2.3)$$

and then using Eqns. 2.1-2.3 we can show that

$$B_1 = A_2 + (A_1 - A_2)F(z)$$

$$B_2 = A_1 + (A_1 - A_2)F(z)$$

where

$$F(z) = \frac{G_1 - G_2}{G_1 + G_2} \frac{h(z)}{h(z)} \quad (2.4)$$

$$h_D(z) \equiv h(s) \quad s \rightarrow \frac{2}{T} \frac{(z-1)}{(z+1)}$$

With  $h(s) = s$  and  $G_1 = 2G_2/T$ , Eqn. 2.4 simplifies to

$$F(z) = z^{-1}$$

A digital realization for a CGIC can thus be deduced as in Fig. 2.3.

Given an interconnection of analog  $n$ -ports, a corresponding digital network can be derived by using the wave synthesis described in Section 1.2.5. Suitable port conductances are first assigned to the ports of the individual  $n$ -ports; subsequently, each  $n$ -port is replaced one-for-one by its digital realization.

Considering the R-GIC configuration of Fig. 2.2, the individual  $n$ -ports can be identified as shown in Fig. 2.4a. Now by assigning the port conductances

$$G_{1A} = TG_0/2, \quad G_{2A} = 2G_2/T, \quad G_{3A} = G_1$$

the general second-order digital section of Fig. 2.4b is derived.



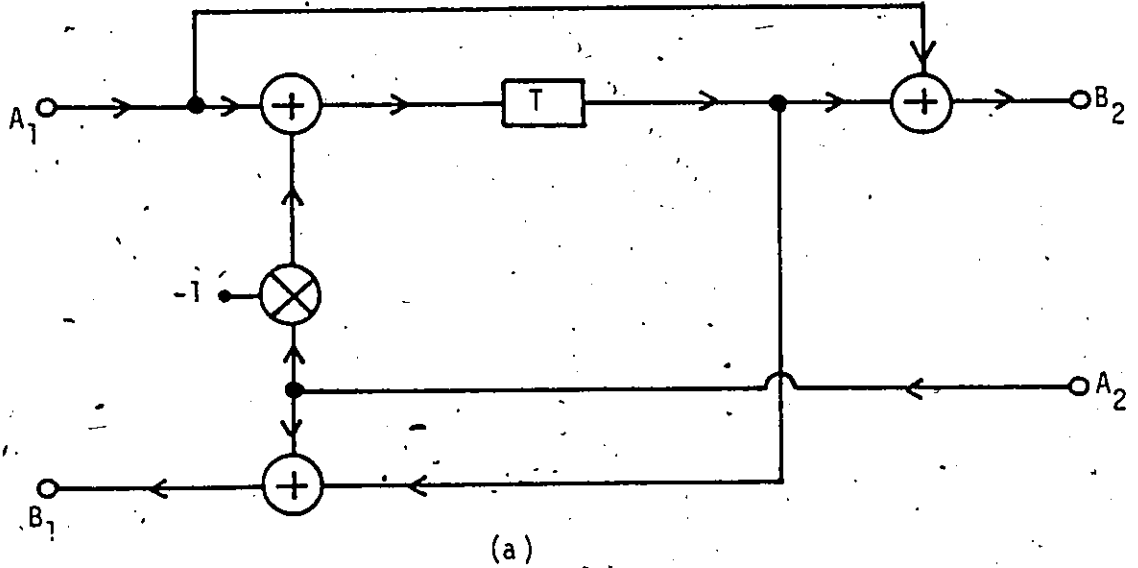


FIG. 2.3 Digital Realization of the CGIC with  $h(s) = s$

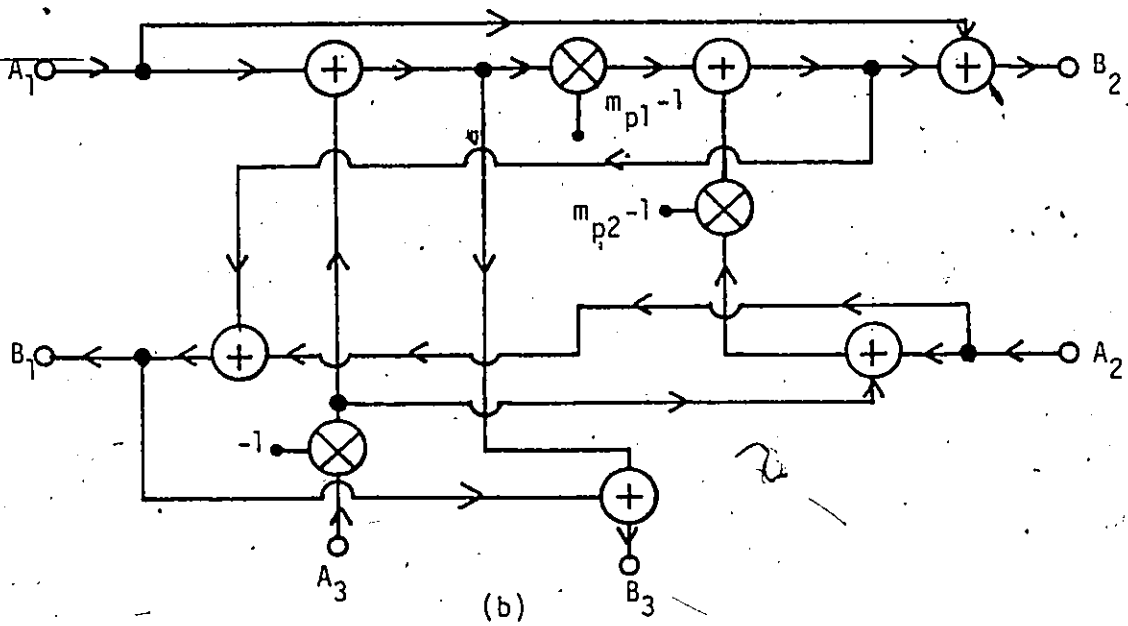


FIG. 2.3 Type-P2 Adaptor

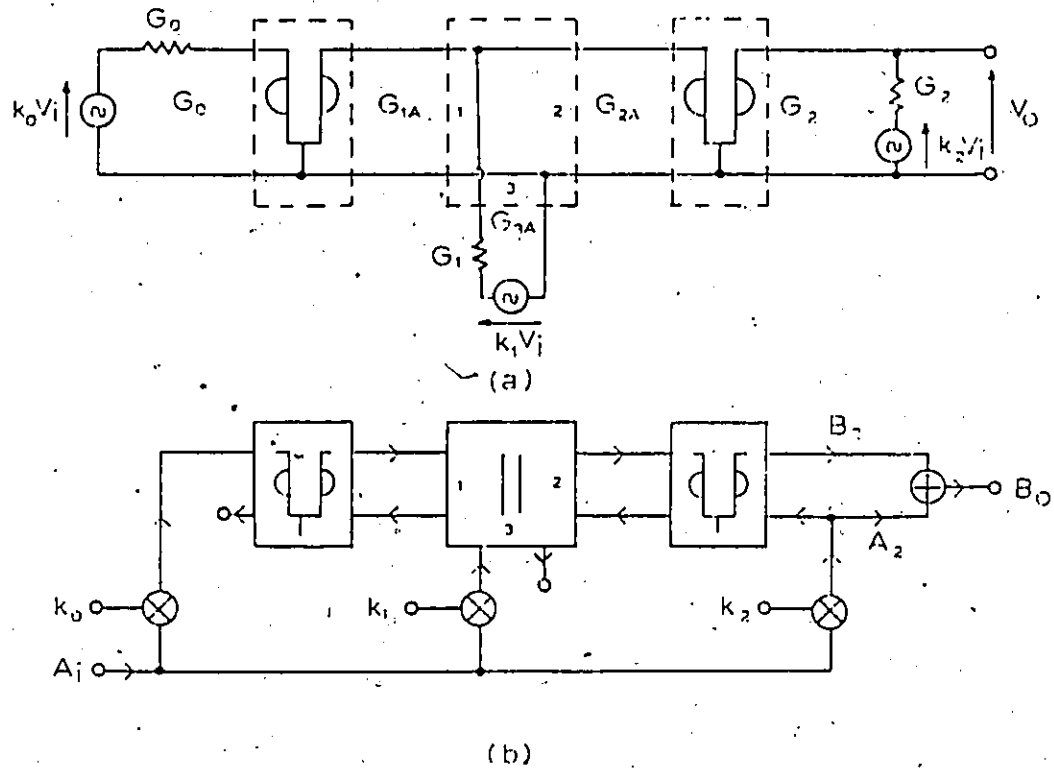


FIG. 2.4 General Second-Order Digital GIC Section

(a) Identification of Individual n-ports wire Interconnection of Fig. 2.2

(b) Digital Realization of Fig. 2.2

An output proportional to  $V_o$  can be formed by using an adder at the input or output of any one of the CGIC's, as in Fig. 2.4b, or at port 3 of the adaptor. This is permissible by virtue of Eqn. 2.1. The transfer function of the derived structure can be obtained from Eqns. 2.1-2.3 as

$$\begin{aligned} H_D(z) &= \frac{B_o}{A_i} = \frac{B_2 + A_2}{A_i} = \frac{2V_o}{V_i} \\ &= 2H(s) \\ s &\rightarrow \frac{2}{T} \frac{(z-1)}{(z+1)} \end{aligned}$$

The realization of Fig. 2.4b, like any other realization based on the bilinear transformation, is subject to the well-known warping effect [9], [10].

### 2.3 REALIZATION OF ANY TRANSFER FUNCTION USING THE GIC SYNTHESIS

Recursive filters are mostly designed by using Butterworth, Tschebycheff, Bessel or elliptic transfer functions which have zeros at the origin of the  $s$  plane, on the imaginary axis or at infinity [36]-[39]. Hence the continuous-time transfer function can be realized as a cascade connection of second-order filter sections characterized by transfer functions of the type

$$H_A(s) = \frac{N_A(s)}{b_0 + b_1 s + s^2}$$

where  $N_A(s)$  can take the form  $b_0$ ,  $s^2$ ,  $b_1 s$  or  $a_0 + s^2$  for a lowpass (LP), highpass (HP), bandpass (BP) or notch (N) section, respectively. Delay equalizers, on the other hand, are designed by using allpass (AP)

sections in which

$$H_A(s) = \frac{b_0 - b_1 s + s^2}{b_0 + b_1 s + s^2}$$

By using the type P2 adaptor of Fig. 2.3b in the configuration of Fig. 2.4b, the above second-order transfer functions can be readily realized as shown in Fig. 2.5 where

$$k_0 = \frac{a_0}{b_0} \quad (2.5)$$

$$m_1 = \frac{\{b_0 - (\frac{z}{T}) b_1 - (\frac{z}{T})^2\}}{\{b_0 + (\frac{z}{T}) b_1 + (\frac{z}{T})^2\}} \quad (2.6)$$

$$m_2 = - \frac{\{b_0 + (\frac{z}{T}) b_1 - (\frac{z}{T})^2\}}{\{b_0 + (\frac{z}{T}) b_1 + (\frac{z}{T})^2\}} \quad (2.7)$$

in each section.

With a set of universal sections available, any standard filter or equalizer can now be designed by using the following procedure:

- 1) Factorize and prewarp the continuous-time transfer function [40]-[42].
- 2) Select suitable sections from Fig. 2.5
- 3) Calculate the multiplier constants using Eqns. 2.5-2.7.
- 4) Connect the various sections in cascade.

Note that the number of unit delays is minimal in each section.

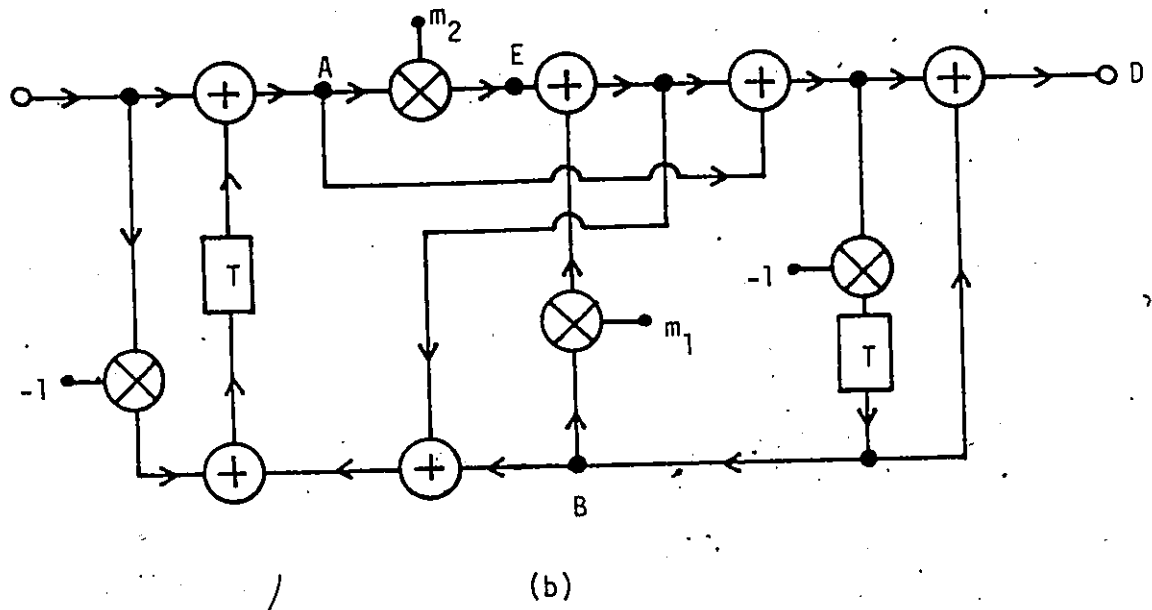
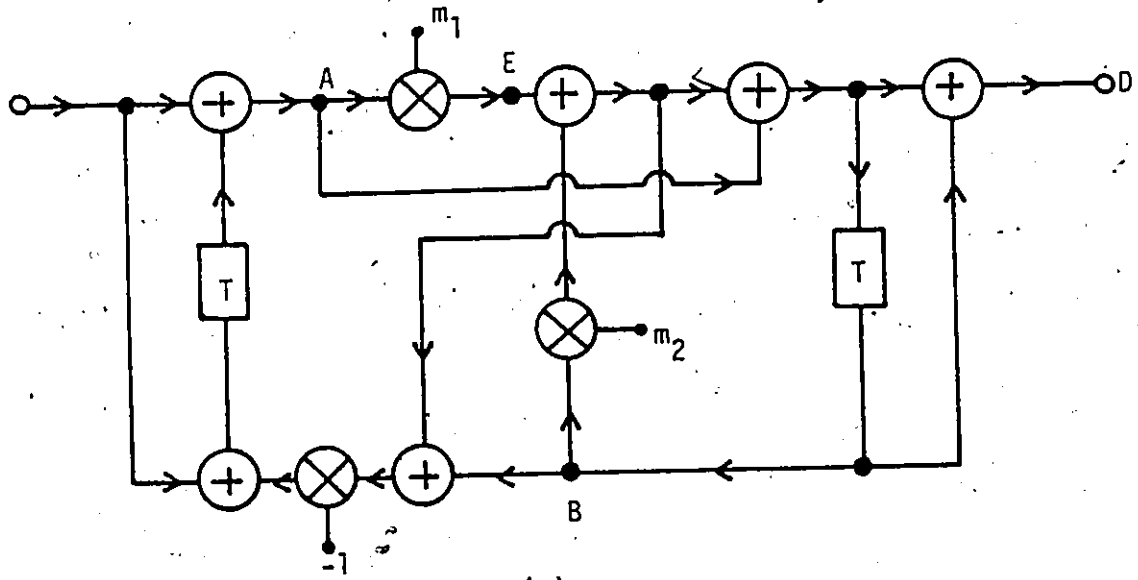
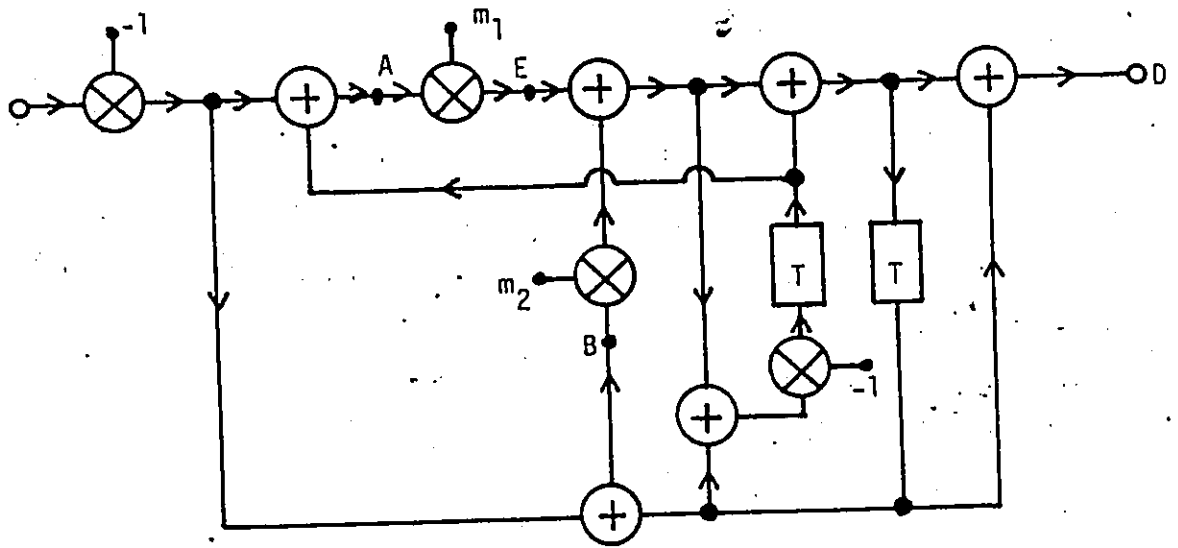
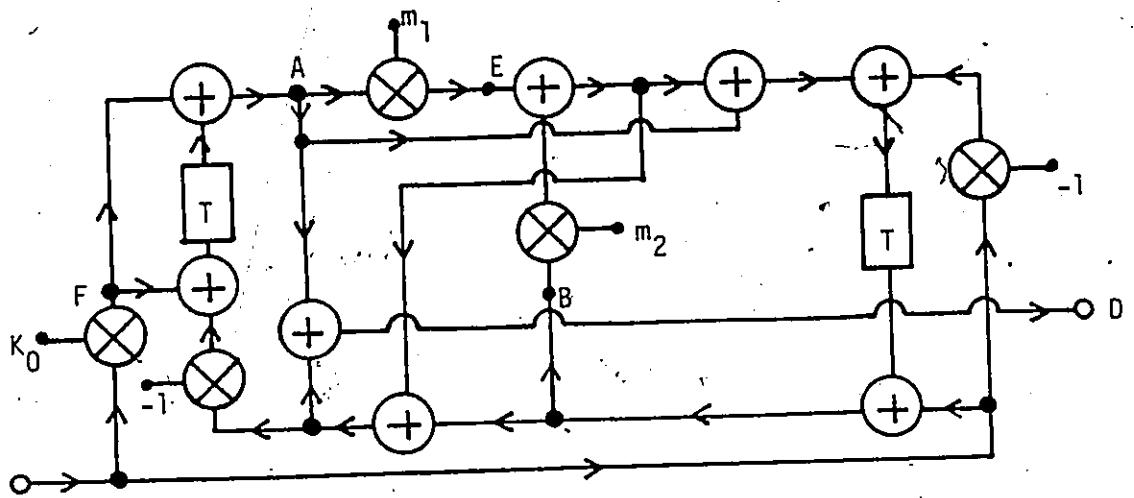


FIG. 2.5 Universal Second-Order Digital GIC Sections  
(a) Lowpass Section  
(b) Highpass Section



(c)



(d)

FIG. 2.5 Universal Second-Order Digital GIC Sections

(c) Bandpass Section

(d) Notch Section

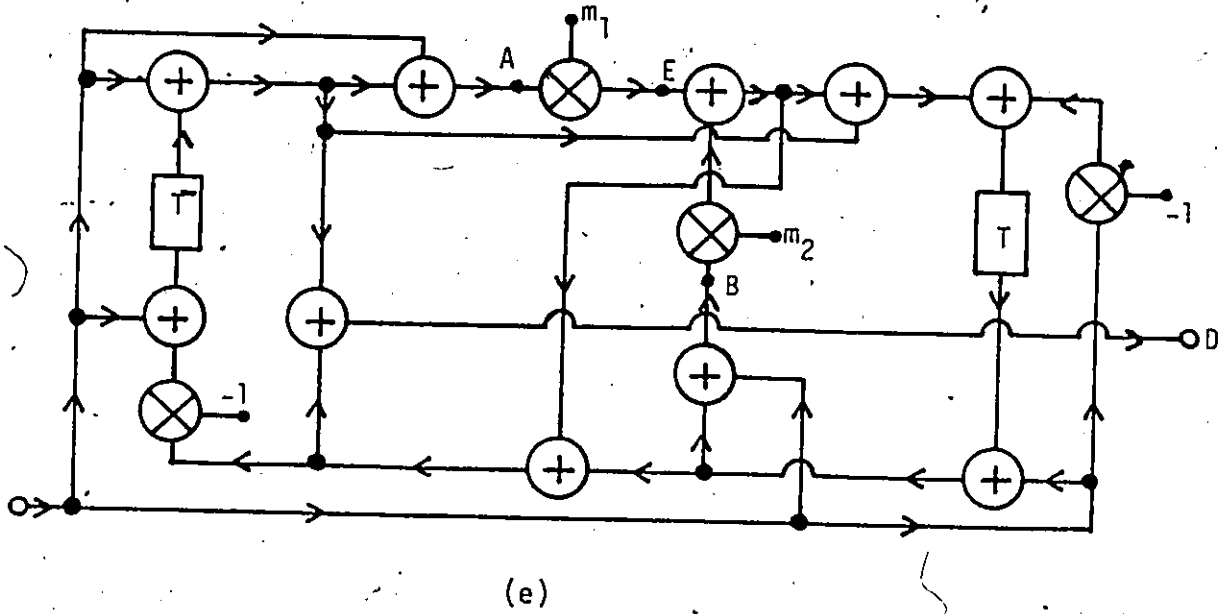


FIG. 2.5 Universal Second-Order Digital GIC Sections

(e) Allpass Section

## 2.4 DESIGN EXAMPLES

For the sake of comparison, the GIC synthesis as well as the conventional cascade canonic synthesis were used to design a number of 6th-order filters, as follows:

- 1) A lowpass, Butterworth filter with a 3-dB cutoff frequency of  $10^3$  rad/s. The sampling frequency was  $10^4$  rad/s.
- 2) A bandstop, elliptic filter with the following specifications:
  - Passband ripple : 1.0 dB
  - Minimum stopband loss : 73.13 dB
  - Passband edges : 3.0, 6.0 rad/s
  - Stopband edges : 4.3, 4.7 rad/s
  - $\omega_s$  : 18 rad/s.
- 3) A bandpass, elliptic filter with the following specifications:
  - Passband ripple : 0.3 dB
  - Minimum stopband loss : 38.7 dB
  - Passband edges : 0.983, 1.018 rad/s
  - Stopband edges : 0.952, 1.051 rad/s
  - $\omega_s$  :  $2.4\pi$  rad/s.
- 4) A delay equalizer for the above bandpass filter.  
The sampling frequency was  $2.4\pi$  rad/s.



The above filters, with the exception of the equalizer, were also designed by using the wave synthesis of Sedlmeyer and Fettweis described in Section 1.2.5.

The continuous-time transfer functions of the various filters are given by

$$H(s) = \prod_{j=1}^3 \frac{a_{0j} + a_{1j}s + a_{2j}s^2}{b_{0j} + b_{1j}s + s^2} \quad (2.8)$$

where  $a_{ij}$  and  $b_{1j}$  are given in Tables 2.1-2.4. The canonic sections employed are shown in Fig. 2.6.

According to the transfer function of Eqn. 2.8 and Table 2.1, the Butterworth lowpass filter can be designed by cascading three LP sections of the type shown in Fig. 2.5a, as illustrated in Fig. 2.7a. The multiplier coefficients of each section can be computed as in Table 2.5 by using the expressions in Eqns. 2.6-2.7.

The same procedure can be applied to the other filters. The realizations for the bandstop, bandpass and allpass filters are given in Figs. 2.7b-2.7d in the form of block diagrams. The values of the multiplier constants for these filters can be calculated as in Tables 2.6-2.8, by using Eqns. 2.5-2.7.

The cascade canonic realizations are obtained by using the canonic sections of Fig. 2.6. The multiplier constants for these realizations are given in Tables 2.9-2.12.

TABLE 2.1 LOWPASS FILTER PARAMETERS

j	$b_{0j}$	$b_{1j}$
1	$1.069676 \times 10^6$	$5.353680 \times 10^2$
2	$1.069676 \times 10^6$	$1.462653 \times 10^3$
3	$1.069676 \times 10^6$	$1.998021 \times 10^3$

$$a_{0j} = b_{0j}, \quad a_{1j} = 0, \quad a_{2j} = 0$$

TABLE 2.2 BANDSTOP FILTER PARAMETERS

j	$a_{0j}$	$b_{0j}$	$b_{1j}$
1	$3.282806 \times 10$	$3.282806 \times 10$	$1.332661 \times 10$
2	$3.705629 \times 10$	$9.644825 \times 10$	2.435375
3	$2.908229 \times 10$	$1.117368 \times 10$	$8.289280 \times 10^{-1}$

$$a_{1j} = 0, \quad a_{2j} = 1$$

TABLE 2.3 BANDPASS FILTER PARAMETERS

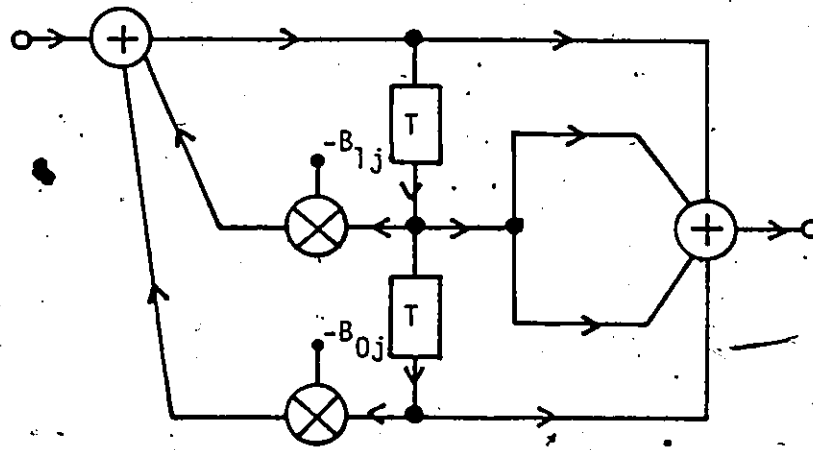
j	$a_{0j}$	$b_{0j}$	$b_{1j}$
1	1.279553	1.178123	$1.455204 \times 10^{-2}$
2	$9.948942 \times 10^{-1}$	1.080529	$1.393597 \times 10^{-2}$
3	0	1.128254	$3.271554 \times 10^{-2}$

$$a_{11} = a_{12} = 0, a_{21} = a_{22} = 1, a_{23} = 0, a_{13} = 4.229751 \times 10^{-3}$$

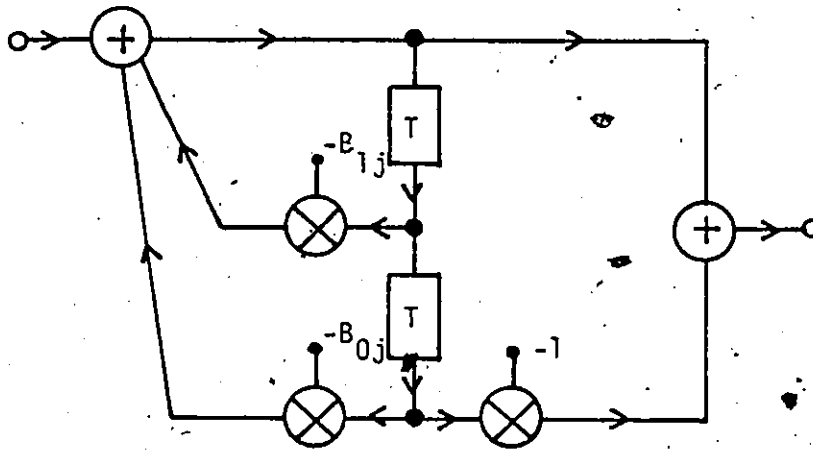
TABLE 2.4 DELAY EQUALIZER PARAMETERS

j	$b_{0j}$	$b_{1j}$
1	$2.90791 \times 10^2$	$2.96640 \times 10^2$
2	$3.71481 \times 10^2$	$5.05382 \times 10^2$
3	$4.27979 \times 10^2$	$5.88548 \times 10^2$

$$a_{0j} = b_{0j}, a_{1j} = -b_{1j}, a_{2j} = 1$$



(a)

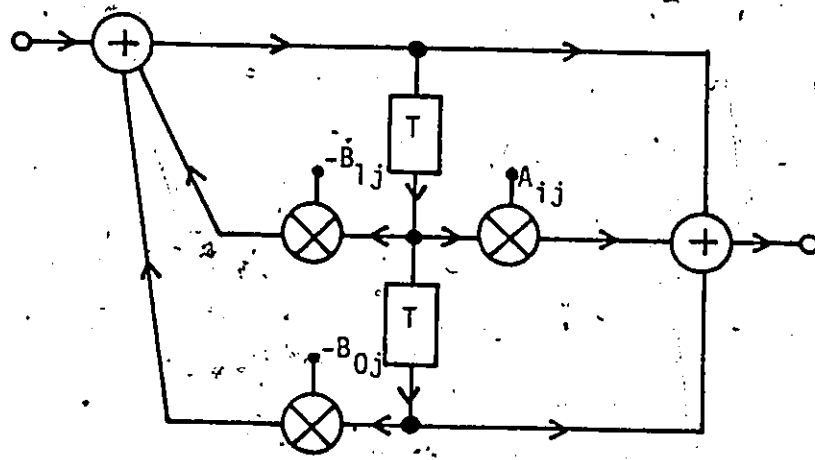


(b)

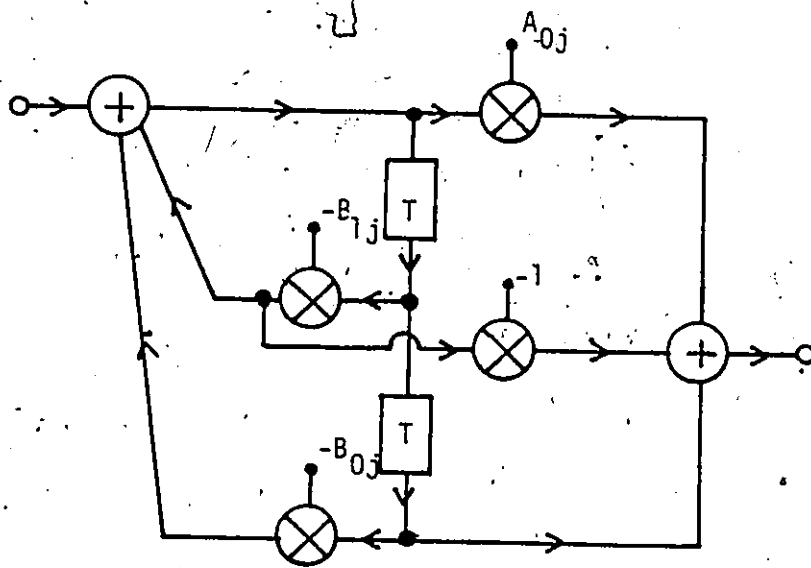
FIG. 2.6 Canonic Second-Order Sections

(a) Lowpass Section

(b) Bandpass Section



(c)

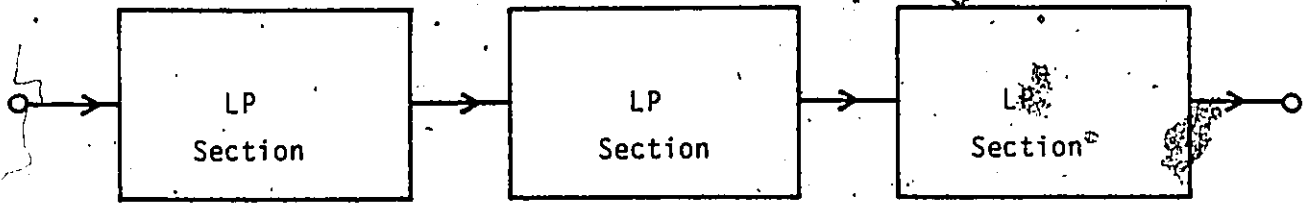


(d)

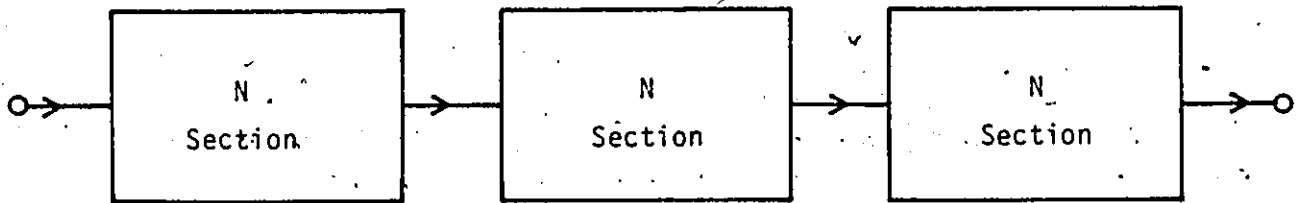
FIG. 2.6 Canonic Second-Order Sections

(c) Notch Section

(d) Allpass Section



(a)

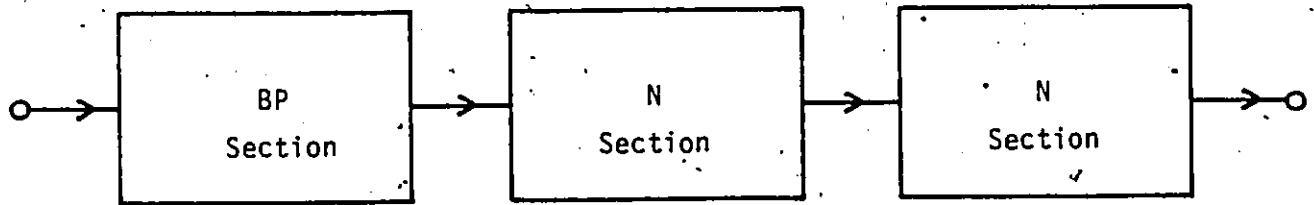


(b)

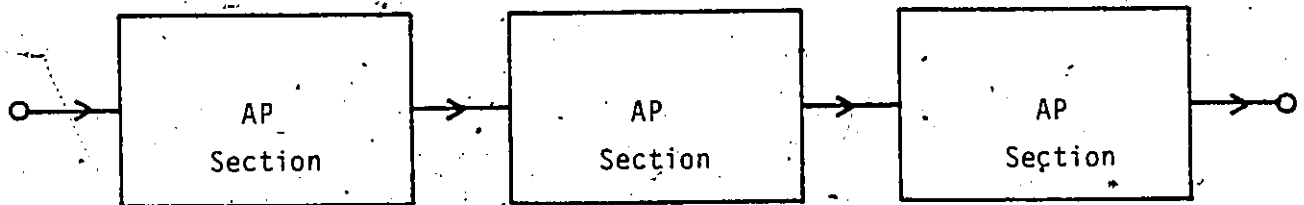
FIG. 2.7 Block Diagram Representations of the Lowpass Filter, Bandstop Filter, Bandpass Filter and the Delay Equalizer

(a) Lowpass Filter

(b) Bandstop Filter



(c)



(d)

FIG. 2.7 Block Diagram Representations of the Lowpass Filter, Bandstop Filter, Bandpass Filter and the Delay Equalizer

(c) Bandpass Filter

(d) Delay Equalizer

TABLE 2.5 LOWPASS FILTER PARAMETERS (GIC SYNTHESIS)

j	$m_{1j}$	$m_{2j}$
1	$-8.34235 \times 10^{-1}$	$5.70150 \times 10^{-1}$
2	$-8.65090 \times 10^{-1}$	$2.77891 \times 10^{-1}$
3	$-8.78181 \times 10^{-1}$	$1.53889 \times 10^{-1}$

TABLE 2.6 BANDSTOP FILTER PARAMETERS (GIC SYNTHESIS)

j	$m_{1j}$	$m_{2j}$
1	$-5.37672 \times 10^{-1}$	$-5.37672 \times 10^{-1}$
2	$3.46761 \times 10^{-1}$	$-5.41604 \times 10^{-1}$
3	$-5.41604 \times 10^{-1}$	$3.46761 \times 10^{-1}$



TABLE 2.7 BANDPASS FILTER PARAMETERS (GIC SYNTHESIS)

j	$m_{1j}$	$m_{2j}$
1	$-6.62093 \times 10^{-1}$	$6.52075 \times 10^{-1}$
2	$-6.85617 \times 10^{-1}$	$6.75886 \times 10^{-1}$
3	$-6.76104 \times 10^{-1}$	$6.53564 \times 10^{-1}$

TABLE 2.8 DELAY EQUALIZER PARAMETERS (GIC SYNTHESIS)

j	$m_{1j}$	$m_{2j}$
1	$-6.75325 \times 10^{-1}$	$6.48386 \times 10^{-1}$
2	$-6.68576 \times 10^{-1}$	$6.47733 \times 10^{-1}$
3	$-6.82027 \times 10^{-1}$	$6.63578 \times 10^{-1}$

TABLE 2.9 LOWPASS FILTER PARAMETERS (CASCADE CANONIC SYNTHESIS)

j	$B_{0j}$	$B_{1j}$
1	0.7359	-1.4044
2	0.4128	-1.1430
3	0.2757	-1.0321

TABLE 2.10 BANDSTOP FILTER PARAMETERS (CASCADE CANONIC SYNTHESIS)

j	$A_{1j}$	$B_{0j}$	$B_{1j}$
1	$0.1700 \times 10^{-7}$	$0.7859 \times 10^{-8}$	-0.0753
2	0.1210	0.8884	0.8052
3	-0.1210	-0.8884	0.8052

TABLE 2.11 BANDPASS FILTER PARAMETERS (CASCADE CANONIC SYNTHESIS)

j	$A_{1j}$	$B_{0j}$	$B_{1j}$
1	0	0.9775	-1.3297
2	-1.2737	0.98998	-1.3141
3	-1.4109	0.9903	-1.3615

TABLE 2.12 DELAY EQUALIZER PARAMETERS (CASCADE CANONIC SYNTHESIS)

j	$B_{0j}$	$B_{1j}$
1	0.9731	-1.3237
2	0.9792	-1.3163
3	0.9816	-1.3456

$$A_{0j} = B_{0j}$$

Wave realizations for the Butterworth lowpass filter, the bandstop elliptic filter, and the bandpass elliptic filter can be obtained by using the following two steps:

- 1) Design a prewarped LC filter for each case.
- 2) Use the wave realization procedure described in Section 1.2.5:

The prewarped LC filter for each can be obtained by using a procedure described by Antoniou in [43]. For the case of the lowpass Butterworth filter the prewarped LC filter is given in Fig. 2.8a, where

$$\begin{aligned} C_1 &= 0.5176 \text{ F} & C_3 &= 1.9319 \text{ F} \\ C_5 &= 1.4142 \text{ F} & L_2 &= 1.4142 \text{ H} \\ L_4 &= 1.9319 \text{ H} & L_6 &= 0.5176 \text{ H} \\ R &= 1.0 \Omega \end{aligned}$$

From step 1 of the design procedure, the wire interconnections can be identified as illustrated in Fig. 2.8b. Hence, from steps 2 and 3, the design can be accomplished as shown below. In this design  $G_{ij}(R_{ij})$  is the port conductance (resistance) assigned to the  $i$ th port of the  $j$ th wire interconnection.

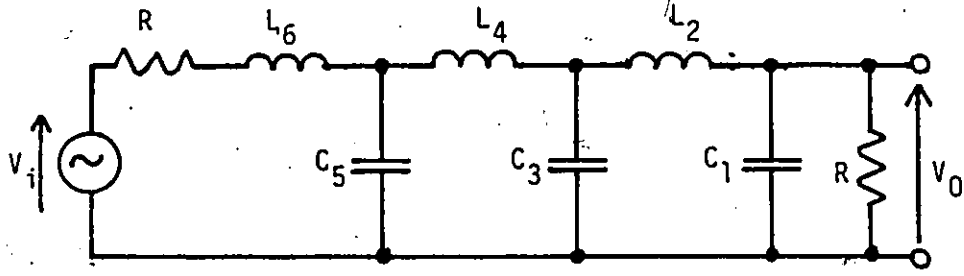
Series Interconnection # 1

$$R_{11} = R = 1.0$$

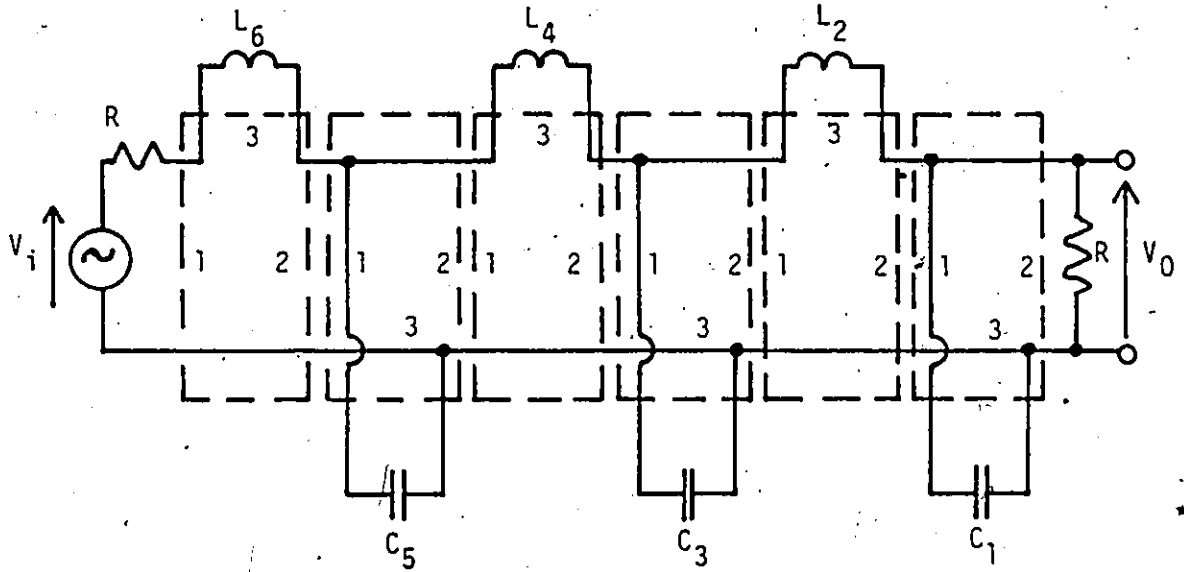
$$R_{31} = \frac{2}{T} L_6 = 1.59301$$

$$R_{21} = R_{11} + R_{31} = 2.59301$$

Hence from Eqn. 1.8



(a)

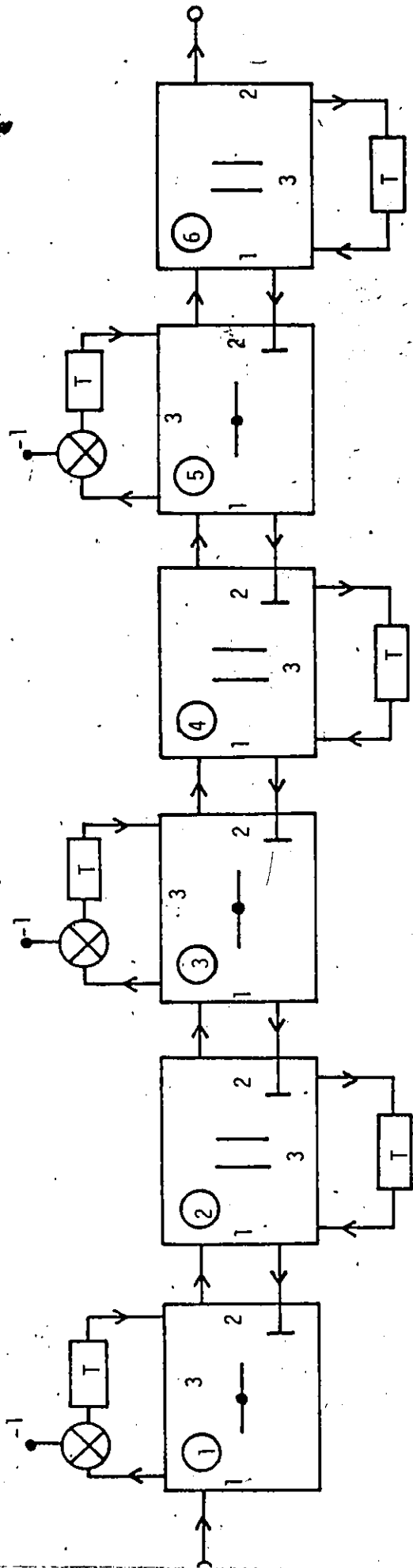


(b)

FIG. 2.8 Butterworth 6th-Order Lowpass Wave Digital Filter

(a) Prewarped Doubly Terminated LC Filter

(b) Identification of Wire Interconnection



(c)

FIG. 2.8 Butterworth 6th-Order Lowpass Wave Digital Filter

(c) Wave Digital Realization

$$m_{s1} = \frac{R_{11}}{R_{21}} = 0.38565$$

Parallel Interconnection # 2

$$G_{12} = \frac{1}{R_{21}} = 0.38565$$

$$G_{32} = \frac{2}{T} C_5 = 4.35247$$

$$G_{22} = G_{12} + G_{32} = 4.73813$$

Hence from Eqn. 1.10

$$m_{p1} = \frac{G_{12}}{G_{22}} = 0.08139$$

Series Interconnection # 3

$$R_{13} = \frac{1}{G_{22}} = 0.21105$$

$$R_{33} = \frac{2}{T} L_4 = 5.9458$$

$$R_{23} = R_{13} + R_{33} = 6.15683$$

$$m_{s1} = \frac{R_{13}}{R_{23}} = 0.03428$$

Parallel Interconnection # 4

$$G_{14} = \frac{1}{R_{23}} = 0.16242$$

$$G_{34} = \frac{2}{T} C_3 = 5.94577$$

$$G_{24} = G_{14} + G_{34} = 6.10819$$

$$m_{p1} = \frac{G_{14}}{G_{24}} = 0.02659$$

Series Interconnection # 5

$$R_{15} = \frac{1}{G_{24}} = 0.16371$$

$$R_{35} = \frac{2}{T} L_2 = 4.35247$$

$$R_{25} = R_{15} + R_{35} = 4.51619$$

$$m_{s1} = \frac{R_{15}}{R_{25}} = 0.03625$$

Parallel Interconnection # 6

$$G_{16} = \frac{1}{R_{25}} = 0.22143$$

$$G_{36} = \frac{2}{T} C_1 = 1.59301$$

$$G_{26} = 1.0$$

Hence from Eqns. 1.10-1.11

$$m_{p1} = \frac{2G_{16}}{G_{16} + G_{26} + G_{36}} = 0.15735$$

$$m_{p2} = \frac{2G_{26}}{G_{16} + G_{26} + G_{36}} = 0.71062$$

The adaptors for interconnections 1,3, and 5 are of type S1 , for interconnections 2, and 4 are of type P1 , and for interconnection 6 is of type P2 . These adaptors are given in Figs. 1.13a-1.13d. Replacing each analog element in Fig. 2.8b with its digital realization, according to step 4, results in the wave digital filter shown in Fig. 2.8c.



For the case of the bandstop elliptic filter, the prewarped LC bandstop filter is given in Fig. 2.9a. The identification of wire interconnections is shown in Fig. 2.9b, and the complete wave digital filter is given in Fig. 2.9c. Similarly, for the bandpass elliptic filter, the prewarped LC bandpass filter is given in Fig. 2.10a, the identification of wire interconnections is illustrated in Fig. 2.10b, while the complete wave digital filter is given in Fig. 2.10c. The multiplier constants for both bandstop and bandpass filters are calculated by using the expression in Eqns. 1.8-1.11, as shown in Tables 2.13-2.14.

## 2.5 GENERAL COMPARISON

One of the principal factors in evaluating a digital filter structure is its computational efficiency. The computational efficiency entails three basic criteria, namely, the number of arithmetic operations, the speed of processing a signal, and the degree of parallelism. Using these criteria, a comparison can now be made between GIC, cascade canonic, and wave structures.

### 2.5.1 Number of Arithmetic Operation

The number of arithmetic operations for the various filter structures obtained in Section 2.4 are tabulated in Table 2.15. As can be seen, the lowpass and bandpass canonic structures are more economical than the corresponding GIC structures, although the difference is marginal in the case of the lowpass filter (one addition per section).

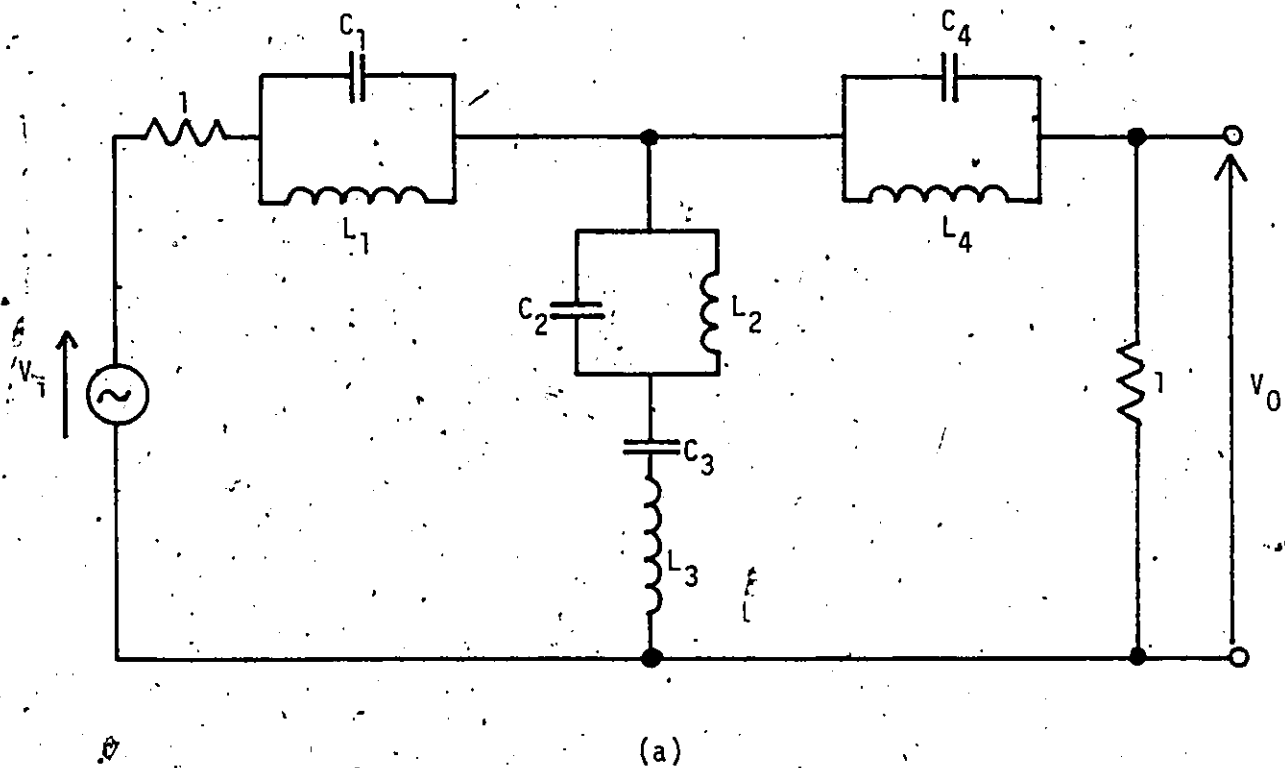


FIG. 2.9 Elliptic 6th-Order Bandstop Wave Digital Filter

(a) Prewarped Doubly Terminated LC Bandstop Filter

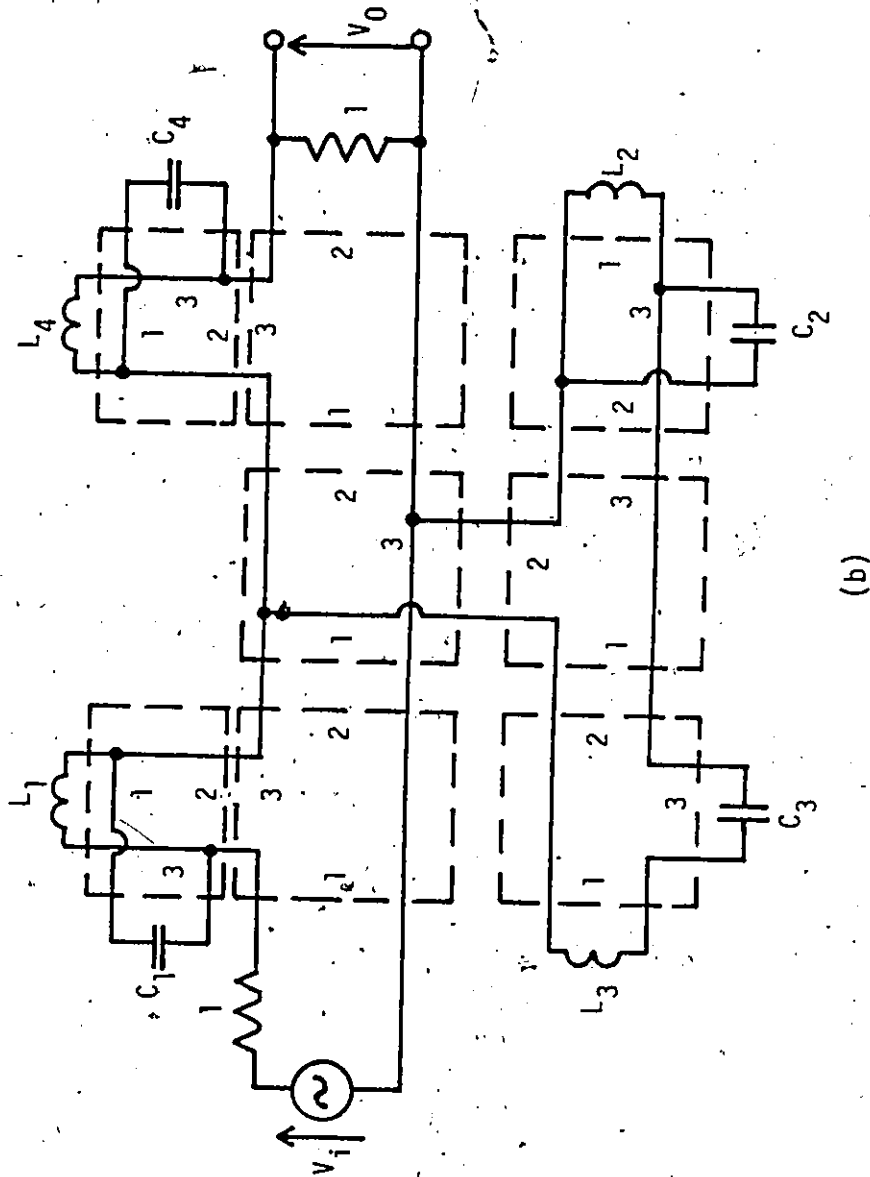


FIG. 2.9 Elliptic 6th-Order Bandstop Wave Digital Filter

(b) Identification of Wire Interconnection

R

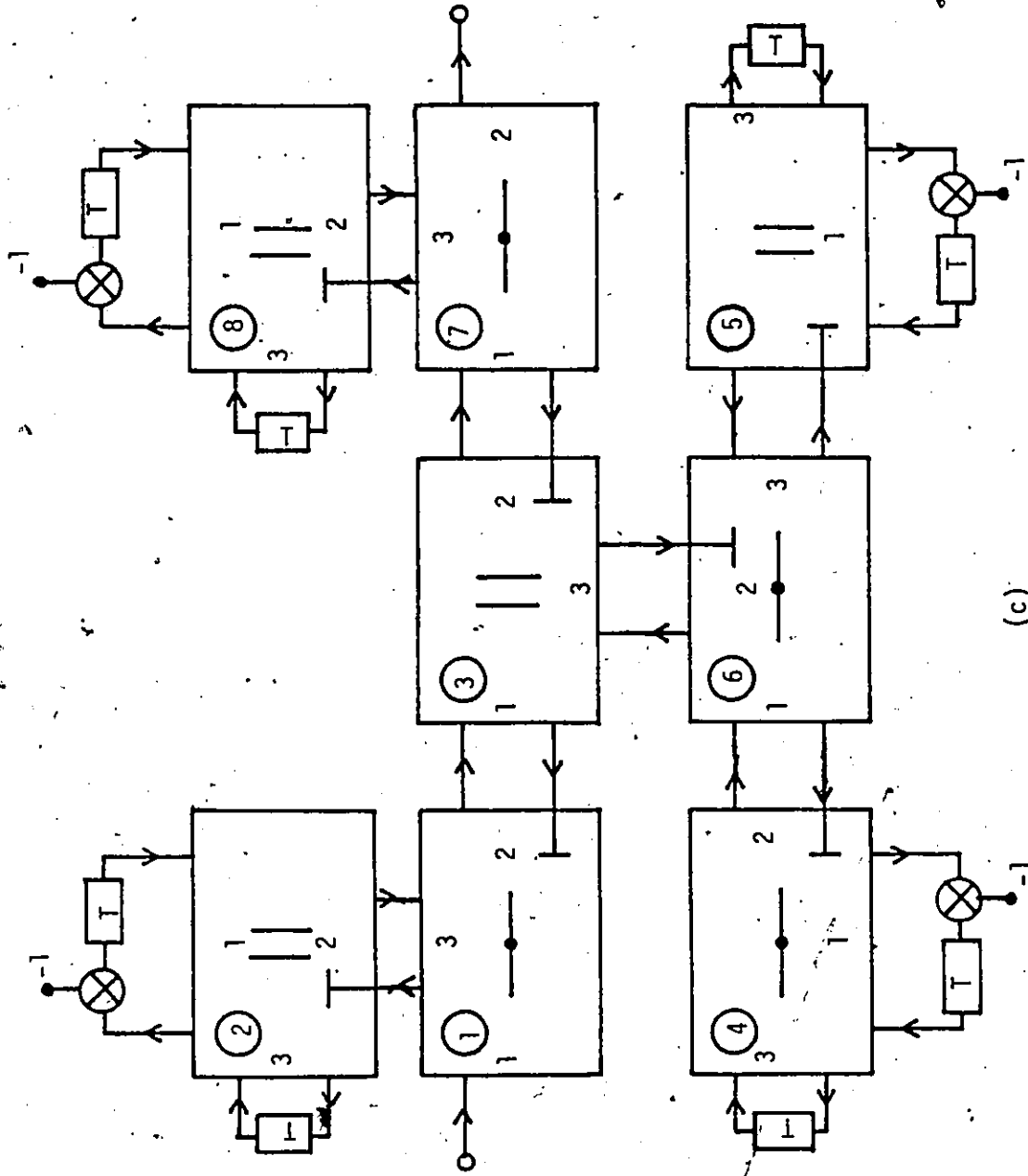


FIG. 2.9 Elliptic 6th-Order Bandstop Wave Digital Filter

(c) Wave Digital Realization

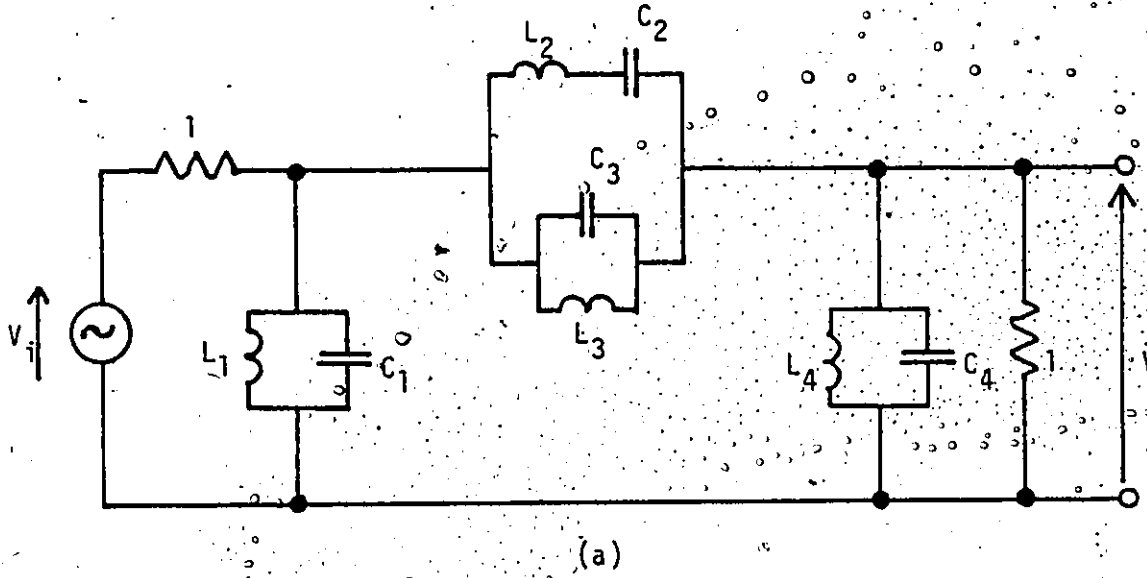


FIG. 2.10 Elliptic 6th-Order Bandpass Wave Digital Filter

(a) Prewarped Doubly Terminated LC Bandpass Filter

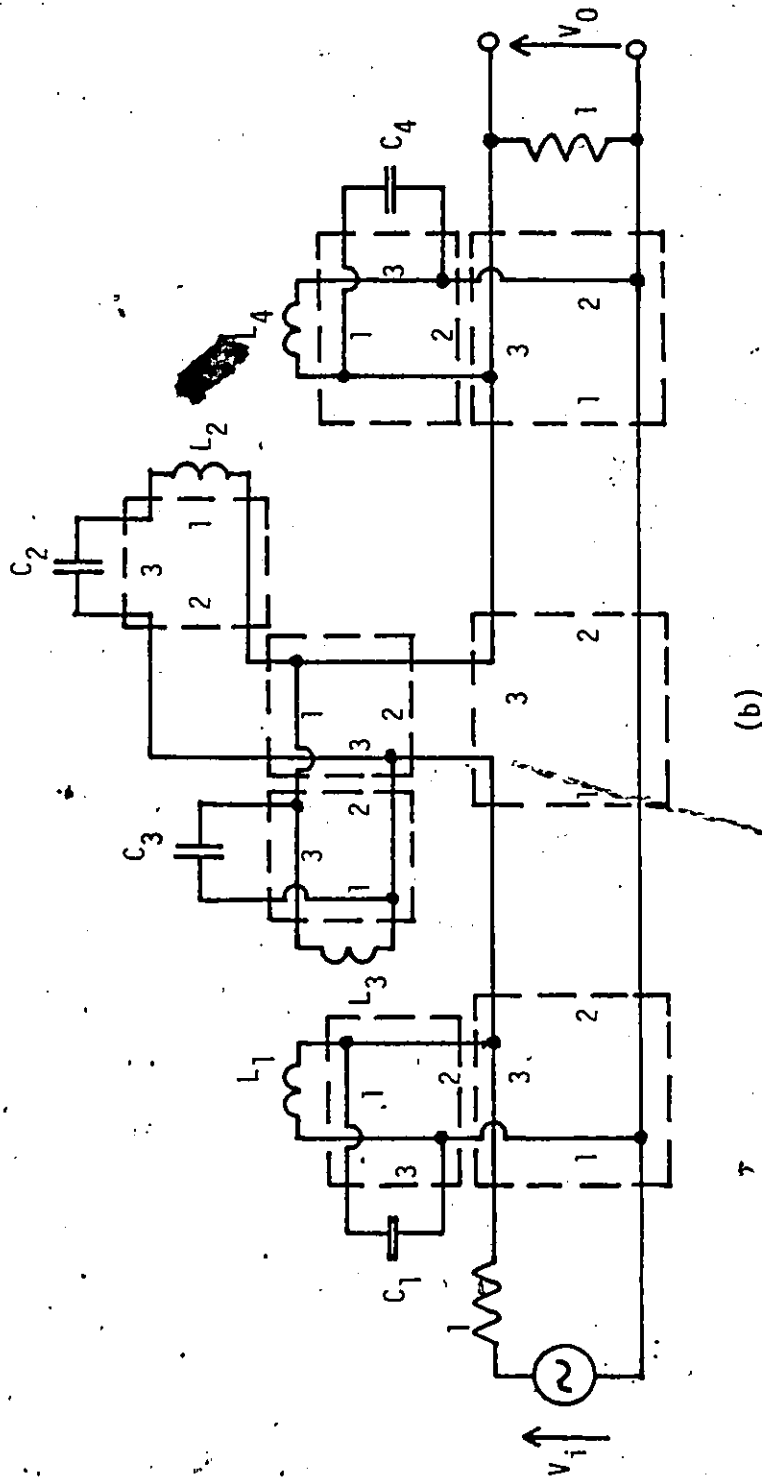
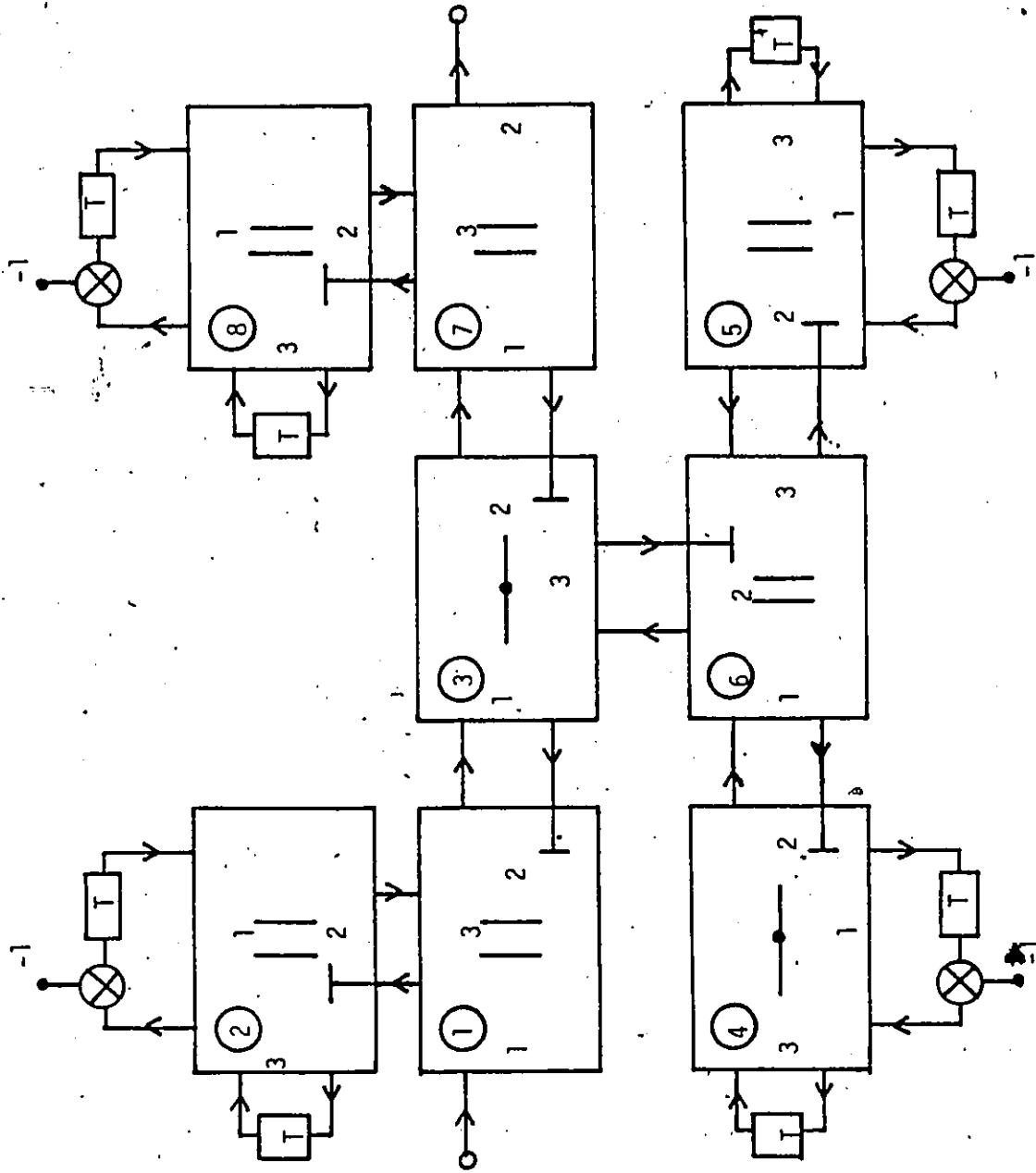


FIG. 2.10 Elliptic 6th-Order Bandpass Wave Digital Filter

(b) Identification of Wire Interconnection



(c)

FIG. 2.10 Elliptic 6th-Order Bandpass Wave Digital Filter  
(c) Wave Digital Realization

TABEL 2.13 MULTIPLIER VALUES OF THE BANDSTOP FILTER (WAVE SYNTHESIS)

Adaptor	Type	K	$m_{pk}$ or $m_{sk}$
1	S1	1	0.46116
2	P1	1	0.5
3	P1	1	0.44706
4	S1	1	0.5
5	P1	1	0.5
6	S1	1	0.99637
7	S2	1	0.61789
		2	0.63737
8	P1	1	0.5



TABLE 2.14 MULTIPLIER VALUES OF THE BANDPASS FILTER (WAVE SYNTHESIS)

Adaptor	Type	K	$m_{pk}$ or $m_{sk}$
1	P1	1	0.01103
2	P1	1	0.16391
3	S1	1	0.06301
4	S1	1	0.83609
5	P1	1	0.16391
6	P1	1	0.0026
7	P2	1	0.11855
		2	0.02075
8	P1	1	0.16391

For the bandstop filter, the canonic and the GIC structures are essentially of the same complexity because the elimination of one multiplication in the case of the GIC structure tends to compensate for the extra additions. For the delay equalizer, however, the GIC structure is more economical, since only six multipliers are necessary, as opposed to the nine required by the canonic structure.

The wave structures, on the other hand, are the least economical as can be seen in Table 2.15. For the lowpass filter, the wave structure requires an extra multiplication and seven extra additions relative to the operations required by the corresponding GIC structure. Similarly, for the bandstop or bandpass filter the wave structure requires two extra inversions, one extra multiplication and ten extra additions.

#### 2.5.2 Processing Speed

The speed of processing a signal in a digital filter depends primarily on the time needed to perform the multiplications throughout the filter since the time needed to perform one multiplication is much greater than that needed to perform one addition or inversion. Therefore, the number of multiplications in a digital-filter structure must be kept as low as possible to minimize the processing time.

Because of the above fact, the canonic and GIC structures for the lowpass filter have nearly the same speed, as can be seen in Table 2.15. For the bandstop filter, the extra multiplication required in the canonic structure is approximately equivalent to the 12 extra additions in the GIC structure. Therefore, both structures will operate at approximately the same speed. The canonic bandpass structure has a somewhat higher speed than the GIC structure because of the extra additions in the



latter case. For the delay equalizer, however, the GIC structure will operate at a higher speed than the canonic structure, since the three extra multiplications in the latter case are much more time consuming than the extra additions in the GIC structure.

Wave structures in general have the lowest speed as compared to the other two types of structures because of the higher number of multiplications and additions required, as can be seen in Table 2.15.

### 2.5.3 Parallelism

A digital-filter structure is called a completely parallel structure [8], [24] if all the arithmetic operations throughout the filter can be completed within the time needed to perform one multiplication. Otherwise, the structure is called partly parallel. The degree of parallelism in a digital-filter structure can be increased by computing as far as possible different multiplications simultaneously. Therefore, a greater degree of parallelism would involve an increase in the number of adders and multipliers [8].

A useful way to study the degree of parallelism is to plot for each structure the time necessary to compute one filter cycle, designated by  $T_{f_c}$ , against  $M$  the number of distinct multipliers used in the implementation [24]. The time necessary to compute one filter cycle can be roughly approximated as

$$T_{f_c} = k_{f_c} \tau_m$$

where  $k_{f_c}$  is an integer and  $\tau_m$  is the time needed to perform one multiplication. A technique for the evaluation of  $T_{f_c}$  was proposed

by Crochiere [24]. This was used to construct the plots of Figs. 2.11a-2.11d for the various types of filters considered.

For the lowpass, bandstop and bandpass filters considered, the cascade canonic structures are the only completely parallel structures, as can be seen in Figs. 2.11a-2.11c. The wave structures and GIC structures are both partly parallel. However, the GIC structures have a higher degree of parallelism than the wave structures, as can be seen in Figs. 2.11a-2.11c. For the delay equalizer, both cascade canonic and GIC structures are partly parallel. However, a higher degree of parallelism is inherent in the GIC structure, as can be seen in Fig. 2.11d,

## 2.6 CONCLUSIONS

A digital-filter synthesis has been described, which uses as a basis an analog configuration comprising of resistors and generalized-immittance converters. The synthesis has been used to derive a set of universal second-order digital sections which can be used in cascade to realize filters or equalizers. The synthesis was illustrated by designing a lowpass filter, a bandstop filter, a bandpass filter and an equalizer. The three filters were then designed by using the cascade canonic and wave syntheses.

The GIC filters obtained were then compared with the cascade canonic and wave digital filters in terms of the number of arithmetic operations, processing speed, and the degree of parallelism. It was found that for the lowpass, bandstop, and bandpass filters, the GIC

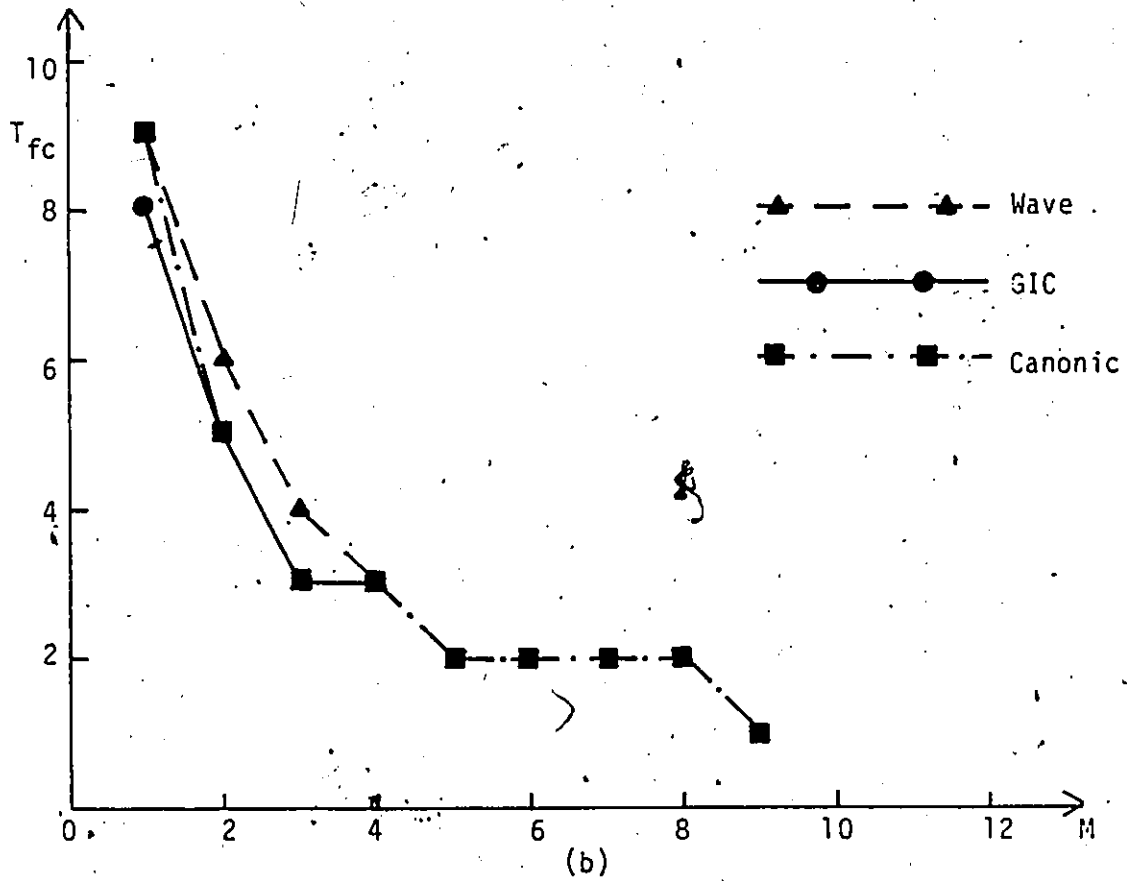
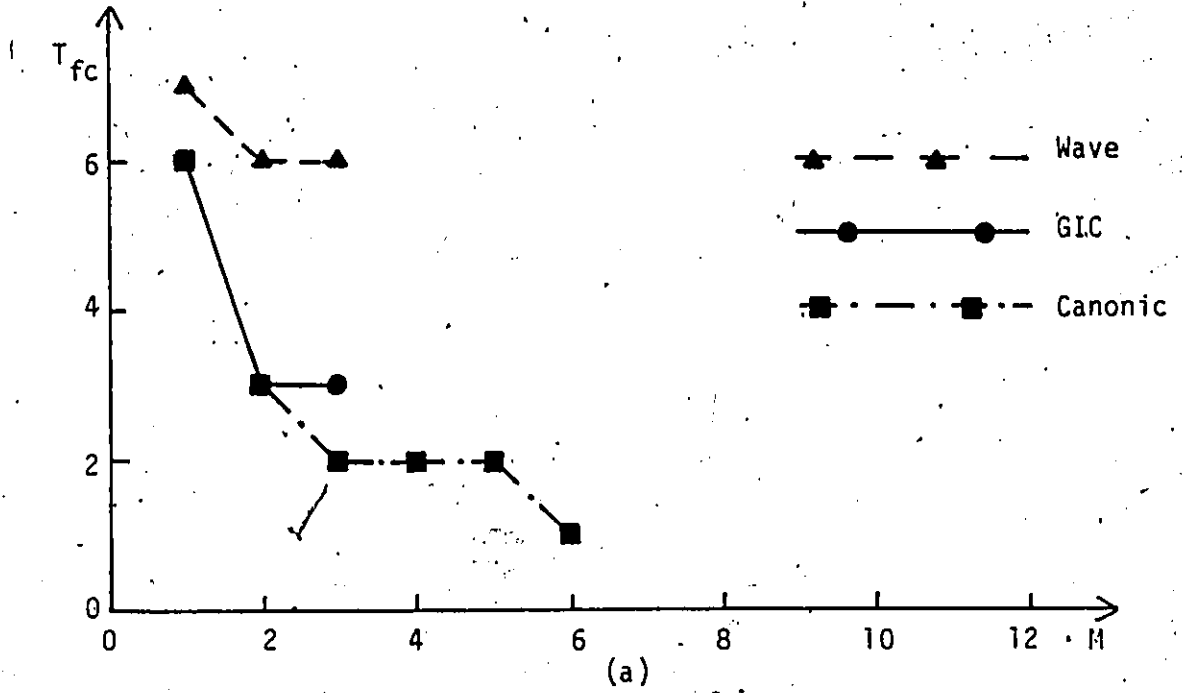


FIG. 2.11 Degree of Parallelism in the Lowpass Filter, Bandstop Filter, Bandpass Filter and the Delay-Equalizer

(a) Lowpass Filter

(b) Bandstop Filter

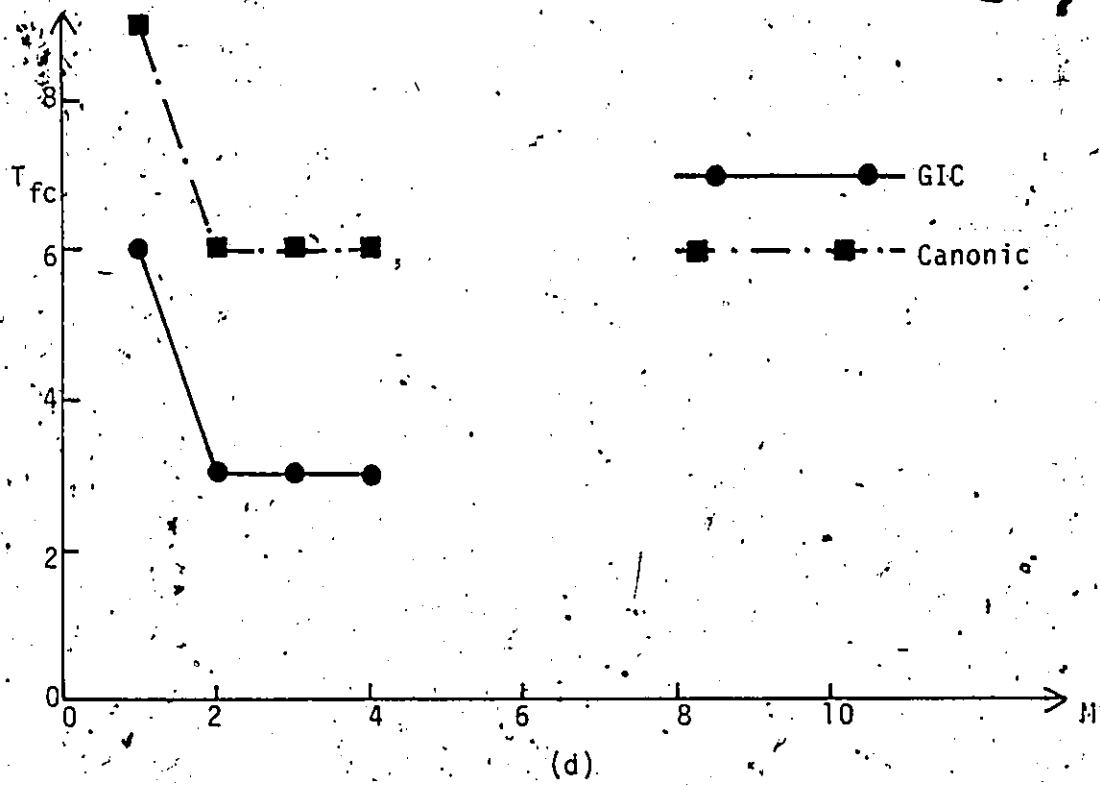
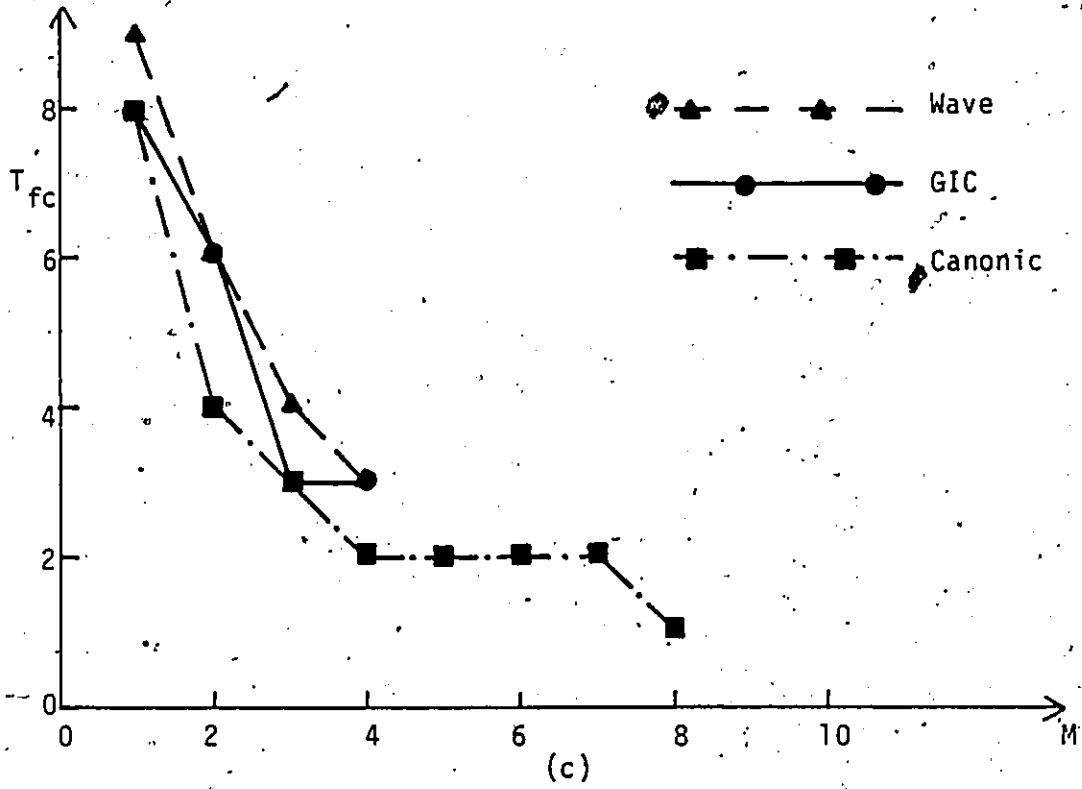


FIG. 2.11 Degree of Parallelism in the Lowpass Filter, Bandstop Filter, Bandpass Filter and the Delay Equalizer

(c) Bandpass Filter  
(d) Delay Equalizer

structures are more efficient than the corresponding wave structures.

The GIC structures for the lowpass and the bandstop filters are of the same computational efficiency as the cascade canonic structures. For the bandpass filter, on the other hand, the cascade canonic structure is more efficient than the GIC structure while for the delay equalizer, the GIC structure is more efficient than the cascade canonic one. It should be pointed out that the number of unit-delays used in the GIC structures is always minimal.



## CHAPTER 3

### PRODUCT QUANTIZATION

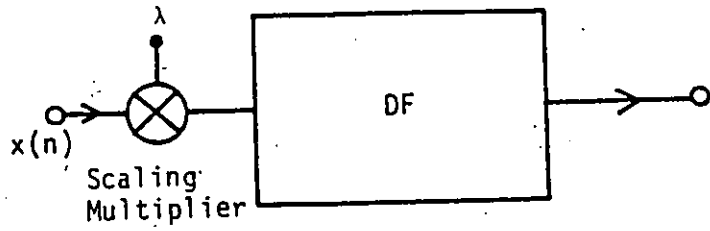
#### 3.1 INTRODUCTION

As was pointed out in Section 1.3, the wordlength in a fixed-point digital-filter implementation must be finite. As a consequence all internal signals must not be allowed to exceed a certain prescribed maximum level. At the same time the signal levels throughout the filter must not be unduly low, since if this is the case the signal-to-noise ratio will be poor. Therefore, for optimum filter performance suitable signal scaling must be employed.

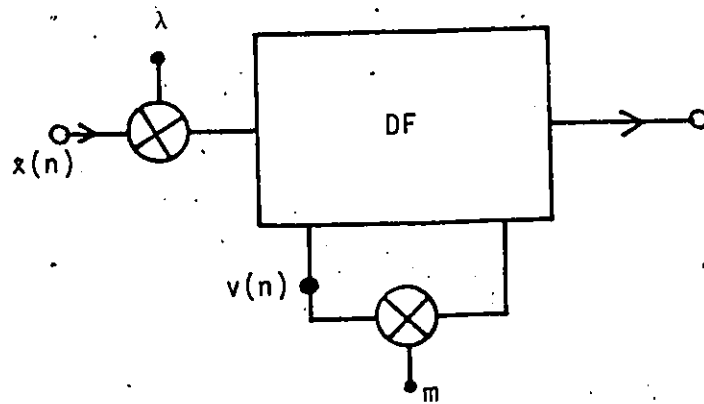
In this chapter, a signal scaling technique is described, and is applied to the various digital filters designed earlier in Section 2.4. The effect of product quantization in these filters is then studied. Subsequently, the GIC synthesis is compared with the cascade canonic and wave syntheses, from the point of view of product quantization. The arithmetic is assumed to be of the fixed-point type throughout while numbers are assumed to be in 2's complement representation.

#### 3.2 SIGNAL SCALING

A commonly used signal scaling technique applicable to fixed-point 2's complement digital-filter implementations is one due to Jackson [44], [45]. In this approach, a scaling multiplier is used at the input of the filter as shown in Fig. 3.1a where  $\lambda$  is chosen such that the magnitude of the largest multiplier input is bounded by  $M$  if



(a)



(b)

FIG. 3.1 Scaling of a Digital Filter

the filter input  $x(n)$  is bounded by  $M$ .

Let us consider a structure with only one multiplier such as that in Fig. 3.1b. The convolution summation yields

$$v(n) = \sum_{k=0}^{\infty} \lambda h_m(k) x(n-k) \quad (3.1)$$

where  $h_m(n)$  is the impulse response between the input of the filter and the input of the multiplier. The z transform gives

$$X(z) = \mathcal{Z}\{x(n)\}$$

$$H_m(z) = \mathcal{Z}\{h_m(n)\}$$

and hence from Eqn. 3.1

$$V(z) = \lambda H_m(z) X(z)$$

The inverse z transform of  $V(z)$  is

$$v(n) = \frac{1}{2\pi j} \oint_{\Gamma} \lambda H_m(z) X(z) z^{n-1} dz \quad (3.2)$$

where  $\Gamma$  may be taken to be the unit circle  $|z| = 1$ . By letting  $z = e^{j\omega T}$ , Eqn. 3.2 can be written as

$$v(n) = \frac{1}{\omega_s} \int_0^{\omega_s} \lambda H_m(e^{j\omega T}) X(e^{j\omega T}) e^{jn\omega T} / d\omega \quad (3.3)$$

where  $\omega_s$  is the sampling frequency. We can now write

$$|v(n)| \leq \left\{ \max_{0 \leq \omega \leq \omega_s} |X(e^{j\omega T})| \right\} \frac{1}{\omega_s} \int_0^{\omega_s} |\lambda H_m(e^{j\omega T})| d\omega \quad (3.4)$$

or

$$|v(n)| \leq \left( \max_{0 \leq \omega \leq \omega_s} |\lambda H_m(e^{j\omega T})| \right) \frac{1}{\omega_s} \int_0^{\omega_s} |X(e^{j\omega T})| d\omega \quad (3.5)$$

This inequality can be expressed in terms of  $L_p$  notation. The  $L_p$  norm of an arbitrary periodic function  $A(e^{j\omega T})$  having a period  $\omega_s$  is defined as

$$\|A\|_p = \left[ \frac{1}{\omega_s} \int_0^{\omega_s} |A(e^{j\omega T})|^p d\omega \right]^{1/p} \quad (3.6)$$

for each  $p \geq 1$ . The  $L_p$  norm exists if

$$\int_0^{\omega_s} |A(e^{j\omega T})|^p d\omega < \infty$$

and if  $A(e^{j\omega T})$  is continuous  $\lim_{p \rightarrow \infty} \|A\|_p$

exists and is given by

$$\|A\|_\infty = \max_{0 \leq \omega \leq \omega_s} |A(e^{j\omega T})| \quad (3.7)$$

Now by using Eqns. 3.6-3.7, Eqn. 3.4 can be put in the form,

$$|v(n)| \leq \|X\|_\infty \cdot \|\lambda H_m\|_1 \quad (3.8)$$

Similarly, from Eqn. 3.5

$$|v(n)| \leq \|\lambda H_m\|_\infty \cdot \|X\|_1 \quad (3.9)$$

Also, by applying the Schwarz inequality to Eqn. 3.3, we have

$$|v(n)| \leq \left\{ \frac{1}{\omega_s} \int_0^{\omega_s} |\lambda H_m(e^{j\omega T})|^2 d\omega \right\}^{1/2} \left\{ \frac{1}{\omega_s} \int_0^{\omega_s} |X(\Omega)|^2 d\Omega \right\}^{1/2}$$

or

$$|v(n)| \leq \|\lambda H_m\|_2 \cdot \|X\|_2 \quad (3.10)$$

In fact it can be shown that Eqns. 3.8-3.10 are particular cases of the general inequality

$$|v(n)| \leq \|\lambda H_m\|_p \cdot \|X\|_q \quad (3.11)$$

(see Ref. 45) where the relation

$$p = \frac{q}{q-1} \quad p, q \geq 1$$

must hold.

In the special case when  $\lambda H_m(e^{j\omega T}) = 1$ , Eqn. 3.11 is still valid. Also from Eqn. 3.2  $y(n) = x(n)$ . Since  $\|1\|_p = 1$  for all  $p \geq 1$ , we obtain from Eqn. 3.11

$$|x(n)| \leq \|X\|_q \quad \text{for all } q \geq 1$$

and if

$$\|X\|_1 \leq M$$

Eqn. 3.11 yields

$$|v(n)| \leq M \|\lambda H_m\|_\infty$$

Therefore,  $|x(n)|$  and  $|v(n)|$  will be bounded by  $M$  provided that

$$\|\lambda H_m\|_\infty \leq 1$$

or

$$\lambda \leq \frac{1}{\|H_m\|_\infty}$$

For maximum signal-to-noise ratio the maximum permissible value of  $\lambda$  should be chosen which is

$$\lambda = \frac{1}{\|H_m\|_\infty} = \frac{1}{\max_{0 \leq \omega \leq \omega_s} |H_m(e^{j\omega T})|}$$

The same technique can be extended to structures having more than one multiplier. In such structures the scaling multiplier must be computed as

$$\lambda = \frac{1}{\max \|H_{mj}\|_\infty}$$

where  $H_{m1}, H_{m2}, \dots$  are the transfer functions between the input of the structure and the inputs of the various multipliers.

To illustrate this technique, consider the second-order section of Fig. 3.2, and let  $H_m(z)$  and  $H(z)$  be the transfer functions between the section input and  $C_1$  and between the section input and section output, respectively. The signals at nodes  $C_2$  and  $C_3$  are delayed versions of the signal at node  $C_1$ . Therefore, the inputs of all multipliers are bounded by  $M$  when  $x(n)$  is bounded by  $M$ , if

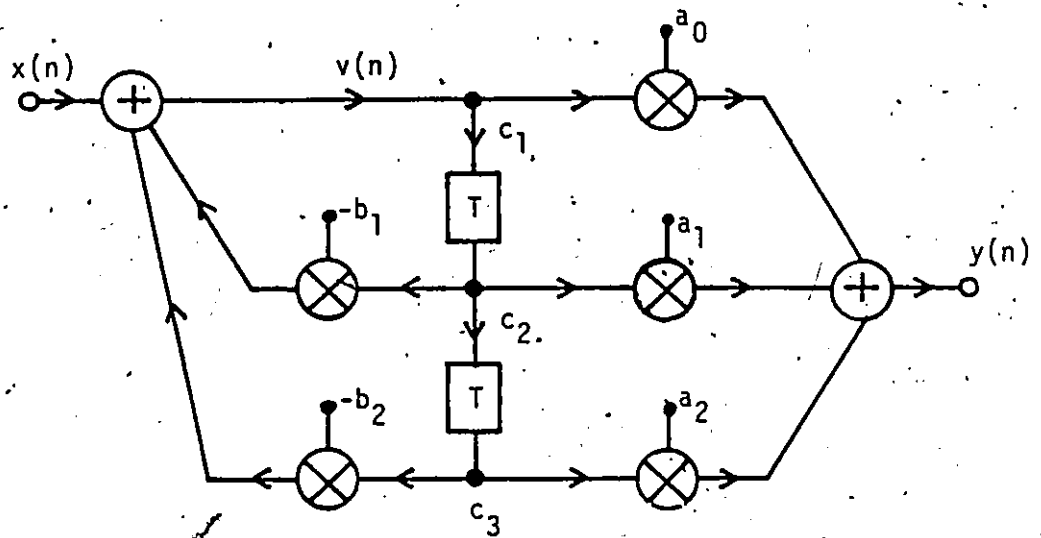


FIG. 3.2 Canonic Second-Order Section

$$\lambda = \frac{1}{\max \{ \|H_m(e^{j\omega T})\|_{\infty}, \|H(e^{j\omega T})\|_{\infty} \}}$$

For a cascade connection of  $L$  second-order canonic sections, the scaling multiplier constants can be determined as

$$\lambda_j = \frac{1}{\prod_{i=0}^{j-1} \lambda_i \max \{ \|H_{mj}\|_{\infty}, \|H_j\|_{\infty} \}}$$

for  $j=1, 2, \dots, L-1$  where,

$$H_{mj} = H_{m(j+1)}(e^{j\omega T}) \prod_{i=1}^j H_i(e^{j\omega T})$$

$$H_j = \prod_{i=1}^{j+1} H_i(e^{j\omega T})$$

The GIC lowpass section shown in Fig. 2.5a, can be represented by the flow graph of Fig. 3.3a, where

$$H_A(z) = N_A(z)/D(z)$$

$$H_B(z) = N_B(z)/D(z)$$

and

$$H_D(z) = N_D(z)/D(z)$$

are the transfer functions between section input and nodes A, B and D, respectively, in Fig. 2.5a. The polynomials  $N_A(z)$ ,  $N_B(z)$ ,  $N_D(z)$  and  $D(z)$  are given in Table 3.1. The optimum value of  $\lambda$  for maximum



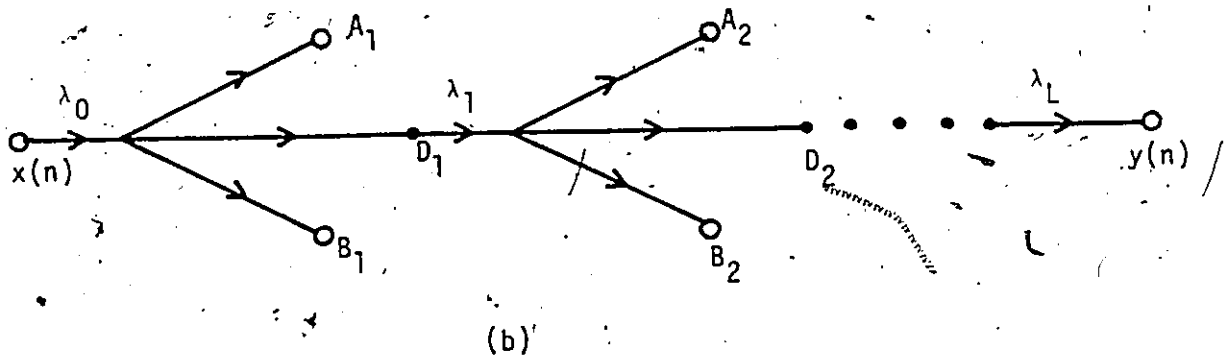
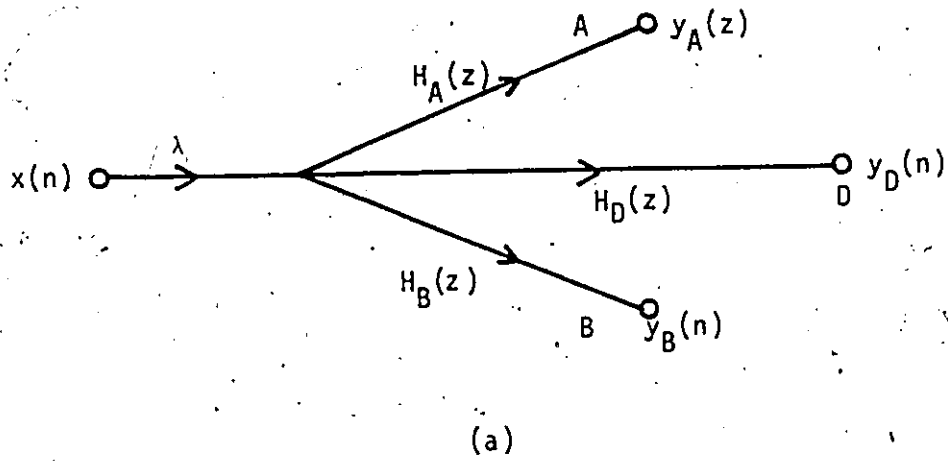


FIG. 3.3 Signal Scaling of GIC Structure

(a) Flow Graph Representation of GIC Section

(b) Flow Graph for Cascade Realization

TABLE 3.1 POLYNOMIALS IN GIC SECTIONS

Type	$N_A(s)$	$N_D(z)$	$N_A(z)$	$N_B(z)$
LP	$b_0$	$(1+m_1)(z+1)^2$	$(z-m_2)(z+1)$	$(1+m_1)(z+1)$
HP	$s^2$	$(1+m_2)(z-1)^2$	$(z+m_1)(z-1)$	$-(1+m_2)(z-1)$
BP	$b_1 s$	$(m_1+m_2)(1-z^2)$	$-(z^2-2m_2z+1)$	$-(z^2+2m_1z+1)$
N	$a_0+s^2$	$k_0(1+m_1)(z+1)^2$ $+ (1+m_2)(z-1)^2$	$k_0(z-m_2)(z+1)$ $-(1+m_2)(z-1)$	$k_0(1+m_1)(z+1)$ $+(z+m_1)(z-1)$
AP	$b_0-b_1s+s^2$	$2\{(1+m_1+m_2)z^2$ $+(m_1-m_2)z+1\}$	$2(z^2-2m_2z+1)$	$2(z^2+2m_1z+1)$
D(z)	$z^2+(m_1-m_2)z+(1+m_1+m_2)$			

signal-to-noise ratio [44], can be shown to be

$$\lambda = \frac{1}{\max \{ \|H_A(e^{j\omega T})\|_\infty, \|H_B(e^{j\omega T})\|_\infty, \|H_D(e^{j\omega T})\|_\infty \}}$$

where, from Eqn. 3.7

$$\|H(e^{j\omega T})\|_\infty = \max_{0 \leq \omega \leq \omega_s} |H(e^{j\omega T})|$$

Similarly, a cascade connection of  $L$  GIC sections can be represented by Fig. 3.3b. In this case, maximum signal-to-noise ratio can be achieved if

$$\lambda_j = \frac{1}{\prod_{i=0}^{j-1} \lambda_i \max \{ \|T_{A_j}\|_\infty, \|T_{B_j}\|_\infty, \|T_{D_j}\|_\infty \}}$$

for  $j=1, 2, \dots, L-1$ , where

$$\lambda_0 = \frac{1}{\max \{ \|H_{A_1}(e^{j\omega T})\|_\infty, \|H_{B_1}(e^{j\omega T})\|_\infty, \|H_{D_1}(e^{j\omega T})\|_\infty \}}$$

and

$$T_{A_j} = H_{A(j+1)}(e^{j\omega T}) \prod_{i=1}^j H_{D_i}(e^{j\omega T})$$

$$T_{B_j} = H_{B(j+1)}(e^{j\omega T}) \prod_{i=1}^j H_{D_i}(e^{j\omega T})$$

$$T_{D_j} = \prod_{i=1}^{j+1} H_{D_i}(e^{j\omega T})$$

If  $\|T_{D(L-1)}\|_{\infty} < \max \{ \|T_{A(L-1)}\|_{\infty}, \|T_{B(L-1)}\|_{\infty} \}$  an additional multiplier with a constant value of

$$\lambda_L = \frac{1}{\prod_{i=0}^{L-1} \lambda_i \|T_{D(L-1)}\|_{\infty}}$$

may be used at the output of the filter to raise the output to the maximum permissible level. Such a multiplier was found to be unnecessary in a number of cascade canonic filters.

The above scaling technique can also be extended to wave digital-filter structures [46]-[47]. Consider the wave digital filter of Fig. 3.4a and let  $v_{1i}(n)$  and  $v_{2i}(n)$  be the inputs of the multipliers in the  $i$ th adaptor. Scaling can be accomplished by using two scaling multipliers at the input of each adaptor, as illustrated in Fig. 3.4b. The scaling multiplier constants for each adaptor must be reciprocal of each other [17], [46], [47] so as to preserve the original transfer function of the filter. Assuming 2-multiplier adaptors, the inputs of the multipliers in adaptor 1, namely  $v_{11}(n)$  and  $v_{21}(n)$ , will be bounded by  $M$  if  $x(n)$  is bounded by  $M$  provided that

$$\lambda_1 = \frac{1}{\max \{ \|H_{11}\|_{\infty}, \|H_{21}\|_{\infty} \}}$$

where  $H_{11}(z)$  and  $H_{21}(z)$  are the transfer functions between the input of the filter and the inputs of the multipliers in adaptor 1. Similarly

$$|v_{12}(n)|, |v_{22}(n)| \leq M$$

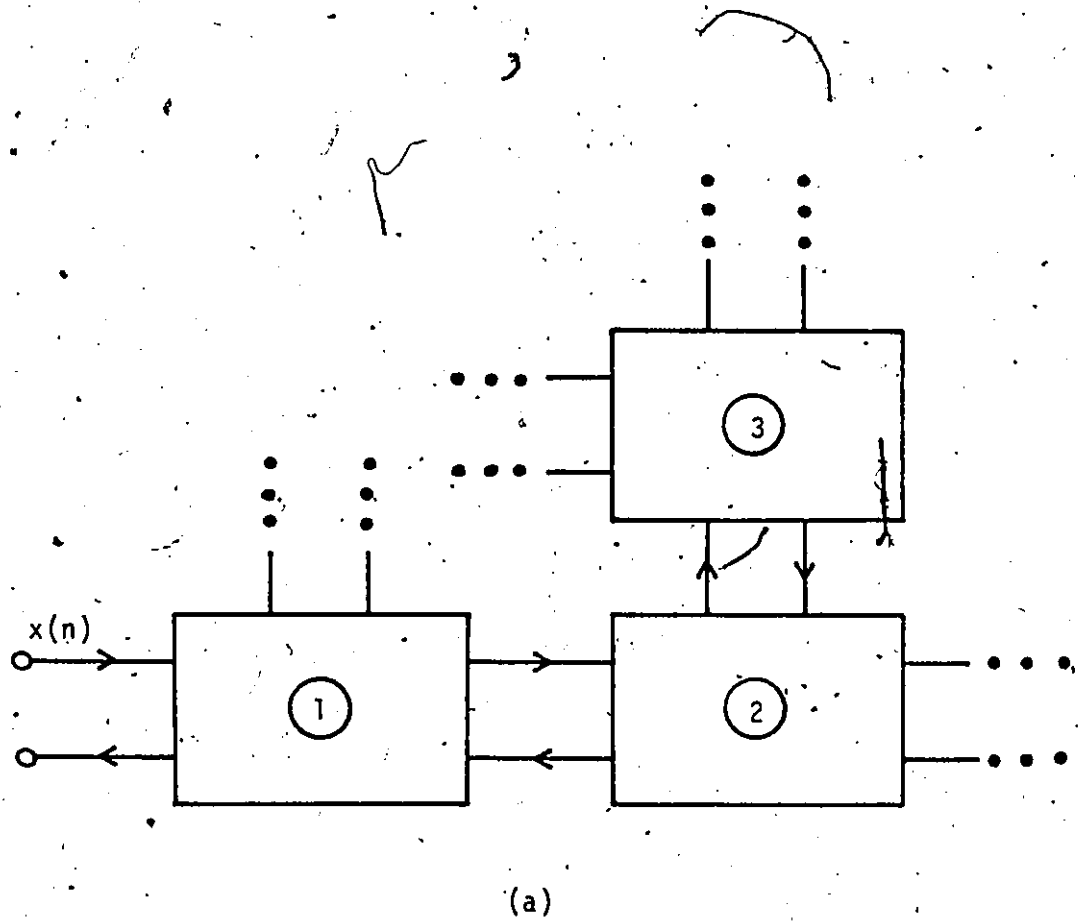


FIG. 3.4 Signal Scaling in Wave Digital-Filter Structure  
(a) The Wave Structure before Scaling

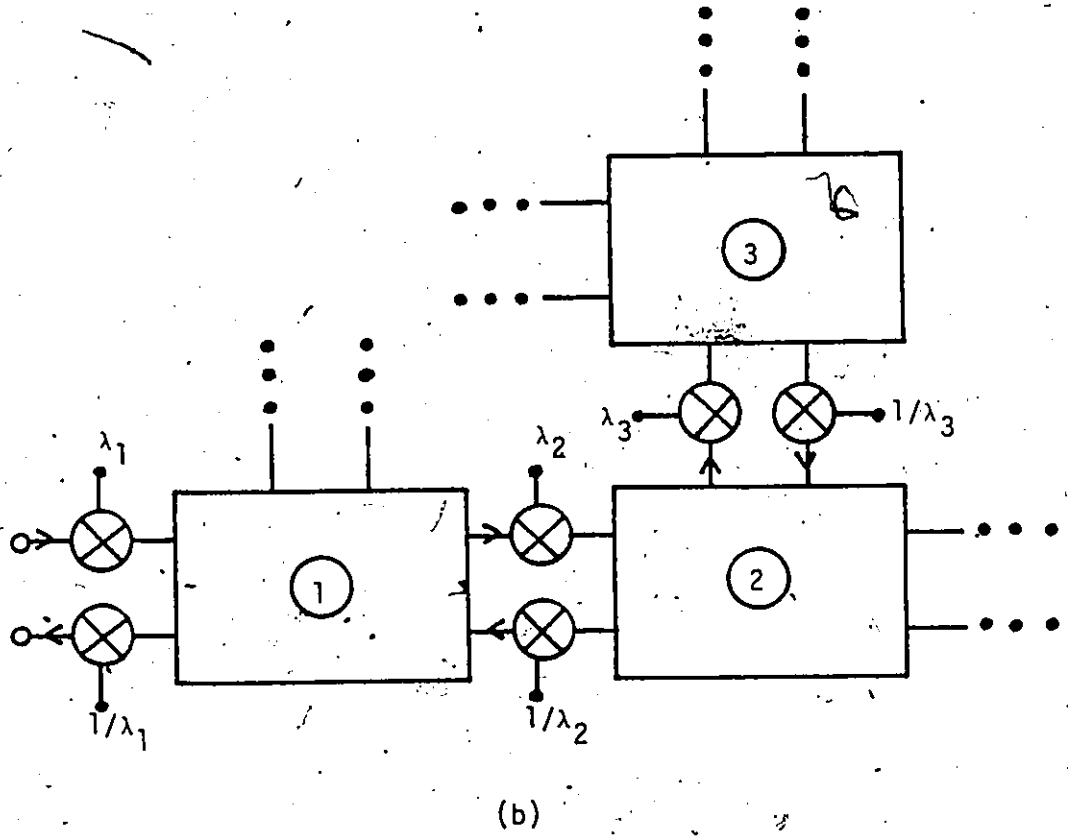


FIG. 3.4 Signal Scaling in Wave Digital-Filter Structure

(b) The Wave Structure after Scaling

when

$$|x(n)| \leq M$$

provided that

$$\lambda_2 = \frac{1}{\max \{ \|H_{12}\|_\infty, \|H_{22}\|_\infty \}}$$

where  $H_{12}(z)$  and  $H_{22}(z)$  are the transfer functions between the input of the filter and the inputs of the multipliers in adaptor 2. Proceeding in the same way  $\lambda_3, \lambda_4, \dots$  can be determined. The same procedure can be applied if some adaptors have only one multiplier. For example if adaptor 1 has only one multiplier we can assign

$$\lambda_1 = \frac{1}{\|H_{11}\|_\infty}$$

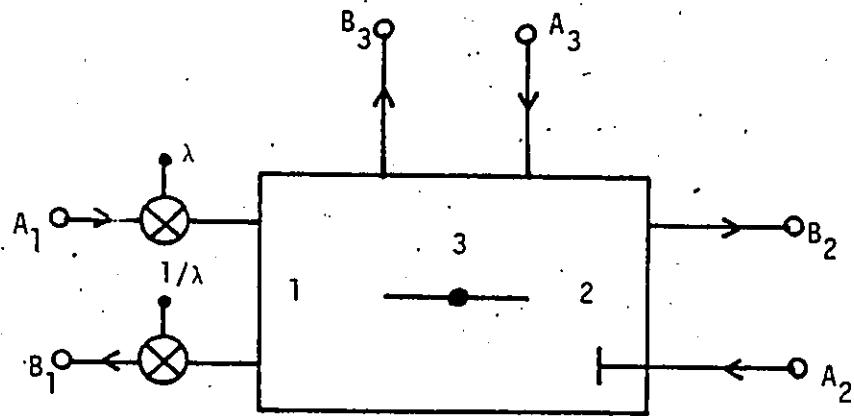
and so on.

The scaling multipliers can be incorporated in the adaptors [17], [47]. For example type S1 adaptor of Fig. 3.5a can be modified as shown in Fig. 3.5b. Similarly, adaptors P1, S2, and P2 can be modified as shown in Figs. 3.6-3.8.

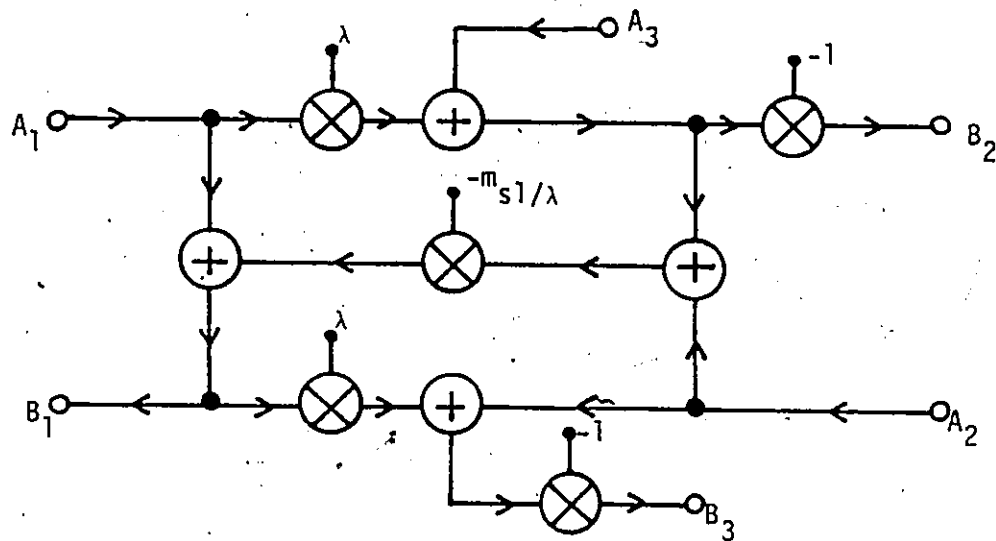
### 3.3 PRODUCT QUANTIZATION ERRORS

The output of a finite wordlength fixed-point multiplier can be written as

$$Q[a_i x(n)] = a_i x(n) + e(n)$$



(a)



(b)

FIG. 3.5 S1-Type Adaptor after Scaling

(a) Block Diagram Representation

(b) Modified Adaptor Incorporating the Scaling Multipliers



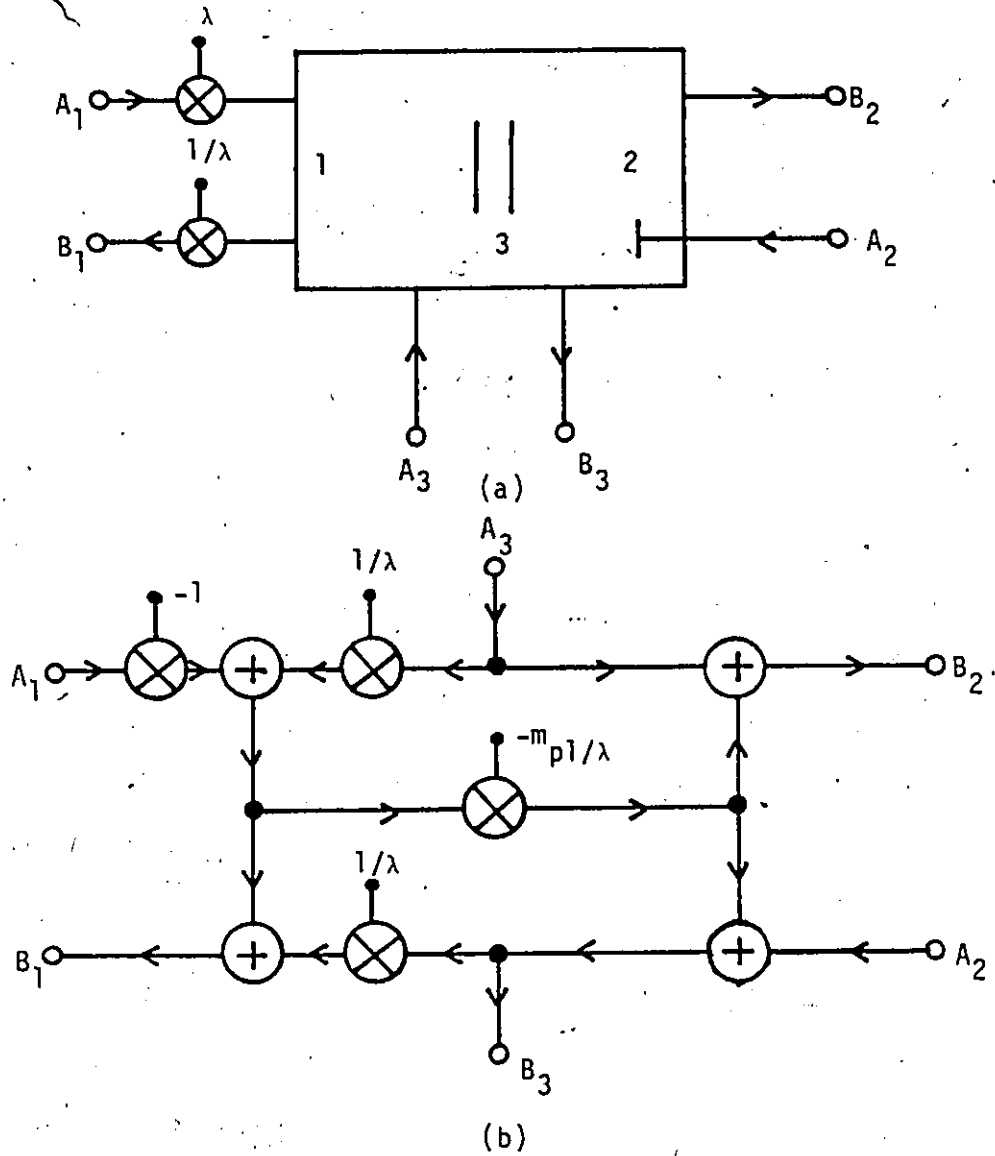


FIG . 3.6 PI-Type Adaptor after Scaling

(a) Block Diagram Representation

(b) Modified Adaptor Incorporating the Scaling Multipliers

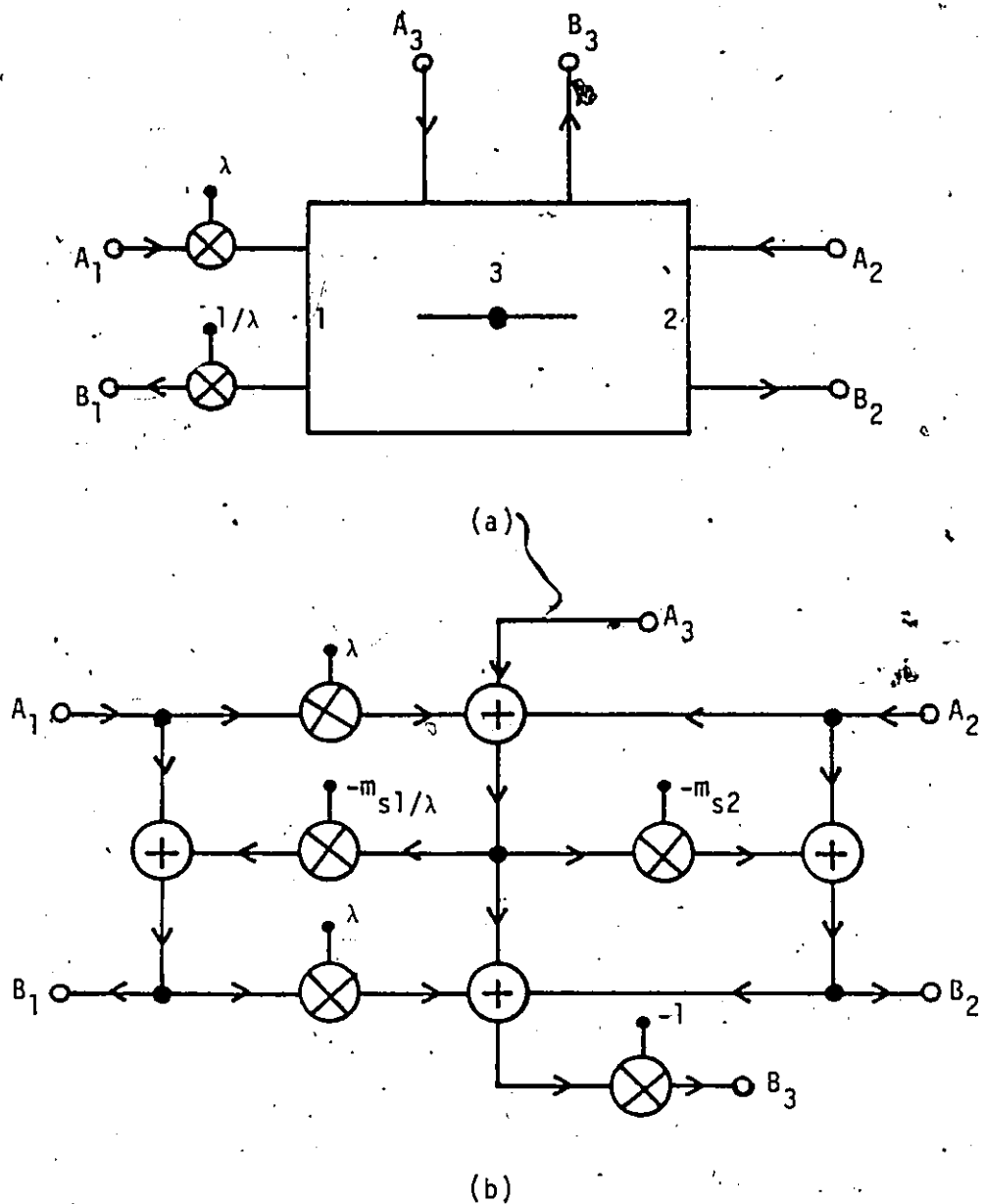


FIG. 3.7 S2-Type Adaptor after Scaling

(a) Block Diagram Representation

(b) Modified Adaptor Incorporating the Scaling Multipliers

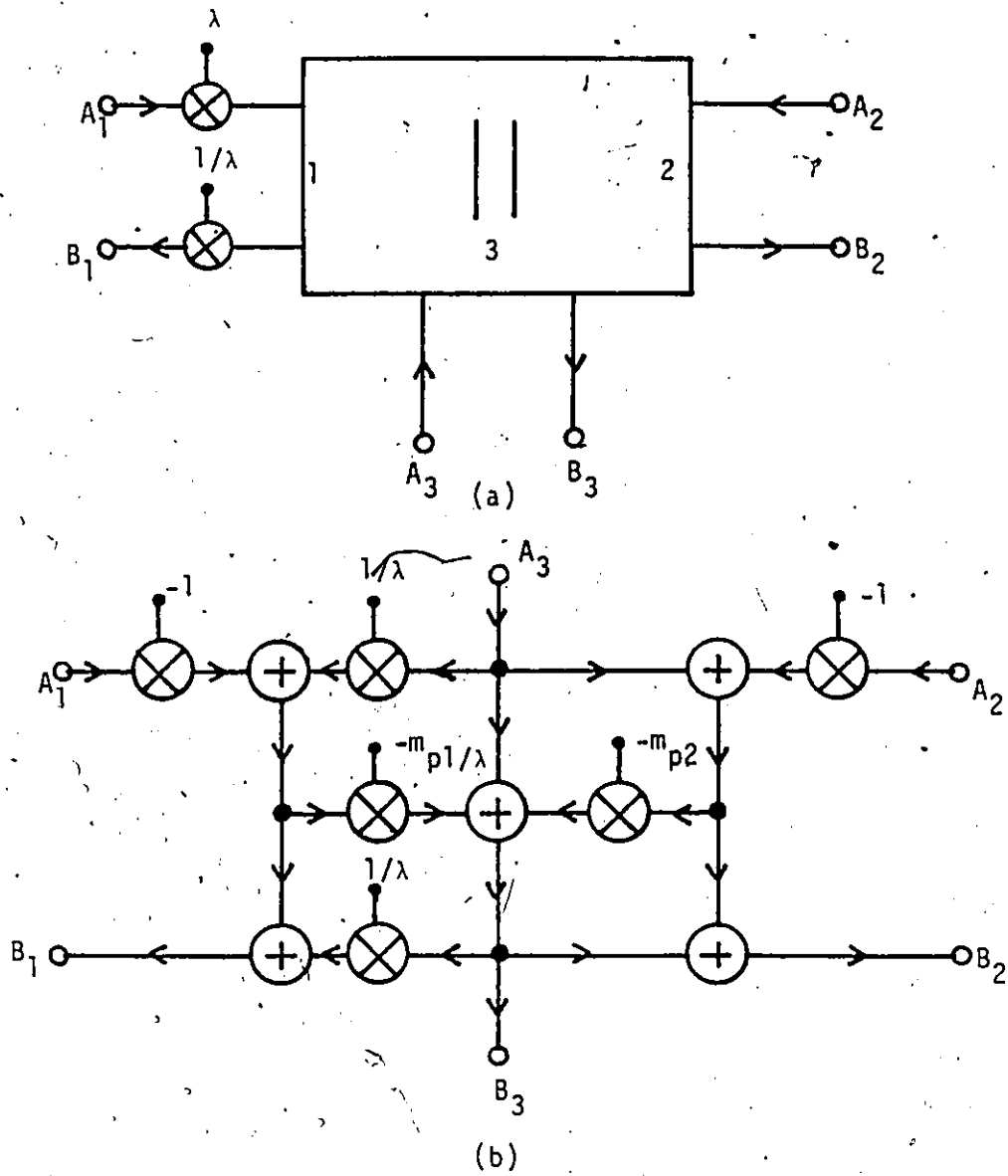


FIG. 3.8 P2-Type Adaptor after Scaling

(a) Block Diagram Representation

(b) Modified Adaptor Incorporating the Scaling Multipliers

where  $a_i x(n)$  and  $e(n)$  are the exact product and the quantization error, respectively. Hence a fixed-point multiplier can be represented by the model of Fig. 3.9a, where the multiplier shown is ideal and  $e(n)$  is a noise source. If product quantization is carried out by rounding,  $e(n)$  is a random variable in the range

$$-\frac{q}{2} \leq e(n) < \frac{q}{2}$$

where  $q$  is the spacing between quantization steps.

In the filter section shown in Fig. 3.2 each multiplier can be replaced by the model of Fig. 3.9a, to yield the equivalent structure shown in Fig. 3.9b. Each noise source  $e_i(n)$  is a random variable with a uniform probability density, that is

$$p\{e_i(n)\} = \begin{cases} 1/q & \text{for } -\frac{q}{2} \leq e_i(n) \leq \frac{q}{2} \\ 0 & \text{otherwise} \end{cases}$$

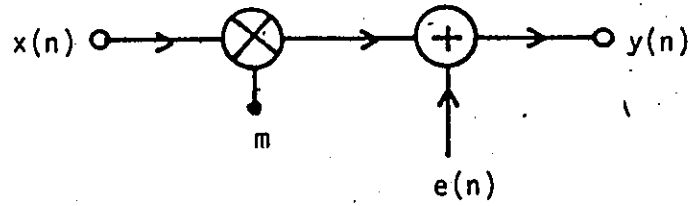
as illustrated in Fig. 3.10. The mean of  $e_i(n)$  is given by

$$\begin{aligned} E\{e_i(n)\} &= \int_{-\infty}^{\infty} e_i(n) p\{e_i(n)\} d\{e_i(n)\} \\ &= 0 \end{aligned} \tag{3.12}$$

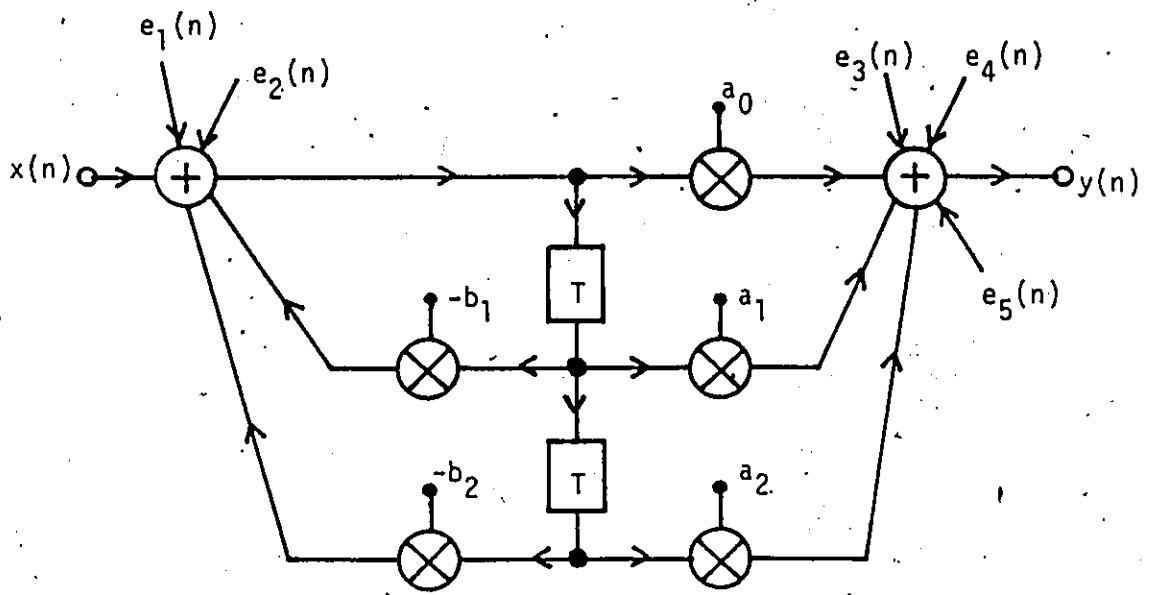
The variance of  $e_i(n)$  can be expressed as

$$\sigma_{e_i}^2 = E\{[e_i(n) - E\{e_i(n)\}]^2\}$$

but since



(a)

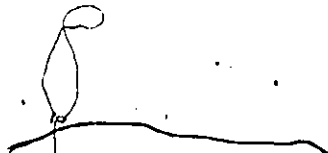


(b)

FIG. 3.9 Multiplier Noise Model

(a) Noise Model for a Single Multiplier,  $m$

(b) Noise Model for a Second-Order Canonic Section



$$E\{e_i(n)\} = 0$$

we have,

$$\sigma_{e_i}^2 = E\{e_i(n)\}^2$$

Therefore, the variance  $\sigma_{e_i}^2$  gives the average power of  $e_i(n)$ . The variance can be determined as

$$\begin{aligned} \sigma_{e_i}^2 &= E\{e_i(n)\}^2 = \int_{-q/2}^{q/2} \{e_i(n)\}^2 p\{e_i(n)\} d\{e_i(n)\} \\ &= \frac{q^2}{12} \end{aligned} \quad (3.13)$$

Now, if the peak value of each noise component is much smaller relative to the value of the signal at any node, the following two assumptions can be made:

- (i)  $e_i(k)$  and  $e_i(n+k)$  are statistically independent for any  $n$  ( $n \neq 0$ ) and any  $k$ .
- (ii)  $e_i(k)$  and  $e_j(n+k)$  are statistically independent for any  $n$  or  $k$  ( $i \neq j$ ).

The implications of the above assumptions are as follows.

The autocorrelation of a random process  $x(k)$  is defined as

$$r_x(n) = E\{x(k)x(k+n)\}$$

Hence, the autocorrelation of the process  $e_i(k)$  can be written as

$$r_{e_i}(n) = E\{e_i(k) e_i(n+k)\}$$

For  $n=0$

$$r_{e_i}(0) = E\{e_i(k)\}^2 \quad (3.14)$$

Thus, from Eqns. 3.13 and 3.14

$$r_{e_i}(0) = \frac{q^2}{12} \quad (3.15)$$

= average power of  $e_i(k)$

On the other hand

$$r_{e_i}(n) \Big|_{n \neq 0} = E\{e_i(k) e_i(n+k)\}$$

and hence by virtue of the first assumption

$$r_{e_i}(n) \Big|_{n \neq 0} = E\{e_i(k)\} E\{e_i(n+k)\}$$

Since the mean of each noise source is zero, the above equation gives

$$r_{e_i}(n) \Big|_{n \neq 0} = 0 \quad (3.16)$$

Therefore, from Eqns. 3.15 and 3.16

$$r_{e_i}(n) = \frac{q^2}{12} \delta(n)$$

where,  $\delta(n)$  is the impulse function.

The power spectral density (PSD) of  $e_i(n)$  is readily obtained as [43]

$$\begin{aligned}
 S_{e_i}(\omega) &= \mathcal{Z} \{ r_{e_i}(n) \}_{z=e^{j\omega T}} \\
 &= \mathcal{Z} \left\{ \frac{q^2}{12} \delta(n) \right\}_{z=e^{j\omega T}} \\
 &= \frac{q^2}{12}
 \end{aligned}$$

that is,  $e_i(k)$  is a "white-noise" process.

The autocorrelation of the sum of processes  $e_i(k)$  and  $e_j(k)$  is

$$r_{e_i+e_j}(n) = E\{[e_i(k)+e_j(k)][e_i(n+k)+e_j(n+k)]\}$$

and from the second assumption, we can write

$$r_{e_i+e_j}(n) = r_{e_i}(n) + r_{e_j}(n)$$

Therefore, the PSD of the sum of processes  $e_i(k)$  and  $e_j(k)$  is given by

$$\begin{aligned}
 S_{e_i+e_j}(\omega) &= \mathcal{Z} \{ r_{e_i+e_j}(n) \}_{z=e^{j\omega T}} \\
 &= \mathcal{Z} \{ r_{e_i}(n) + r_{e_j}(n) \}_{z=e^{j\omega T}} \\
 &= S_{e_i}(\omega) + S_{e_j}(\omega)
 \end{aligned}$$

i.e. the PSD of a sum of two statistically independent processes  $e_i(k)$  and  $e_j(k)$  is equal to the sum of their respective PSD's. Because of this property, the noise PSD at the output of a digital filter can be



readily deduced by using superposition.

For a digital filter with input  $x(k)$ , output  $y(k)$  and transfer function  $H(z)$ , the  $z$  transform of  $r_y(n)$  is related to that of  $r_x(n)$  by [43], [48]

$$S_y(z) = H(z) H(z^{-1}) S_x(z)$$

where,  $S_x(z)$ ,  $S_y(z)$  are the input and output PSD's respectively.

By using the superposition theorem in the filter section of Fig. 3.9b, we obtain

$$\begin{aligned} S_y(z) &= H(z)H(z^{-1})\{S_{e_1}(z)+S_{e_2}(z)\}+\{S_{e_3}(z)+S_{e_4}(z)+S_{e_5}(z)\} \\ &= S_i(z)\{2H(z)H(z^{-1})+3\} \end{aligned}$$

where the quantity  $S_i(\omega)$  is the PSD of the noise generated by one multiplier, which is equal to  $\frac{q^2}{12}$ . Therefore, the output PSD due to all the noise sources is deduced as

$$S_y(\omega) = S_i(\omega) [2|H(e^{j\omega T})|^2 + 3]$$

A similar analysis can also be applied to the GIC structures and the wave structures. The GIC universal sections of Fig. 2.5 with scaling employed, can be represented by the flow graph of Fig. 3.11, where the dotted branch pertains to the N-section only. Straight forward analysis gives the transfer functions between nodes E, F and output (see Fig. 2.5) as

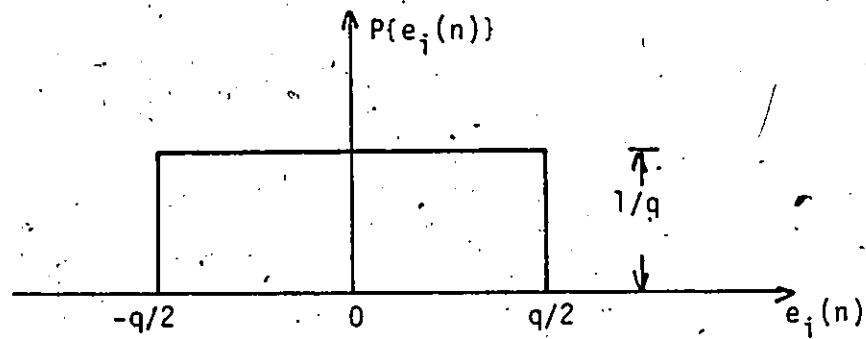


FIG. 3.10 Probability Density Function of the Quantization Noise in Fixed-Point Arithmetic

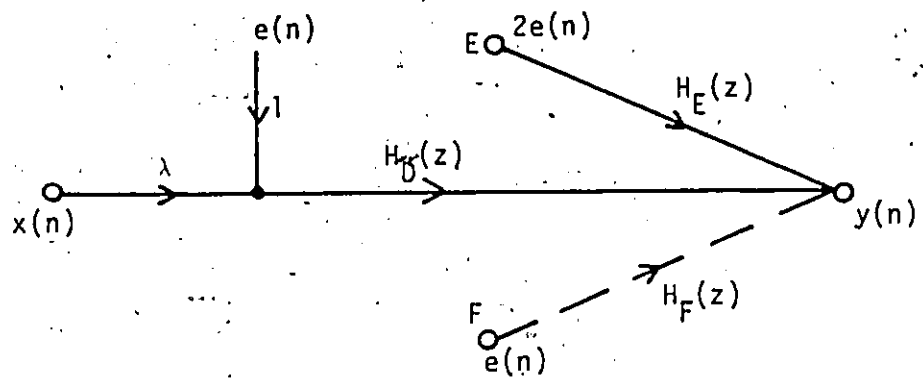


FIG. 3.11 Quantization-Noise Model for GIC Sections

$$H_E(z) = \frac{(z+1)(z-1)}{D(z)}$$

$$H_F(z) = \frac{(1+m_1)(z+1)^2}{D(z)}$$

where,  $D(z)$  is given in Table 3.1.

The output noise PSD for each section can be readily expressed as

$$S_o(\omega) = S_i(\omega) \{ |H_D(e^{j\omega T})|^2 + |H_F(e^{j\omega T})|^2 + 2 |H_E(e^{j\omega T})|^2 \}$$

where,  $H_F(e^{j\omega T}) = 0$  for LP, HP, BP, and AP sections.

An interesting and important observation can be made at this point.  $H_E(z)$  is a bandpass transfer function in each of the five sections. Hence, noise generated by multipliers  $m_1$  and  $m_2$  will be attenuated at low as well as high frequencies, becoming zero at  $\omega=0$  and  $\omega_s/2$ . This feature is particularly useful in lowpass and highpass filters because it will lead to reduced inband noise PSD. By contrast, the cascade canonic section, noise components due to denominator multipliers are subjected to the same transfer function as the signal and those due to numerator multipliers appear unattenuated at the output [45]. Hence the output noise PSD in this case will tend to have the form of the filter response.

For a cascade realization comprising  $L$  sections (LP, HP, BP or AP), and scaled according to Fig. 3.3b, the output noise PSD for GIC structures can be shown to be:

$$S_o(\omega) = S_i(\omega) \left[ 1 + \sum_{j=1}^L \{ |H_{D_j}(e^{j\omega T})|^2 + 2 |H_{E_j}(e^{j\omega T})|^2 \} \prod_{i=j}^L \lambda_i^2 \prod_{i=j+1}^L |H_{D_i}(e^{j\omega T})|^2 \right]$$

Similarly, for cascade canonic structures with the sections employed of the type shown in Fig. 3.2, we have

$$S_o(\omega) = S_i(\omega) \left[ 1 + \sum_{i=1}^L \{ 3 |H_{D_i}(e^{j\omega T})|^2 + 3 \} \prod_{j=i}^L \lambda_j^2 \prod_{j=i+1}^L |H_{D_j}(e^{j\omega T})|^2 \right]$$

For the wave structures, similar expressions can be derived; however, these are extremely complicated and are not given here.

### 3.4 COMPARISON

The digital filter structures obtained in Section 2.4, were investigated from the point of view of product-quantization effects. Then the various filters were compared. Each filter structure was scaled according to the procedure given in Section 3.2.

The noise PSD of these filters were obtained according to the following steps:

- (i) The canonic and GIC structures of each filter were scaled for all possible section sequences [45].
- (ii) The noise spectrum for each filter structure was obtained by computing the relative PSD given by

$$\text{PSD} = 10 \log_{10} \{ S_o(\omega) / S_i(\omega) \}$$

- (iii) The optimum section sequence from the point of view of signal-to-noise ratio was chosen for each synthesis.

The scaling multipliers and filter parameters for both canonic and GIC structures of the four filters designed in Section 2.4 are summarized in Tables 3.2-3.5. For the wave structures, the scaling multipliers were incorporated in the adaptors.

The results obtained for the noise spectrum computed according to step 2 above are given in Figs. 3.12-3.15. As can be seen in Figs. 3.12-3.15, the GIC synthesis leads to a significant improvement in the inband signal-to-noise ratio in the lowpass and bandstop filters and also in the delay equalizer. For the bandpass filter, however, a better performance can be achieved by using the Sedlmeyer-Fettweis approach.

For the lowpass and bandpass filters, the wave structures have better inband signal-to-noise ratio than the corresponding cascade canonic structures. For the bandstop filter, however, the cascade canonic structure is preferable to the wave structure.

### 3.5 CONCLUSIONS

The effect of product quantization has been examined by evaluating the PSD of the quantization noise superimposed on the output signal in the digital filter structures considered. The digital filter structures of interest have been scaled by employing a scaling technique due to Jackson. The various structures were then compared.

TABLE 3.2 LOWPASS FILTER PARAMETERS AFTER SCALING (GIC AND CASCADE CANONIC SYNTHESSES)

j	$b_{0j}$	$b_{1j}$	$m_{1j}$	$m_{2j}$	$\lambda_j$ GIC Structure	$\lambda_j$ Canonic Structure
0	-	-	-	-	1.278562e-1	4.144133e-2
1	1.069676e+6	5.353680e+2	-8.342350e-1	5.701500e-1	4.191412e-1	8.654204e-2
2	1.069676e+6	1.462653e+3	-8.650900e-1	2.778910e-1	6.459184e-1	9.495136e-2
3	1.069676e+6	1.998021e+3	-8.781810e-1	1.538890e-1	3.611187e 0	-

~~$a_{0j} = b_{0j}$~~   
 $a_{1j} = 0$   
 $a_{2j} = 0$

TABLE 3.3 BANDSTOP FILTER PARAMETERS AFTER SCALING (GIC AND CASCADE CANONIC SYSTHESES)

j	$a_{0j}$	$b_{0j}$	$b_{1j}$	$m_{1j}$	$m_{2j}$	$\lambda_j$ GIC Structure	$\lambda_j$ Canonic Structure
0	-	-	-	-	-	$3.006675 \times 10^{-1}$	$4.623281 \times 10^{-1}$
1	$3.282806 \times 10$	$3.282806 \times 10$	$1.332661 \times 10$	$-5.376719 \times 10^{-1}$	$-5.376719 \times 10^{-1}$	$6.080126 \times 10^{-1}$	$4.001785 \times 10^{-1}$
2	$3.705629 \times 10$	$9.644825 \times 10$	2.435375	$3.467606 \times 10^{-1}$	$-5.416035 \times 10^{-1}$	$6.178220 \times 10^{-1}$	1.548355
3	$2.908229 \times 10$	$1.117368 \times 10$	$8.289280 \times 10^{-1}$	$-5.416035 \times 10^{-1}$	$3.467606 \times 10^{-1}$	1.106745	-

$a_{1j} = 0$

$a_{2j} = 1$

$k_{0j} = a_{0j}/b_{0j}$

TABLE 3.4 BANDPASS FILTER PARAMETERS AFTER SCALING (GIC AND CASCADE CANONIC SYNTHESSES)

j	$a_{0j}$	$b_{0j}$	$b_{1j}$	$m_{1j}$	$m_{2j}$	$\lambda_j^j$ GIC Structure	$\lambda_j^j$ Canonic Structure
0	-	-	-	-	-	$5.980234 \times 10^{-2}$	$7.532642 \times 10^{-3}$
1	1.279553	1.178123	$1.455204 \times 10^{-2}$	$-6.620924 \times 10^{-1}$	$6.520753 \times 10^{-1}$	$2.926817 \times 10^{-1}$	$4.757409 \times 10^{-1}$
2	$9.948942 \times 10^{-1}$	1.080529	$1.393597 \times 10^{-2}$	$-6.956174 \times 10^{-1}$	$6.758861 \times 10^{-1}$	$5.275565 \times 10^{-1}$	$4.033963 \times 10^{-1}$
3	0	1.128254	$3.271554 \times 10^{-2}$	$-6.761042 \times 10^{-1}$	$6.535637 \times 10^{-1}$	1.750283	-

$$a_{11} = a_{12} = 0, \quad a_{13} = 4.229751 \times 10^{-3}$$

$$a_{21} = a_{22} = 1, \quad a_{23} = 0$$

$$k_{0j} = a_{0j}/b_{0j}$$



TABLE 3.5 DELAY EQUALIZER PARAMETERS AFTER SCALING (GIC AND CASCADE CANONIC SYNTHESSES)

j	$b_{0j}$	$b_{1j}$	$m_{1j}$	$m_{2j}$	$\lambda_j$ GIC Structure	$\lambda_j$ Canonic Structure
0	-	-	-	-	2.44872e-1	2.03188e-2
1	2.90791e+2	2.96640e+2	-6.75325e-1	6.48386e-1	4.15957e-1	8.58102e-1
2	3.71481e+2	5.05382e+2	-6.68576e-1	6.47733e-1	5.63558e-1	1.30512e 0
3	4.27979e+2	5.88548e+2	-6.82027e-1	6.63578e-1	2.17763e 0	4.39453e+1

$a_{0j} = b_{0j}$

$a_{1j} = -b_{1j}$

$a_{2j} = 1$

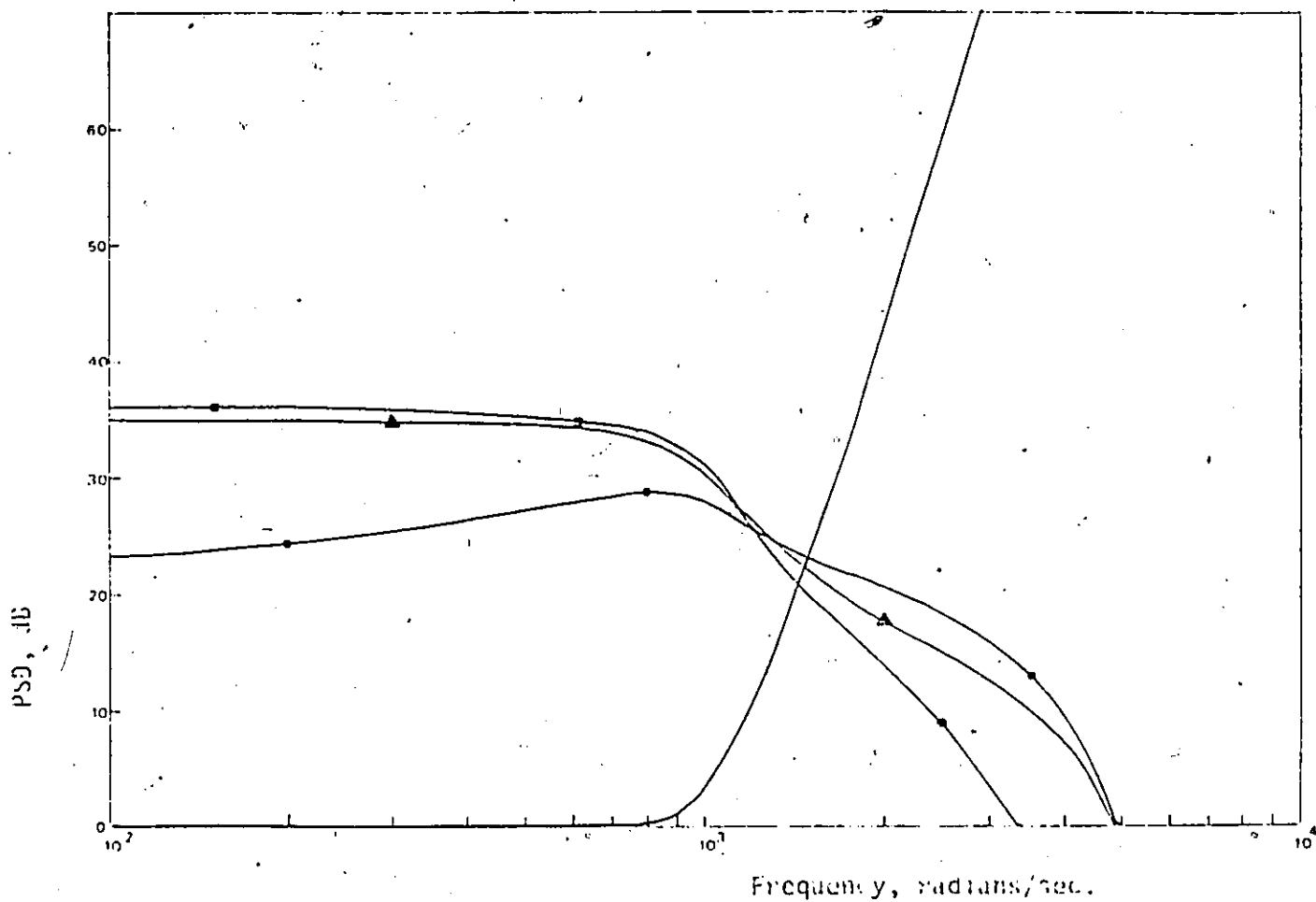


FIG. 3.12 PSD versus Frequency (Butterworth Lowpass Filter)

- — ● GIC
- — ■ Canonic
- ▲ — ▲ Wave
- Loss Characteristic

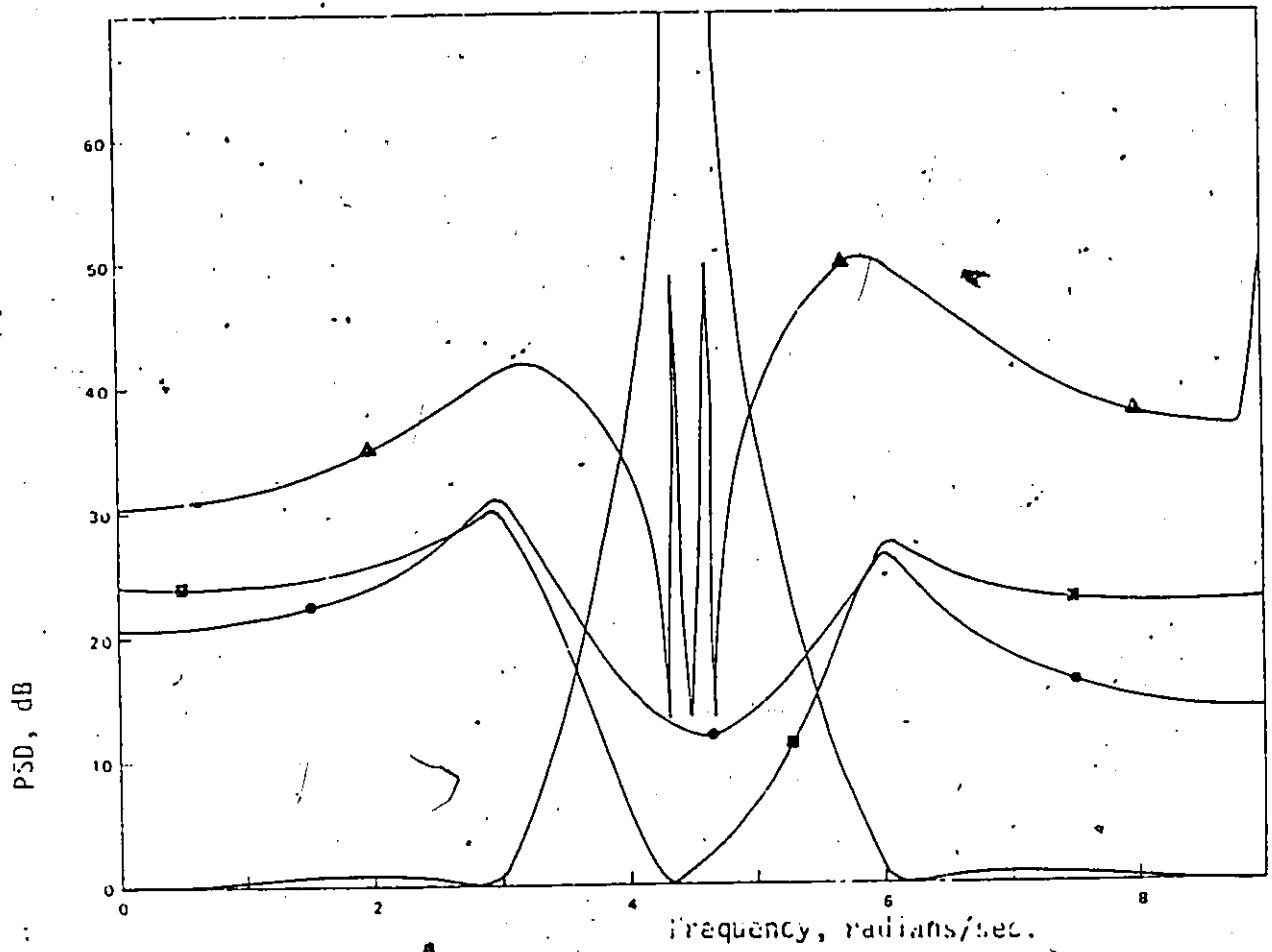


FIG. 3.13 PSD versus Frequency (Elliptic Bandstop Filter)

- — ● GIC
- — ■ Canonic
- ▲ — ▲ Wave
- Loss Characteristic

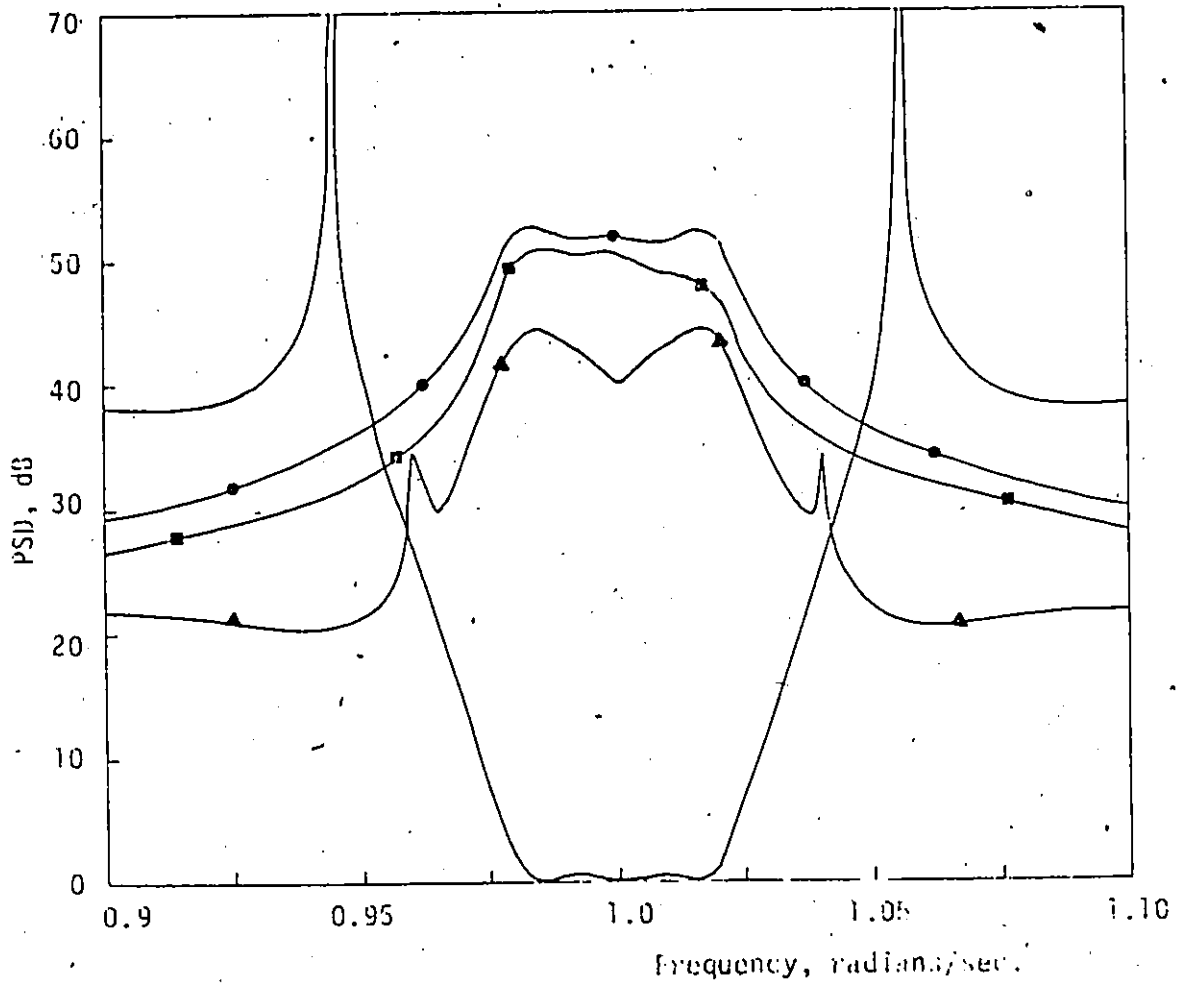


FIG. 3.14 PSD versus Frequency (Elliptic Bandpass Filter)

- — ● GIC
- — ■ Canonic
- ▲ — ▲ Wave
- Loss Characteristic

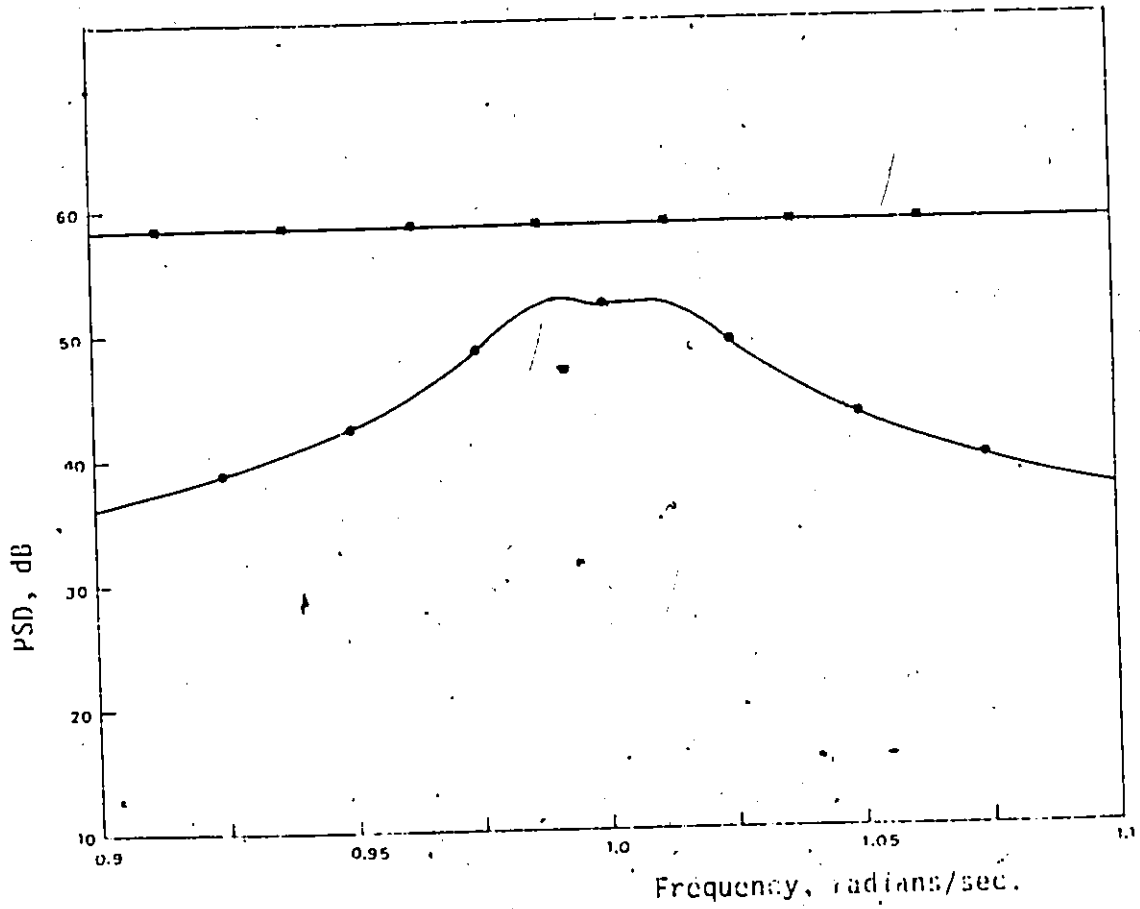


FIG. 3.15 PSD versus Frequency (Delay Equalizer)

—●— GIC  
—■— Canonic

An attractive feature in the GIC structures is that the quantization noise generated by multipliers  $m_1$  and  $m_2$  is subjected to a bandpass transfer function in each of the universal sections. Because of this fact, the GIC synthesis yields lowpass and bandstop filters, and also digital equalizers with improved inband signal-to-noise ratio relative to that in the cascade canonic and wave syntheses.

For the lowpass and bandpass filters, the wave structures have better inband signal-to-noise ratio than the corresponding cascade canonic structures. For the bandstop filter, however, the cascade canonic structure is preferable to the wave structure.

## CHAPTER 4

### COEFFICIENT QUANTIZATION

#### 4.1 INTRODUCTION

As was pointed out in Chapter 1 quantization of the transfer function coefficients introduces perturbations in the zeros and poles of the transfer function. Therefore, coefficient quantization errors manifest themselves as errors in the frequency response, which tend to increase as the wordlength used in the implementation is decreased.

In this chapter, a brief review for the sensitivity analysis of a digital filter is first given. Next, a procedure for evaluating the exact wordlength as well as a procedure for evaluating a statistical wordlength are described. By using these procedures, the required wordlengths for the various digital filters considered in Section 2.4 are obtained. Subsequently, a comparison is made between the GIC synthesis and the cascade canonic and wave syntheses.

#### 4.2 SENSITIVITY ANALYSIS

This section provides a sensitivity analysis which can be used to study the effects of coefficient quantization.

Consider the digital network shown in Fig. 4.1, and let  $H(z)$  be the transfer function between input and output. The sensitivity of  $H(z)$  with respect to variations in coefficient  $a_j$  is defined as

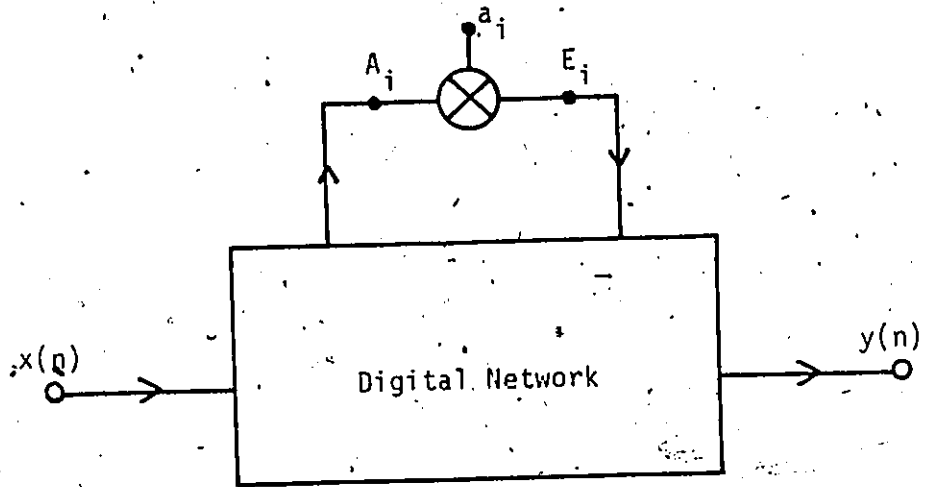


FIG. 4.1 Digital-Network Model for Sensitivity Analysis



$$S_{a_i} = \frac{\partial \{H(z)\}}{\partial a_i} \quad (4.1)$$

This formula can be expressed as

$$S_{a_i} = \frac{\partial \{H(z)\}}{\partial a_i} = H_{A_i}(z) \cdot H_{E_i}(z) \quad (4.2)$$

by using the transpose or adjoint approach [49], [50], where  $H_{A_i}(z)$ , is the transfer function between the input to the filter and node  $A_i$ , and  $H_{E_i}(z)$  is the transfer function between node  $E_i$  and the output of the filter. By letting

$$H(e^{j\omega T}) = M(\omega) e^{j\theta(\omega)} \quad (4.3)$$

where  $M(\omega)$ , and  $\theta(\omega)$  are the gain and phase shift of the filter, respectively, Eqn. 4.1 gives

$$\begin{aligned} \frac{\partial H(e^{j\omega T})}{\partial a_i} &= \frac{\partial \{M(\omega) e^{j\theta(\omega)}\}}{\partial a_i} \\ &= e^{j\theta(\omega)} S_{a_i}^M + jM(\omega) e^{j\theta(\omega)} S_{a_i}^\theta \end{aligned} \quad (4.4)$$

$$= \text{Re} \left\{ \frac{\partial H(e^{j\omega T})}{\partial a_i} \right\} + j \text{Im} \left\{ \frac{\partial H(e^{j\omega T})}{\partial a_i} \right\} \quad (4.5)$$

where

$$S_{a_i}^M = \frac{\partial M(\omega)}{\partial a_i}, \quad S_{a_i}^\theta = \frac{\partial \theta(\omega)}{\partial a_i}$$

After some manipulation, Eqns. 4.4 and 4.5 give

$$\frac{\partial M(\omega)}{\partial a_i} = \cos\{\theta(\omega)\} \left[ \operatorname{Re} \left\{ \frac{\partial H(e^{j\omega T})}{\partial a_i} \right\} \right] + \sin\{\theta(\omega)\} \left[ \operatorname{Im} \left\{ \frac{\partial H(e^{j\omega T})}{\partial a_i} \right\} \right] \quad (4.6)$$

The quantity  $\partial M/\partial a_i$  is known as the sensitivity of the gain with respect to variations in coefficient  $a_i$ . The gain sensitivity can be evaluated by using the following steps:

- (i) Form the real and imaginary parts of the quantity  $S_{a_i}$  by using Eqn. 4.2
- (ii) Find the phase angle  $\theta(\omega)$  of  $H(e^{j\omega T})$
- (iii) Compute  $\partial M(\omega)/\partial a_i$  by using Eqn. 4.6.

The above sensitivity analysis can be readily carried out by obtaining the various transfer functions of the digital filter structure under investigation. For the canonic section of Fig. 4.2 the required transfer functions are

$$H_{A_1}(z) = \frac{(1+m_1)z}{z^2 + B_1z + B_0}$$

$$H_{A_2}(z) = \frac{1+m_1}{z^2 + B_1z + B_0}$$

and

$$H_{E_1}(z) = H_{E_2}(z) = \frac{z^2 + 2z + 1}{z^2 + B_1z + B_0}$$

Similarly, for the GIC section of Fig. 4.3 the required transfer functions are

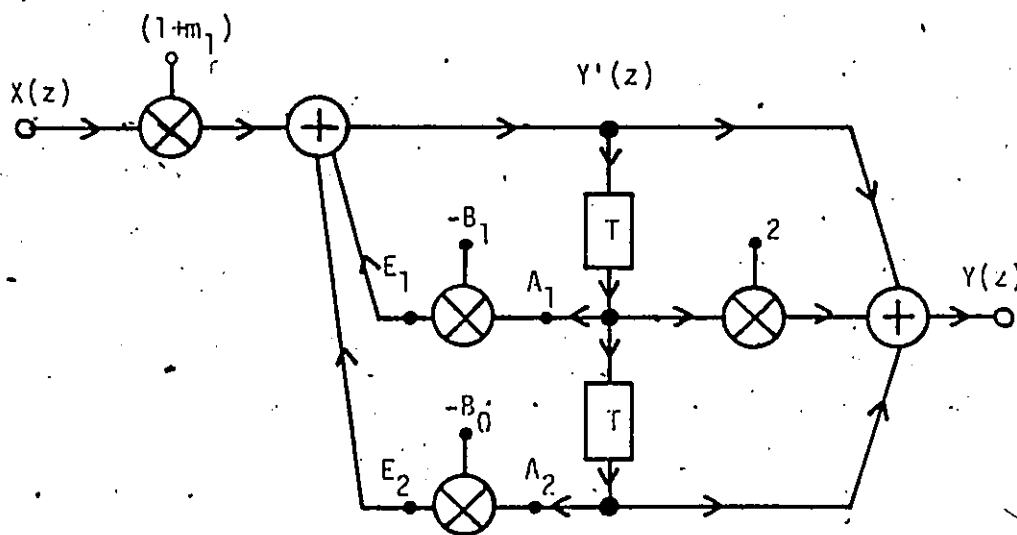


FIG. 4.2 Second-Order Canonic Lowpass Section Model for Sensitivity Analysis

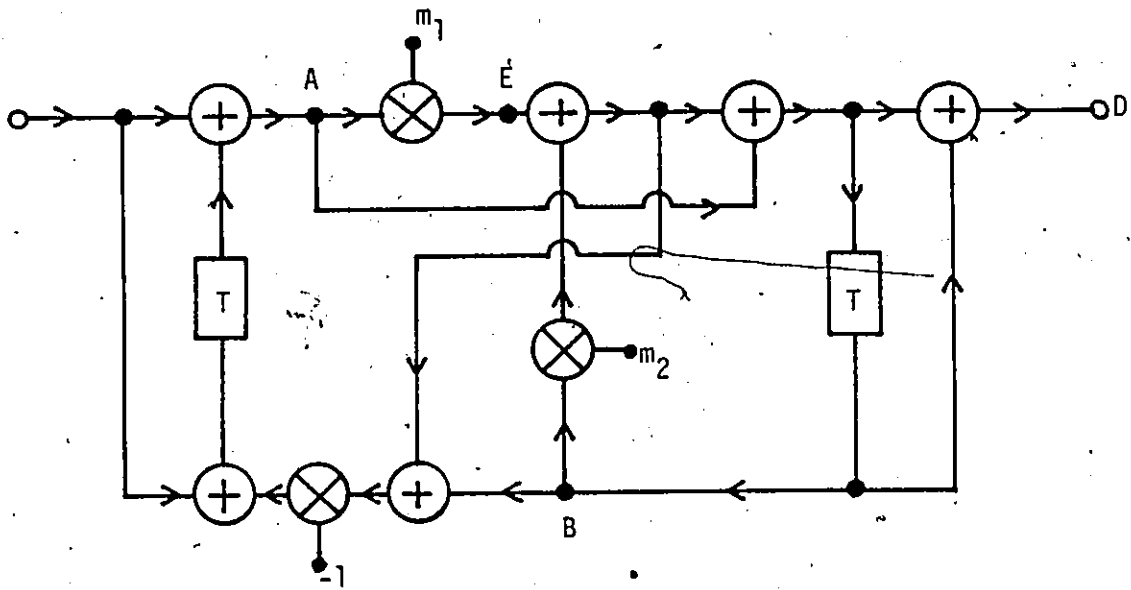


FIG. 4.3 Lowpass GIC Second-Order Section Model for Sensitivity Analysis

$$H_A(z) = \frac{z^2 + (1-m_2)z - m_2}{z^2 + (m_1 - m_2)z + 1 + m_1 + m_2}$$

$$H_B(z) = \frac{(z+1)(1+m_1)}{z^2 + (m_1 - m_2)z + 1 + m_1 + m_2}$$

and

$$H_E(z) = \frac{z^2 - 1}{z^2 + (m_1 - m_2)z + 1 + m_1 + m_2}$$

The above sensitivity analysis can also be applied to wave structures. The only difference is the expressions for the required transfer functions are somewhat complicated.

#### 4.3 EXACT WORDLENGTH

The wordlength necessary to represent the coefficients of a digital-filter transfer function such that the desired specifications can be exactly satisfied, is called the exact wordlength. This section describes a procedure which can be used to evaluate the exact wordlength. Consider, a digital filter characterized by  $H(z)$ , and let:

$M(\omega)$  = amplitude response without coefficient quantization ( $= |H(e^{j\omega T})|$ ) .

$M_Q(\omega)$  = amplitude response with the coefficients quantized.

$M_I(\omega)$  = idealized amplitude response.

$\delta_p$  ( $\delta_a$ ) = passband (stopband) tolerance of the amplitude response.

These quantities are illustrated in Fig. 4.4.

The effect of coefficient quantization is to introduce an error  $\Delta M$  in  $M(\omega)$  given by

$$\Delta M = M(\omega) - M_Q(\omega) \quad (4.7)$$

The maximum permissible value of  $|\Delta M|$ , denoted by  $\Delta M_{\max}(\omega)$  can be deduced from Fig. 4.4 as

$$\Delta M_{\max}(\omega) = \begin{cases} \delta_p - |M(\omega) - M_I(\omega)| & \text{for } \omega \leq \omega_p \\ \delta_a - |M(\omega) - M_I(\omega)| & \omega \geq \omega_a \end{cases}$$

and if

$$|\Delta M| \leq \Delta M_{\max}(\omega) \quad (4.8)$$

the desired specifications will be satisfied. The required wordlength can be determined exactly by evaluating  $|\Delta M|$  as a function of frequency for successively larger values of the wordlength until Eqn. 4.8 is satisfied.

#### 4.4 STATISTICAL WORDLENGTH

Recently, a number of alternative approaches for the study of coefficient quantization effects have been suggested [51]-[63].

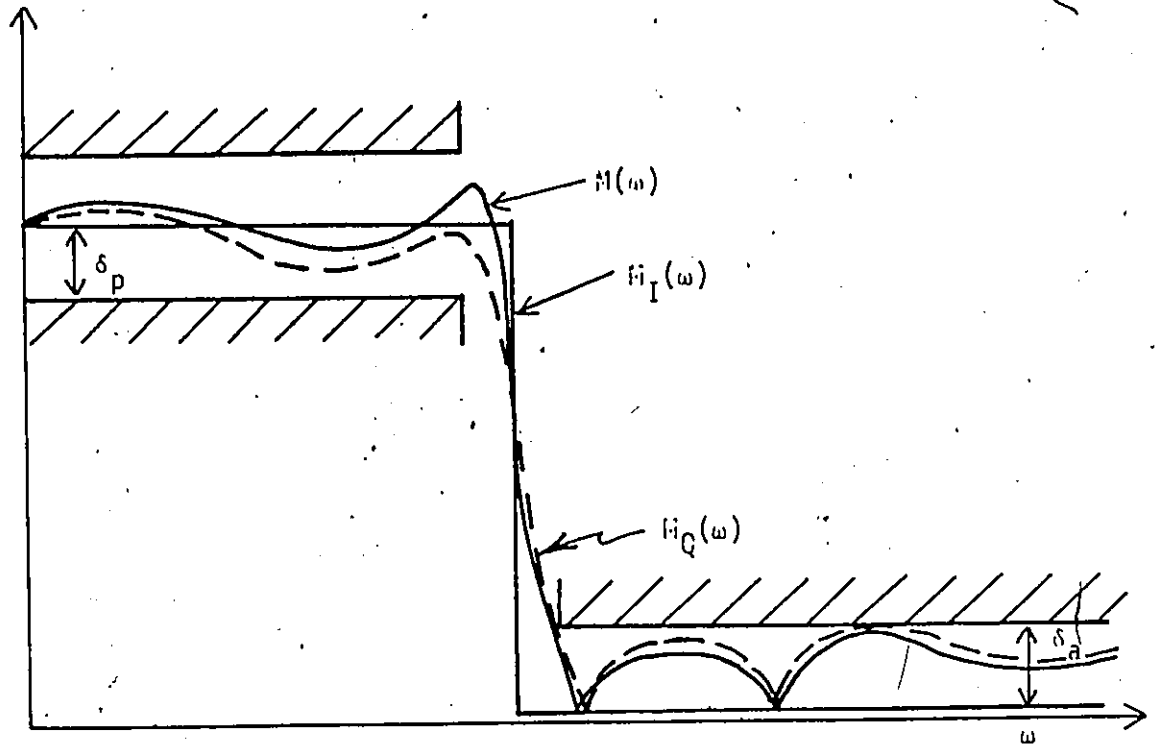


FIG. 4.4 Amplitude Response of a Digital Filter

Of particular interest here is the statistical approach proposed by Avenhaus [59] and latter modified by Crochiere [60]. As will be shown, this method leads to a fairly accurate estimate for the required wordlength. The details of this approach are as follows.

Consider a fixed-point implementation and assume that quantization is carried out by rounding. The error in coefficient  $a_i$  ( $i=1,2,\dots,m$ ), denoted by  $\Delta a_i$  brought about by quantization can assume any value in the range  $-q/2$  to  $q/2$ , i.e.  $\Delta a_i$  is a random variable. If  $\Delta a_i$  is assumed to have a uniform probability density, that is

$$p(\Delta a_i) = \begin{cases} 1/q & -q/2 \leq \Delta a_i \leq q/2 \\ 0 & \text{otherwise} \end{cases}$$

then from Eqns. 3.12 and 3.13

$$E\{\Delta a_i\} = 0 \quad (4.9)$$

and

$$\sigma_{\Delta a_i}^2 = \frac{q^2}{12} \quad (4.10)$$

The variation  $\Delta M$  in  $M(\omega)$  is also a random variable and is given by

$$\Delta M = \sum_{i=1}^m \Delta a_i S_{a_i}^M$$

where

$$S_{a_i}^M = \frac{\partial M(\omega)}{\partial a_i}$$



is the sensitivity of  $M(\omega)$  with respect to variations in  $a_i$ .

Evidently,

$$\begin{aligned} E\{\Delta M\} &= \sum_{i=1}^m S_{a_i}^M E\{\Delta a_i\} \\ &= 0 \end{aligned}$$

according to Eqn. 4.9. If  $\Delta a_i$  and  $\Delta a_j$  ( $i \neq j$ ) are assumed to be statistically independent, it can be shown that

$$\sigma_{\Delta M}^2 = \sum_{i=1}^m \sigma_{\Delta a_i}^2 (S_{a_i}^M)^2$$

and therefore, from Eqn. 4.10

$$\sigma_{\Delta M}^2 = q^2 S_T^2 / 12 \quad (4.11)$$

where

$$S_T^2 = \sum_{i=1}^m (S_{a_i}^M)^2$$

For a large value of  $m$ ,  $\Delta M$  is approximately Gaussian, with zero mean, and thus

$$p(\Delta M) = \frac{1}{\sigma_{\Delta M} \sqrt{(2\pi)}} e^{-\Delta M^2 / 2\sigma_{\Delta M}^2} \quad -\infty \leq \Delta M \leq \infty$$

Consequently,  $\Delta M$  will be in some range  $-\Delta M_1 \leq \Delta M \leq \Delta M_1$  with a confidence factor  $\gamma$  given by

$y = \text{probability } [|\Delta M| \leq \Delta M_1]$

$$= \frac{2}{\sigma_{\Delta M} \sqrt{2\pi}} \int_0^{\Delta M_1} e^{-\Delta M^2 / 2\sigma_{\Delta M}^2} d(\Delta M) \quad (4.12)$$

By letting

$$\left. \begin{aligned} \Delta M &= x \sigma_{\Delta M} \\ \Delta M_1 &= x_1 \sigma_{\Delta M} \end{aligned} \right\} \quad (4.13)$$

Eqn. 4.12 can be simplified to

$$y = \frac{2}{\sqrt{2\pi}} \int_0^{x_1} e^{-x^2/2} dx$$

Once an acceptable confidence factor  $y$  is selected, a corresponding value for  $x_1$  can be obtained from published tables or by using a numerical method. The quantity  $\Delta M_1$  is essentially a statistical bound on  $\Delta M$ . Therefore, if the wordlength is chosen such that

$$\Delta M_1 \leq \Delta M_{\max}(\omega) \quad (4.14)$$

the desired specifications will be satisfied to within a confidence factor  $y$ . The resulting wordlength is said to be the 'statistical wordlength'. From Eqns. 4.11, 4.13, and 4.14

$$\Delta M_1 = x_1 q S_T / \sqrt{12} \leq \Delta M_{\max}(\omega)$$

and, therefore

$$q \leq \sqrt{12} \Delta M_{\max}(\omega) / x_1 S_T \quad (4.15)$$

The register length should be sufficiently large to accommodate the largest coefficient. If the quantized value of the largest coefficient is

$$\sum_{i=-k}^j b_i 2^i$$

where  $b_j$  and  $b_{-k} \neq 0$ , then the required wordlength must be

$$W(\omega) = 1+j+k \quad (4.16)$$

By noting that  $q = 2^{-K}$  or

$$K = \log_2 (1/q) \quad (4.17)$$

and then using Eqns. 4.15, 4.16, and 4.17, the required result is obtained provided that the coefficient wordlength,  $W$  is chosen as:

$$W \geq w(\omega) = 1+j+\log_2 \left\{ \frac{x_1 S_T}{\sqrt{12} \Delta M_{\max}(\omega)} \right\} \quad (4.18)$$

where  $W(\omega)$  is the statistical wordlength.

The value of  $x_1$  is usually assumed to be 2 [24], [60]. This corresponds to a confidence factor  $\gamma = 0.95$ . The sensitivities  $S_{a_i}^M$  can be computed efficiently by using the approach described in Section 4.2.

The statistical wordlength is generally easier to compute than the exact wordlength because the latter involves essentially a trial-and-error procedure.

#### 4.5 COMPARISON

The coefficient wordlength required in each of the digital filter structures designed in Section 2.4, has been computed first by using an exact method and then by using a statistical method. The results obtained were then used to compare the various structures.

The exact wordlength, for each filter structure was evaluated by analyzing the structure on a general-purpose digital computer. The coefficients were assumed to be in fixed-point, 2's complement representation. The wordlength was assumed to take values in the range 6-20 bits. The frequency response of each filter was evaluated and compared with the desired response and the maximum value of  $|\Delta M|$  over the passband was determined by using Eqn. 4.7. The average of  $|\Delta M|$  and the normalized standard deviation over the passband were also obtained for the same wordlength. These three parameters are plotted against the wordlength in Figs. 4.5-4.13. From these plots, the following results are evident:

- (i) For the lowpass and bandpass filters, the GIC structures are less sensitive to coefficient quantization as compared to the cascade canonic and the wave structures.

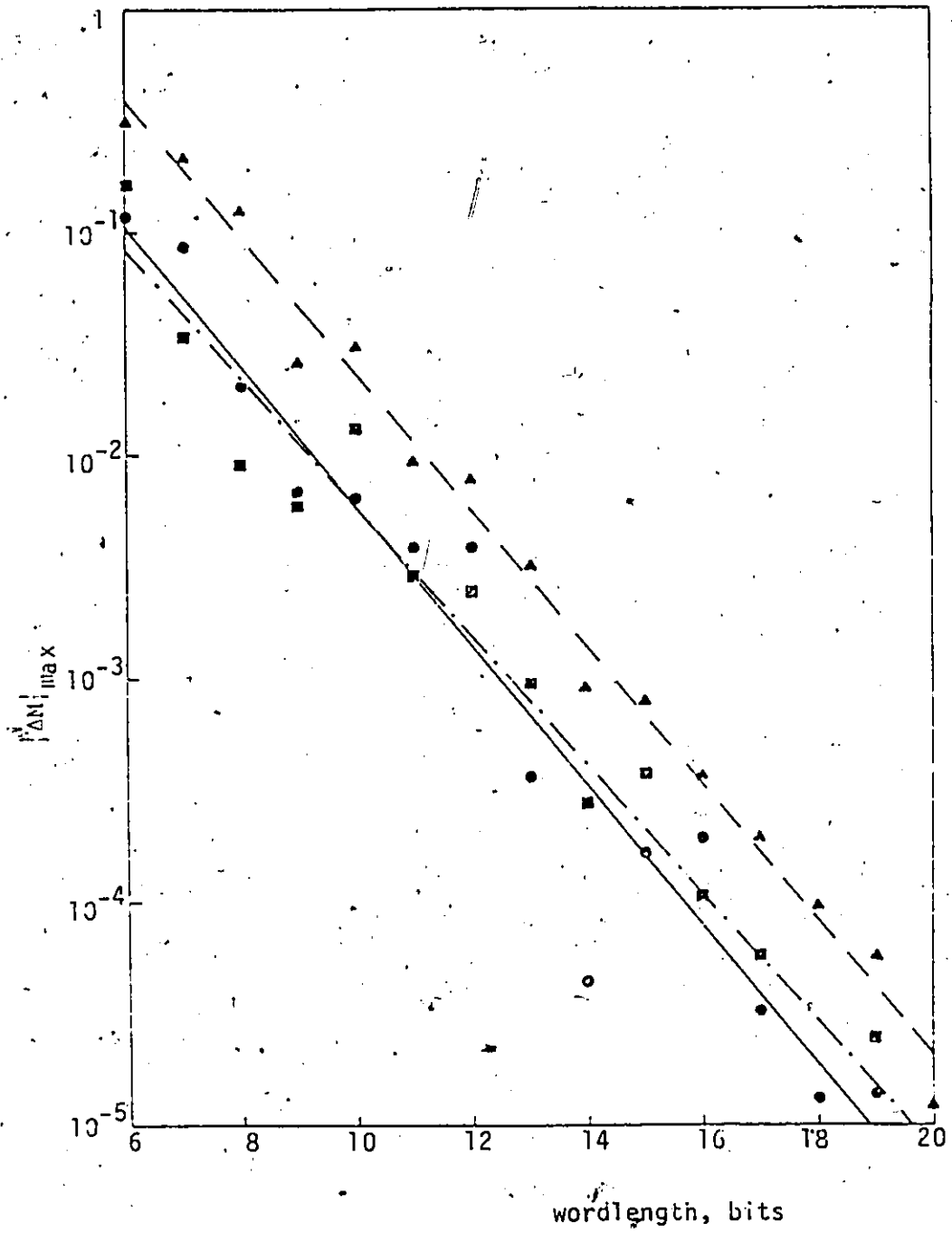
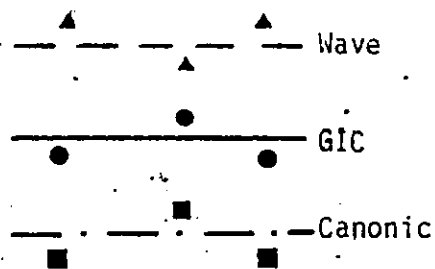


FIG. 4.5  $|\Delta M|_{max}$  versus Wordlength (Butterworth Lowpass Filter)



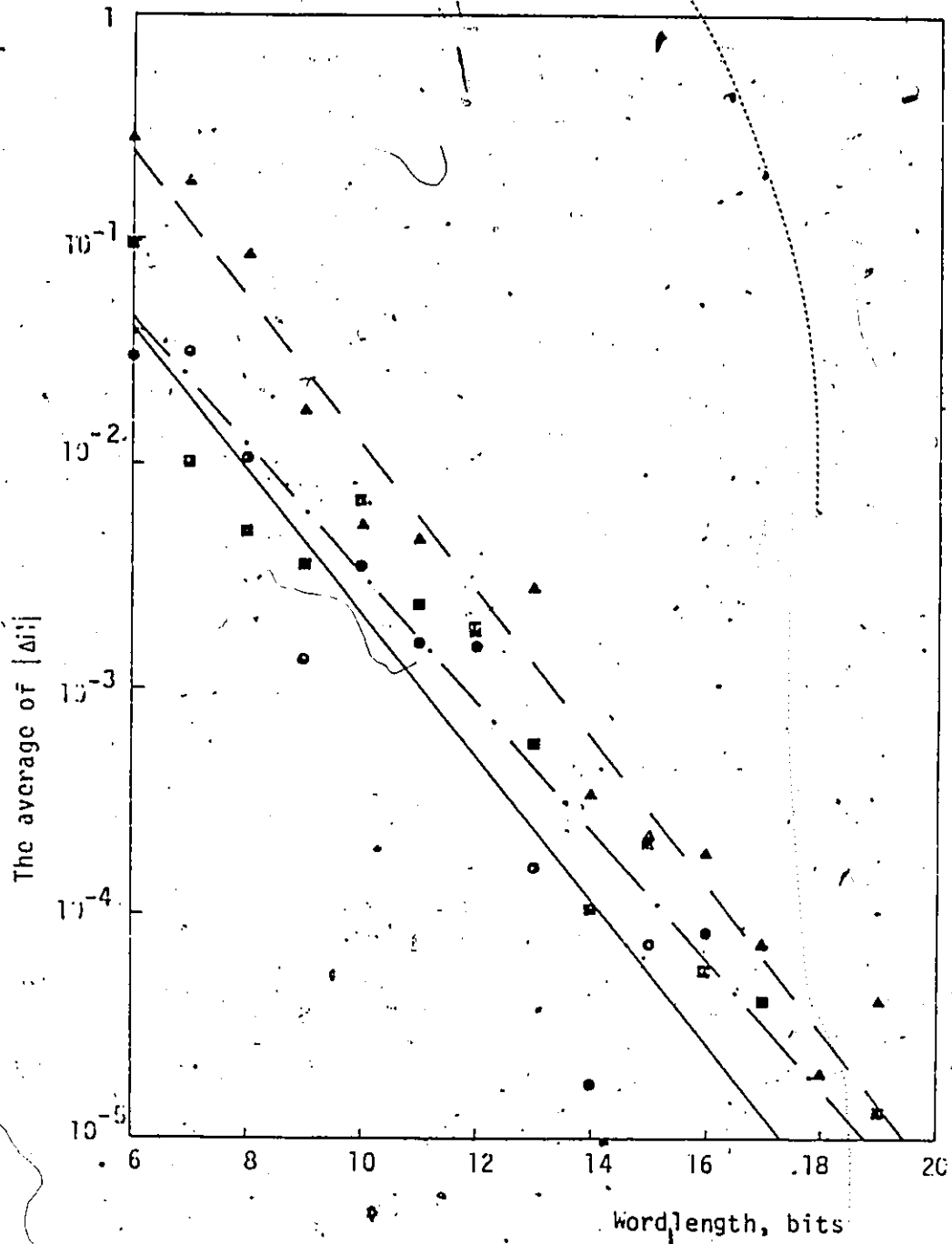
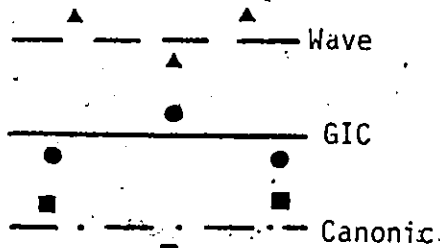


FIG. 4.6 The Average of  $|\Delta M|$  versus Wordlength (Butterworth Lowpass Filter)



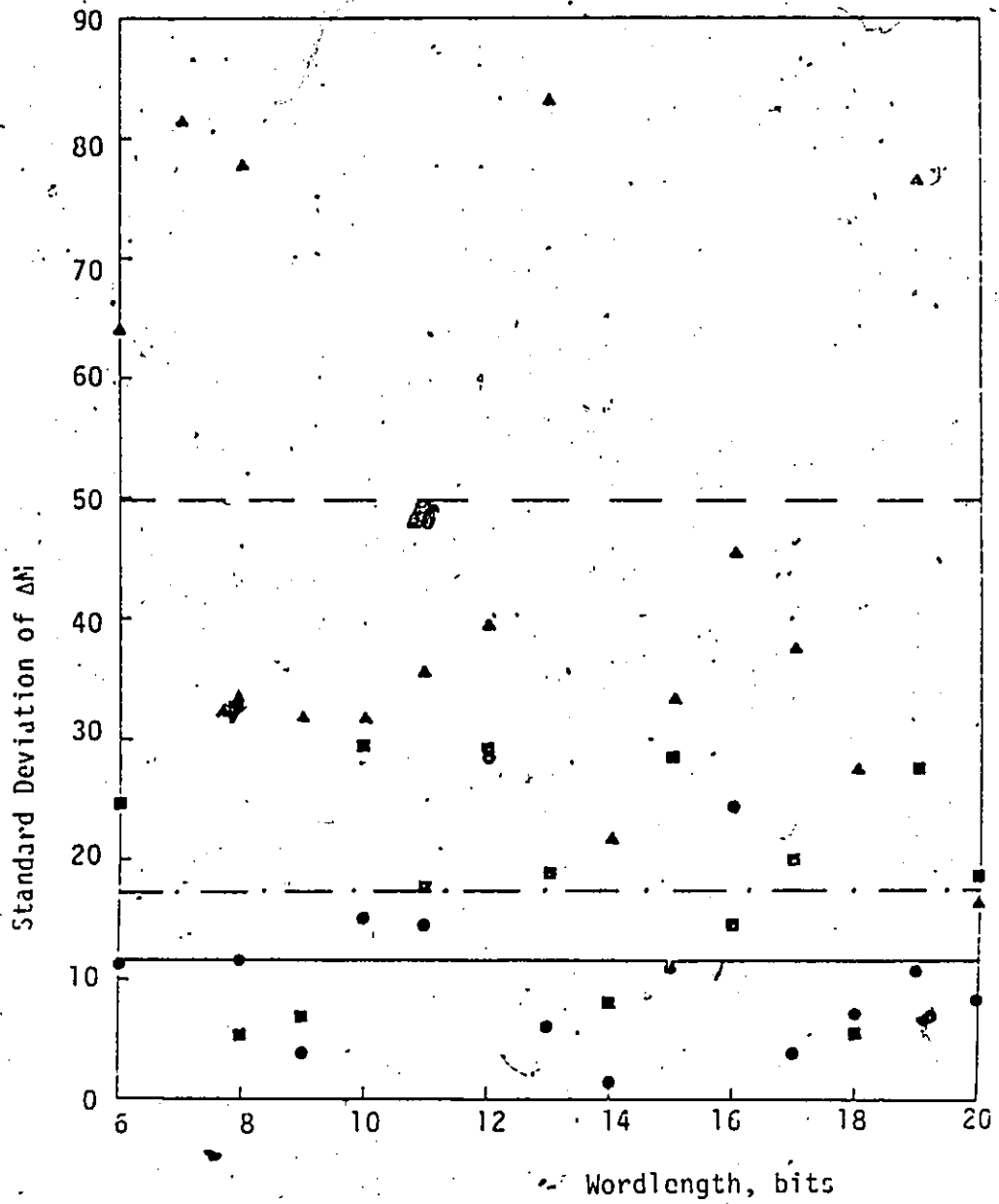
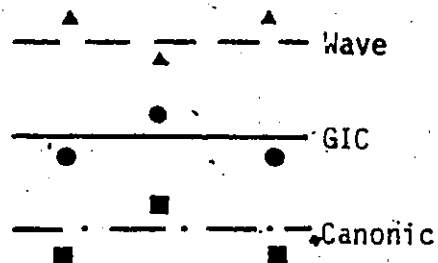


FIG. 4.7 Standard Deviation of  $\Delta M$  versus Wordlength (Butterworth Lowpass Filter)



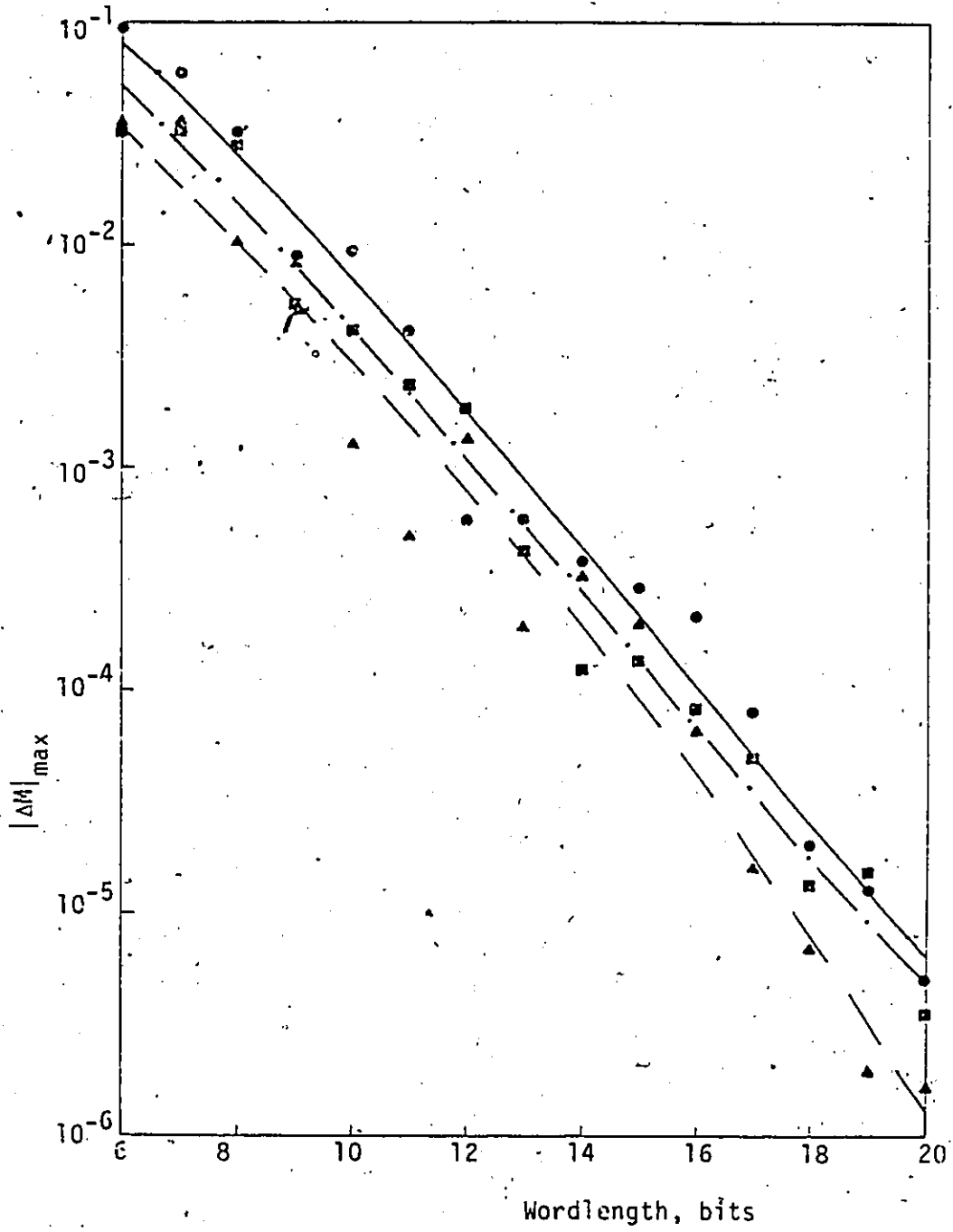
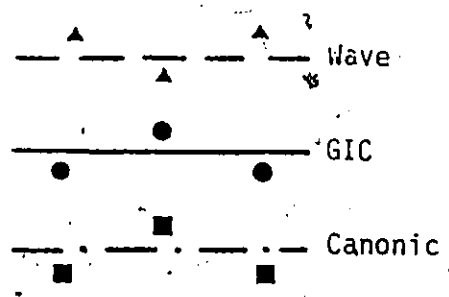


FIG. 4.8  $|\Delta M|_{\max}$  versus Wordlength (Elliptic Bandstop Filter)





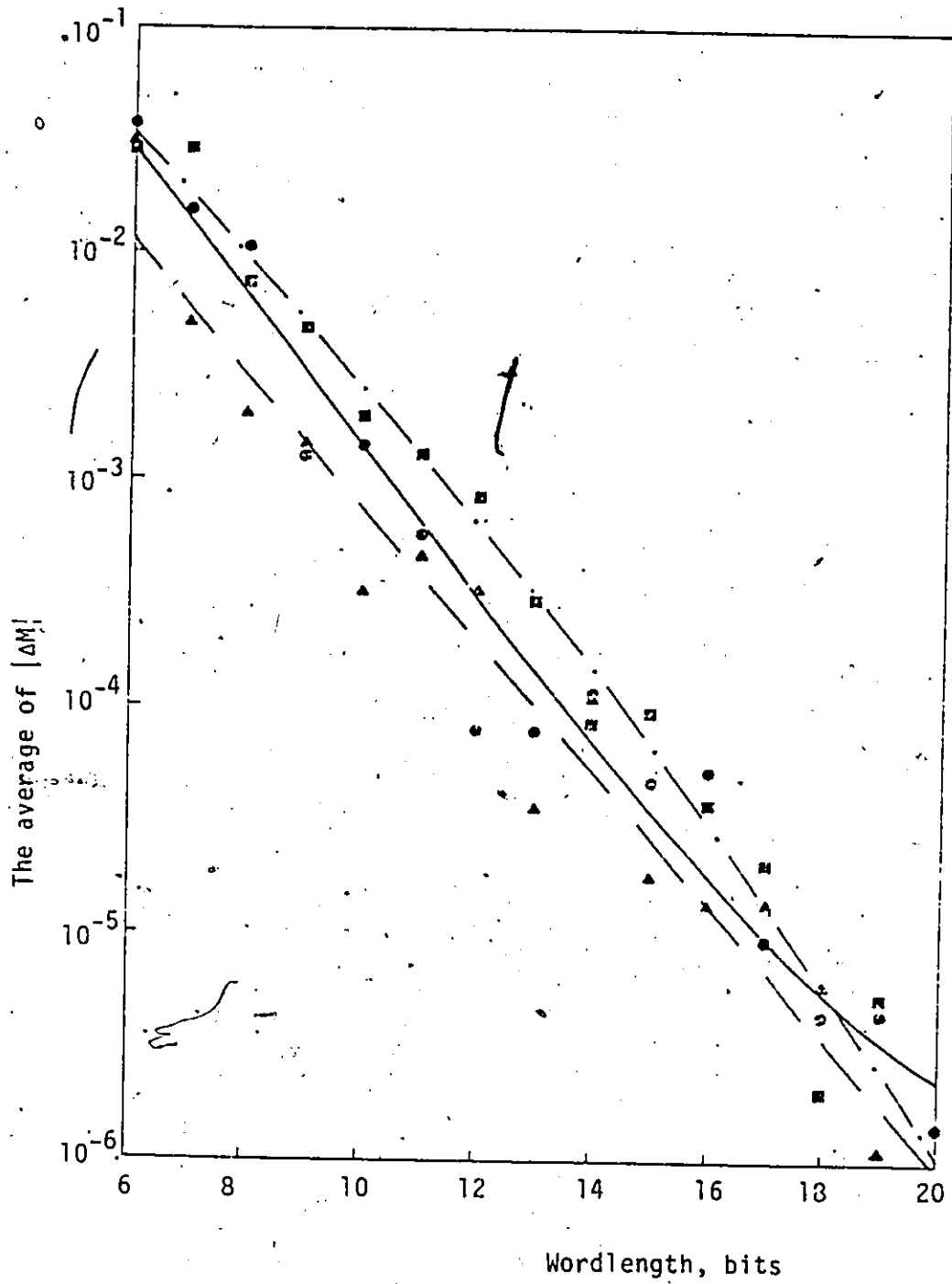
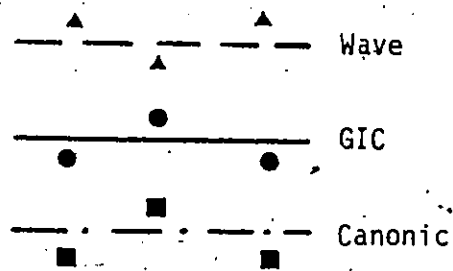


FIG. 4.9 The Average of  $|\Delta M|$  versus Wordlength (Elliptic Bandstop Filter)



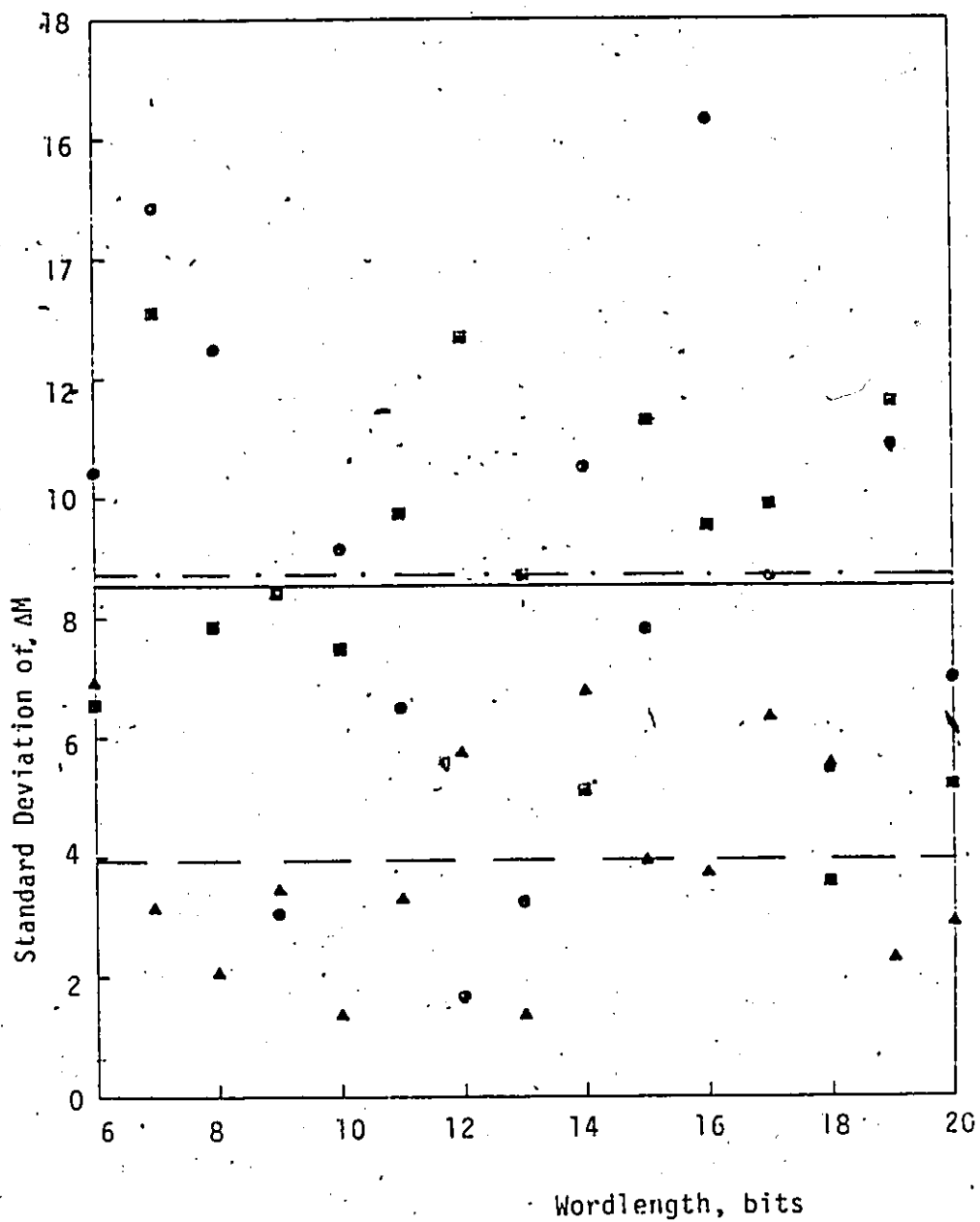
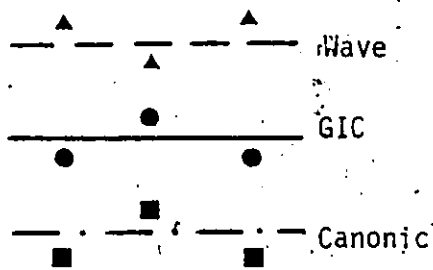


FIG. 4.10 Standard Deviation of  $\Delta M$  versus Wordlength (Elliptic Bandstop Filter).



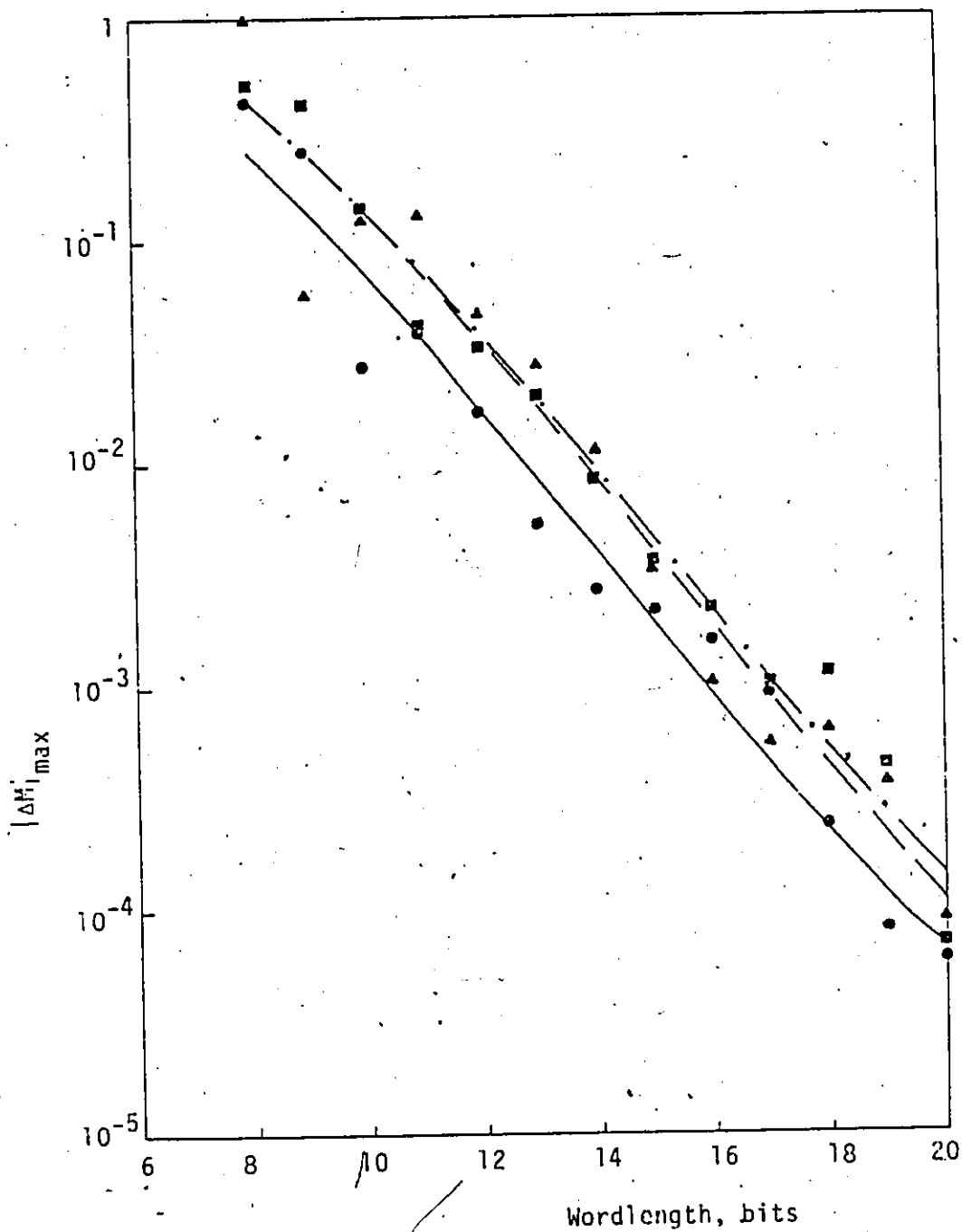
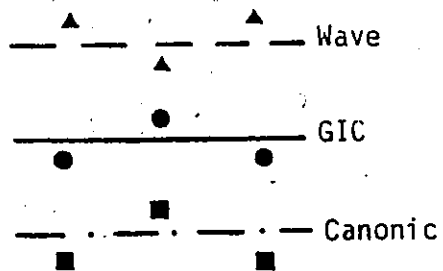


FIG. 4.11  $|\Delta M|_{\max}$  versus Wordlength (Elliptic Bandpass Filter)



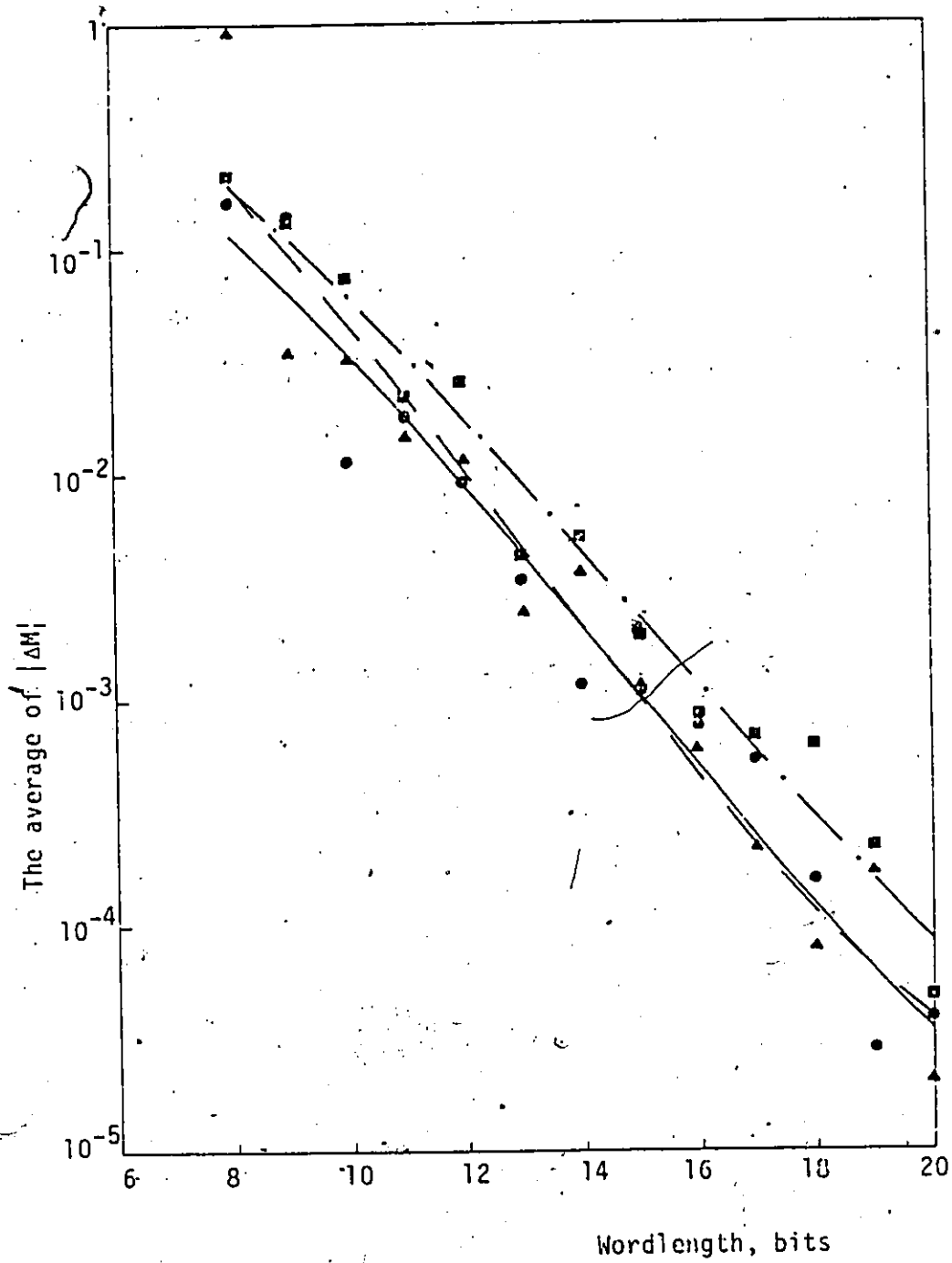
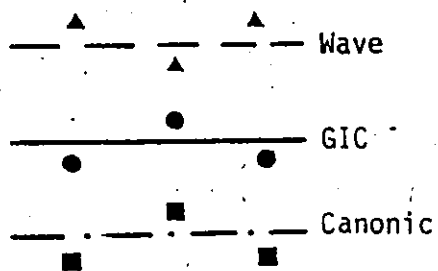


FIG. 4.12 The Average of  $|\Delta M|$  versus Wordlength (Elliptic Bandpass filter)



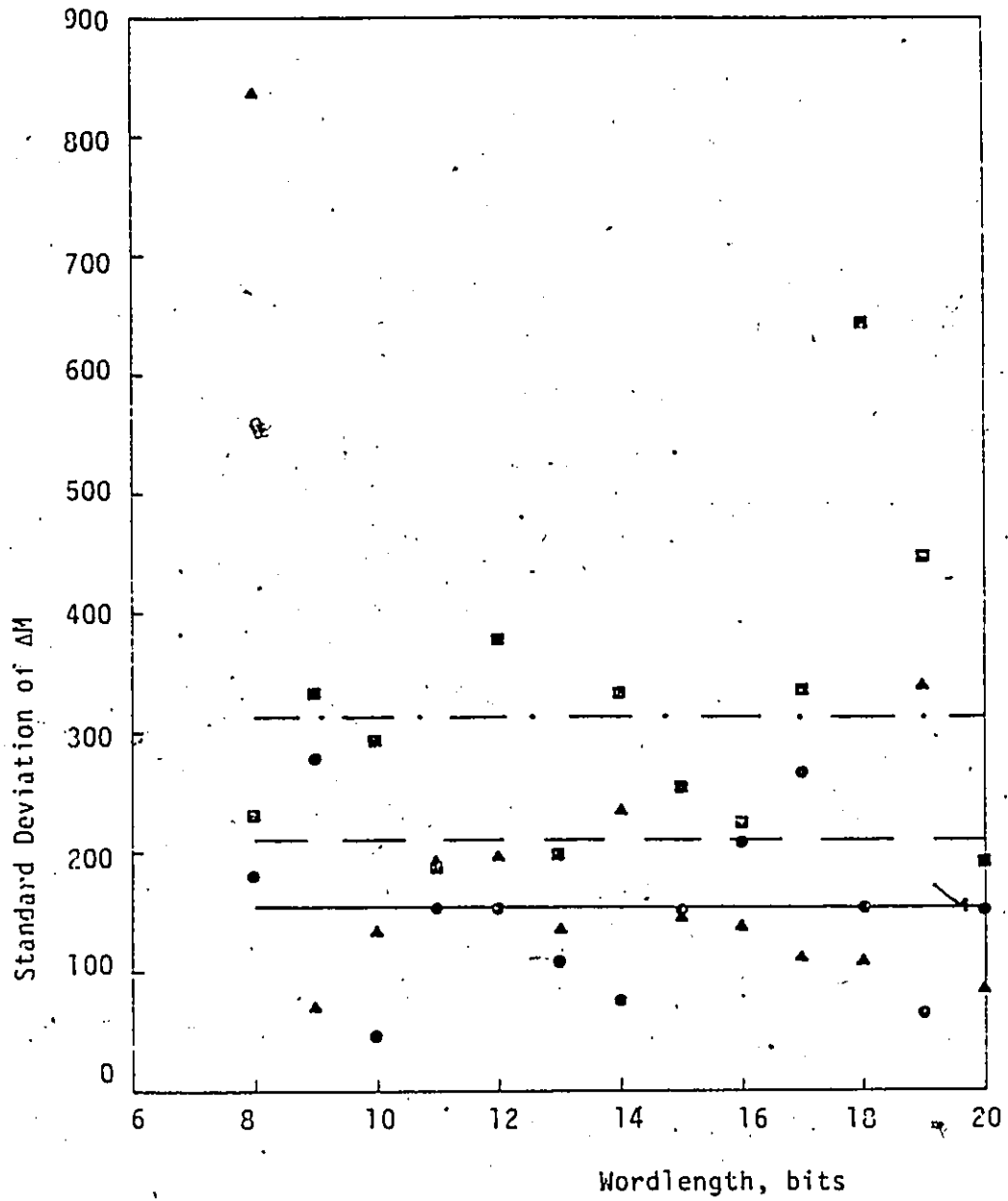
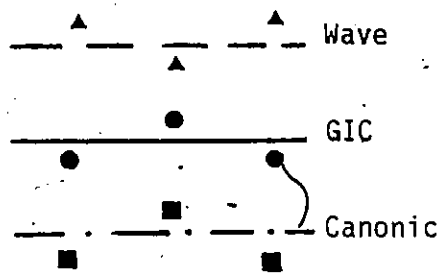


FIG. 4.13 Standard Deviation of  $\Delta M$  versus Wordlength (Elliptic Bandpass Filter)



- (ii) The lowpass cascade canonic structure gives better results than the corresponding wave structure. On the other hand, the bandpass wave structure gives slightly better results than the corresponding cascade canonic structure.
- (iii) For the bandstop filter, the wave structure gives the best results among the three types of structures. For this filter, the choice between cascade canonic and GIC structures is not clear cut. In the cascade canonic structure the quantity  $|\Delta M|_{\max}$  is slightly lower, while in the GIC structure the average of  $|\Delta M|$  and the average of the normalized standard deviation are slightly lower.

The statistical wordlength  $W(\omega)$  was computed as a function of frequency for each filter structure. The values of  $x_1$  and  $\Delta M_{\max}(\omega)$  in Eqn. 4.18 were assumed to be 2 and 0.02, respectively. The results obtained are given in Figs. 4.14-4.17. From these plots the following conclusions can be made:

- (i) For the lowpass and bandpass filters, the maximum value of  $W(\omega)$  is approximately the same in the GIC and cascade canonic structures while it is higher in the wave structures. However, the average value of  $W(\omega)$  over each passband is lower in the GIC structures relative to that in the corresponding cascade canonic and wave structures.

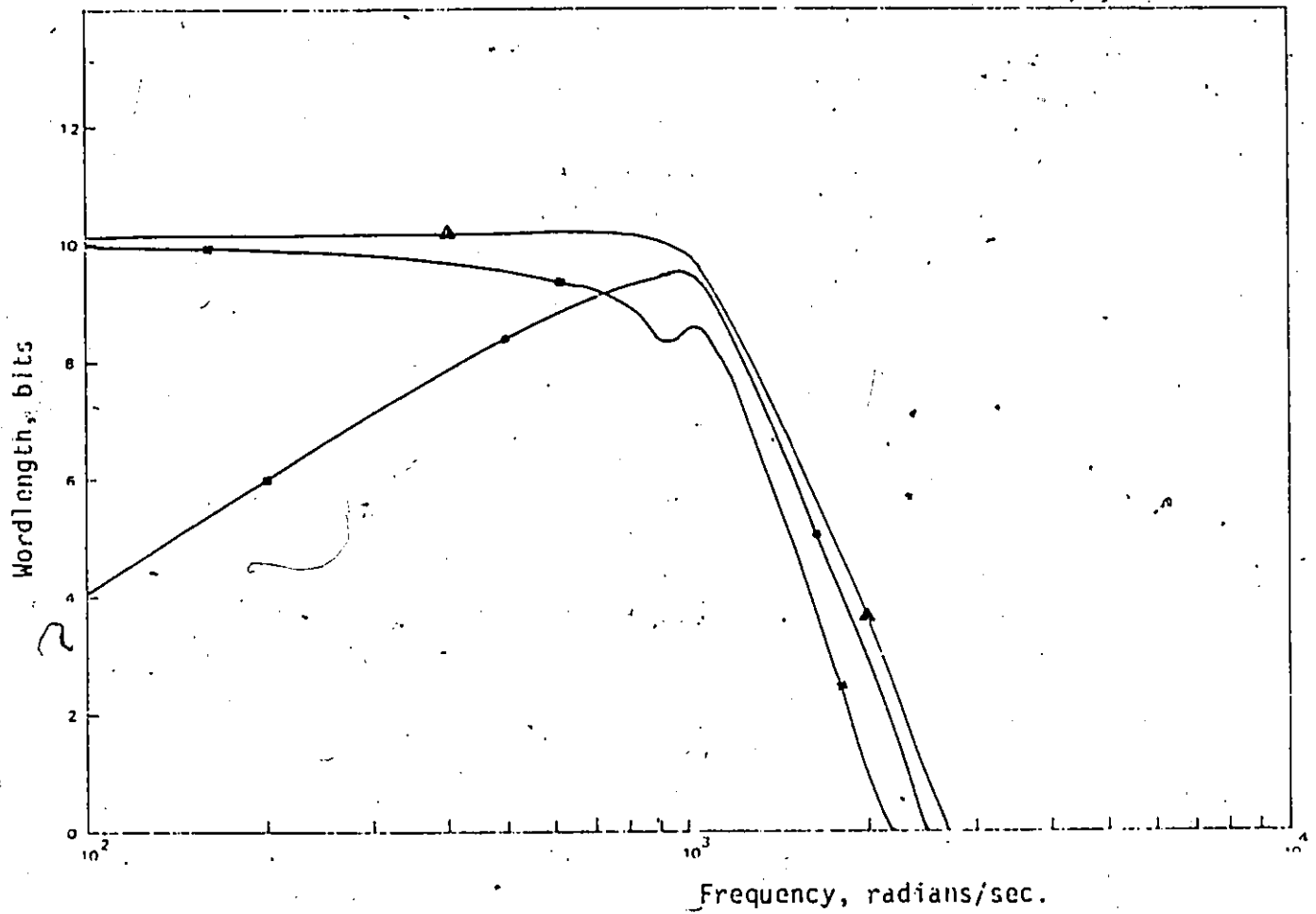


FIG. 4.14  $W(\omega)$  versus Frequency (Butterworth Lowpass Filter)

- — ● GIC
- — ■ Canonic
- ▲ — ▲ Wave

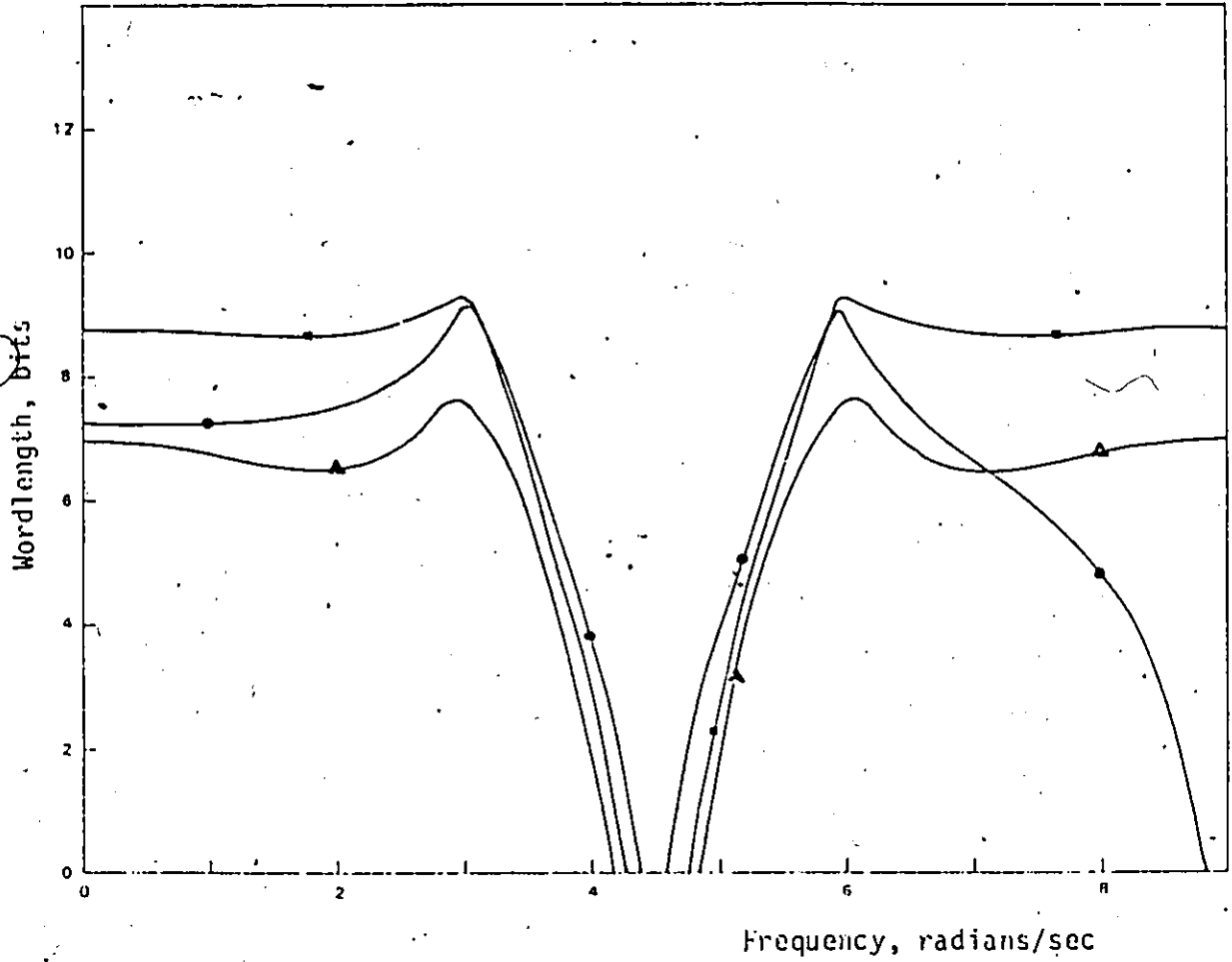


FIG. 4.15  $W(\omega)$  versus Frequency (Elliptic Bandstop Filter)

- — GIC
- — Canonic
- ▲ — Wave



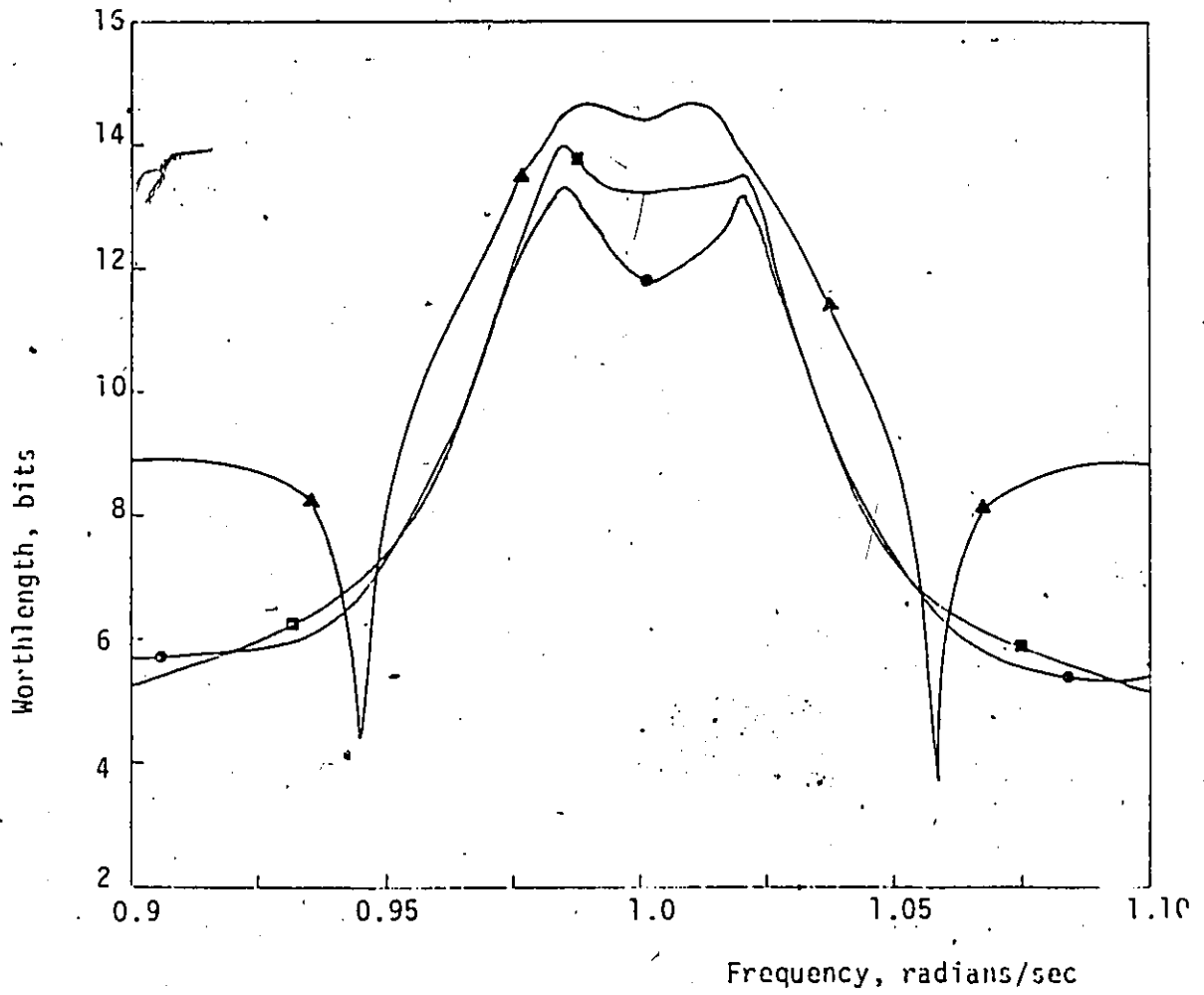


FIG. 4.16  $W(\omega)$  versus Frequency (Elliptic Bandpass Filter)

- — ● GIC
- — ■ Canonic
- ▲ — ▲ Wave

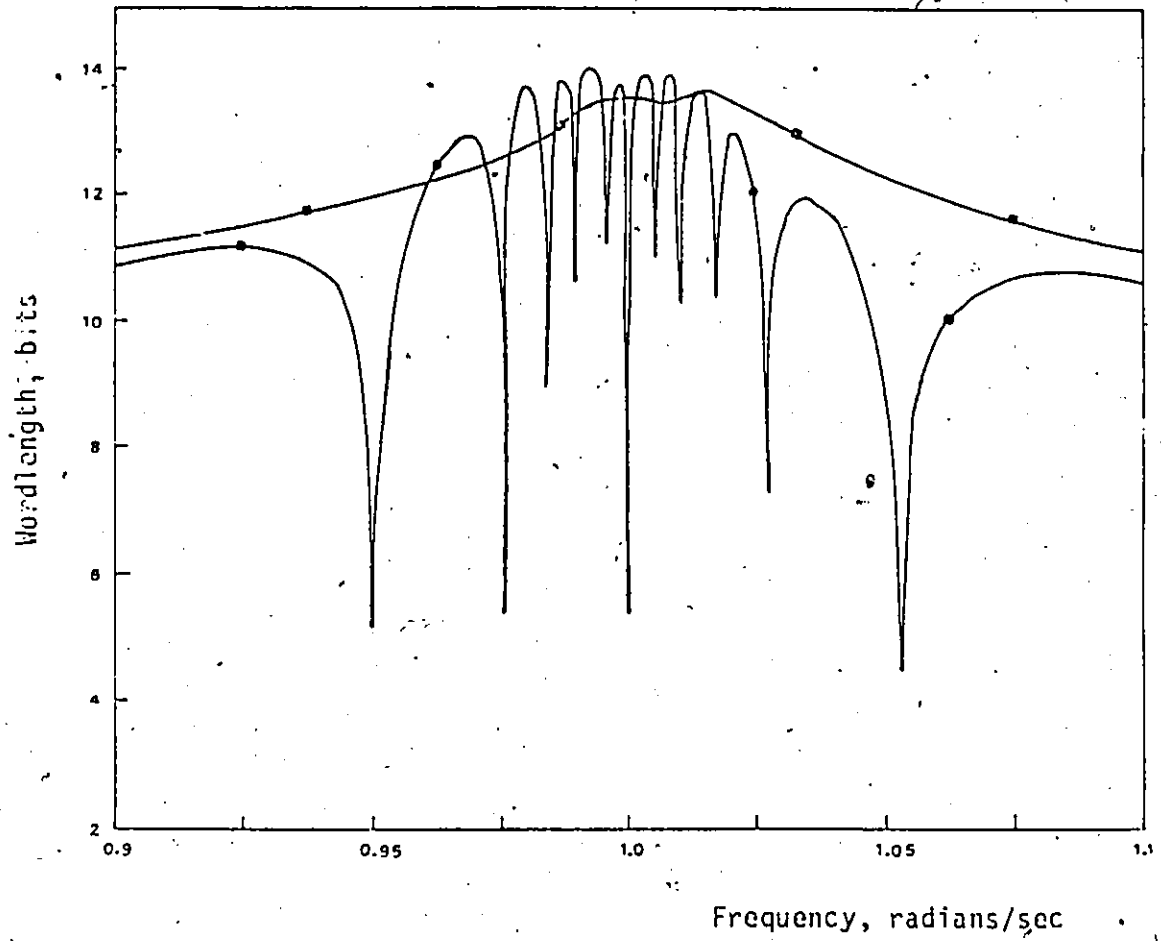


FIG. 4.17  $W(\omega)$  versus frequency (Delay Equalizer)

● — ● GIC  
■ — ■ Canonic

- (ii) In the lowpass and bandpass cascade canonic structures, the average value of  $W(\omega)$  over each passband is lower relative to that in the corresponding wave structures.
- (iii) For the bandstop filter, the maximum value of  $W(\omega)$  and also the average of  $W(\omega)$  over the passband are lowest in the wave structure as compared to the other two types of structures. For this filter, the maximum value of  $W(\omega)$  is approximately the same in both GIC and cascade canonic structures. However, the average of  $W(\omega)$  over the passband is lower in the GIC structure.
- (iv) For the delay equalizer, the maximum value of  $W(\omega)$  is approximately the same in the GIC and the cascade canonic structures.

Evidently, the conclusions based on the statistical wordlength confirm the conclusions based on the exact wordlength. In fact for  $x_1=2$ , the statistical wordlength is equal to the exact wordlength to within 1 or 2 bits.

In the above analysis, variations in scaling multiplier constants were neglected. The reason is that these constants are usually assumed to be powers of two in practice.

#### 4.6 CONCLUSIONS

The coefficient wordlength required for the digital filters designed in Section 2.4, has been computed first by using an exact method and then by using a statistical method. It is found that, the statistical wordlength evaluated with  $x_1=2$  and  $\Delta M_{\max}(\omega) = 0.02$  agrees with the exact wordlength to within 1 or 2 bits.

By using the three parameters  $|\Delta M|_{\max}$ , the average of  $|\Delta M|$ , and the average of the normalized standard deviation of the error in the frequency response, the various structures were compared. For the lowpass and bandpass filters the GIC structures give better results than the corresponding cascade canonic and wave structures. However, for the bandstop filter, the wave structure gives the best results.

The same digital filter structures were then compared by using the statistical wordlength as a criterion. The results obtained agree closely with the results obtained by using the exact wordlength as a criterion.

CHAPTER 5

CONCLUSIONS

5.1 SUMMARY

A digital-filter synthesis procedure has been described in which an analog configuration comprising resistors and generalized-immittance converters is simulated by employing digital elements. By using the synthesis, five universal second-order digital-filter sections have been derived, which can be used in cascade to realize filters or equalizers. The synthesis was used to design a number of digital filters, namely, a Butterworth lowpass filter, an elliptic bandstop filter, an elliptic bandpass filter, and a delay equalizer. All these filters were also designed by using the cascade canonic synthesis. In addition, the first three of these filters, were also designed by using the wave synthesis of Fettweis and Sedlmeyer.

By using the computational efficiency as a criterion, the GIC digital filters were compared with the cascade canonic and wave digital filters. For the lowpass, bandstop, and bandpass filters, the GIC structures are more efficient than the corresponding wave structures. For the lowpass and bandstop filters, the GIC structures have the same computational efficiency as the cascade canonic structures. However, for the bandpass filter, the cascade canonic structure is more efficient than the GIC structure. For the delay equalizer, the GIC structure is more efficient than the cascade canonic one.

The digital filter structures obtained in Chapter 2 have been scaled by employing a technique due to Jackson. The effect of product

quantization in these structures has been examined by evaluating the power spectral density of the quantization noise superimposed on the output signal. An attractive feature found in the GIC structures is that the quantization noise generated by the internal multipliers is subjected to a bandpass transfer function in each of the universal sections. Because of this fact, the GIC synthesis yields lowpass and bandstop filters, and also delay equalizers with improved inband signal-to-noise ratio relative to that in cascade canonic and wave structures. For the lowpass and bandpass filters, the wave structures give better results than the corresponding cascade canonic structures. However, for the bandstop filter, the cascade canonic structure is preferable to the wave structure.

The coefficient wordlength required for the digital filters designed in Chapter 2, has been computed first by using an exact method and then by using a statistical method. By using the exact wordlength as a criterion, the various structures were compared. It was found that, for the lowpass and bandpass filters, the GIC structures give better results than the corresponding cascade canonic and wave structures. However, for the bandstop filter, the wave structure gives the best results. The same conclusions were obtained when the statistical wordlength was used as a criterion for comparison.

## 5.2 AREAS FOR FUTURE RESEARCH

Further investigation can be carried out in the area of error analysis. The effects of product and coefficient quantization in GIC

structures as well as sensitivity properties of these structures should be studied for 1's complement and sign-magnitude number representation and for the case of floating-point arithmetic.

GIC structures, like other digital filter structures are subject to nonlinear effects such as limit cycles. Therefore, the existence of limit-cycles in these structures should be studied and methods should be found for their elimination. Alternatively, limit cycle bounds should be deduced.

It has been shown in Chapter 2 that GIC structures are more attractive than corresponding wave structures from the point of view of computational efficiency. Hence the implementation of GIC structures by means of microprocessors and other modern LSI circuits should be pursued.

Chapters 3 and 4 have shown that GIC structures often result in digital filters with reduced product quantization noise and reduced sensitivities. Hence the use of GIC structures should be considered for various applications such as time-division multiplexing to frequency-division multiplexing translation, channel filtering and so on.

REFERENCES

1. Peled, A., and Liu, B., Digital Signal Processing, John Wiley and Sons Book Co., 1976.
2. Jackson, L.B., et al., "An Approach to the Implementation of Digital Filters", IEEE Trans. Audio Electroacoust., Vol. AU-16, pp. 413-421, Sept. 1968.
3. Kurth, C.F., "SSD/FDM Utilizing TDM Digital Filters", IEEE Trans. on Communication Tech., Vol. COM-19, pp. 63-70, Feb. 1971.
4. Freeny, S.L., Kieburz, R.B., Mina, K.V. and Tewksbury, S.K., "Design of Digital Filters for an All Digital Frequency Division Multiplex-Time Division Multiplex Translator", IEEE Trans. on Circuits and Theory, Vol. CT-18, pp. 702-711, Nov. 1971.
5. Tierney, J., Rader, C.M. and Gold, B., "A Digital Frequency Synthesizer", IEEE Trans. on Audio and Electroacoust., Vol. AU-19, pp. 48-56, Mar. 1971.
6. Kaul, P., "An All Digital Telephony Signalling Module", Proc. 1975 IEEE Intern. Symp. on Circuits and Systems, pp. 392-395.
7. Fettweis, A. and Mandeville, G.J., "Design of Wave Digital Filters for Communications Applications", Proc. 1975 IEEE Intern. Symp. on Circuits and Systems, pp. 162-165.
8. Gabel, R.A., "A Parallel Arithmetic Hardware Structure for Recursive Digital Filters", IEEE Trans. Acoustics, Speech and Signal Processing, Vol. ASSP-22, pp. 255-258, Aug. 1974.



9. Rabiner, R.L. and Gold, B., Theory and Application of Digital Signal Processing, Prentice-Hall Book Co., 1975.
10. Oppenheim, A. and Schaffer, R.W., Digital Signal Processing, Prentice-Hall Book Co., 1975.
11. Bogner, R.E. and Constantinides, A.G., Introduction to Digital Filtering, John Wiley and Sons Book Co., London, 1975.
12. Fettweis, A., "Some Principles of Designing Digital Filters Imitating Classical Filter Structures", IEEE Trans. Circuit Theory, Vol. CT-18, pp. 314-316, Mar. 1971.
13. Fettweis, A., "Digital Filter Structures Related to Classical Filter Networks", Arch. Elektron. Und Uebertrogungstech., 25, pp. 79-89, 1971.
14. Fettweis, A., "Wave Digital Filters with Reduced Number of Delays", Intern. J. Circuit Theory and Applications, Vol. 2, pp. 319-330, 1974.
15. Sedlmeyer, A. and Fettweis, A., "Realization of Digital Filters with True Ladder Configuration", Proc. 1973 IEEE Intern. Symp. on Circuit Theory, pp. 149-152.
16. Sedlmeyer, A. and Fettweis, A., "Digital Filters with True Ladder Configuration", Intern. J. Circuit Theory and Applications, Vol. 1, pp. 5-10, 1973.
17. Fettweis, A. and Meerkötter, K., "On Adaptors for Wave Digital Filters", IEEE Trans. on Acoustics, Speech and Signal Processing, Vol. ASSP-23, pp. 516-525, Dec. 1975.

18. Constantinides, A.G., "Alternative Approach to Design of Wave Digital Filters", Electronics Letters, Vol. 10, pp. 59-60, Mar. 1974.
19. Swamy, M.N.S. and Thyagarajan, K.S., "A New Wave Digital Filter", Proc. 2nd Inter-American Conference on Systems and Informatics, Mexico, Paper No. 265, Nov. 1974.
20. Lawson, S.S. and Constantinides, A.G., "A Method for Deriving Digital Filter Structures from Classical Filter Networks", Proc. 1975 IEEE Intern. Symp. on Circuits and Systems, pp. 170-173.
21. Swamy, M.N.S. and Thyagarajan, K.S., "A New Type of Wave Digital Filter", Proc. 1975 IEEE Intern. Symp. on Circuits and Systems, pp. 174-178.
22. Swamy, M.N.S. and Thyagarajan, K.S., "A New Type of Wave Digital Filter", Journal of The Franklin Institute, Vol. 300, pp. 41-58, July 1975.
23. Constantinides, A.G., "Design of Digital Filters from LC Ladder Networks", Proc. IEE, Vol. 123, pp. 1307-1312, Dec. 1976.
24. Crochiere, R.E. and Oppenheim, A.V., "Analysis of Linear Digital Networks", Proc. IEEE, Vol. 63, pp. 581-595, April 1975.
25. Jenkins, W.K. and Leon, B.J., "An Analysis of Quantization Error in Digital Filters Based on Interval Algebras", IEEE Trans. on Circuits and Systems, Vol. CAS-22, pp. 223-232, Mar. 1975.
26. Long, J.L. and Trick, T.N., "Sensitivity and Noise Comparison of Some Fixed-Point Recursive Digital Filter Structures", Proc. 1975 IEEE Intern. Symp. on Circuits and Systems, pp. 56-59.

27. Crochiere, R.E., "Digital Ladder Structures and Coefficient Sensitivity", IEEE Trans. on Audio and Electroacoust, Vol. AU-20, pp. 240-246, Oct. 1972.
28. Ku, W.H. and Ng, S.M., "Floating-Point Coefficient Sensitivity and Roundoff Noise of Recursive Digital Filters Realized in Ladder Structures", IEEE Trans. on Circuits and Systems, Vol. CAS-22, pp. 927-936, Dec. 1975.
29. Fettweis, A., "On the Connection Between Multiplier Wordlength Limitation and Roundoff Noise in Digital Filters", IEEE Trans. on Circuit Theory, Vol. CT-19, pp. 486-491, Sept. 1972.
30. Antoniou, A. and Rezk, M.G., "Digital-Filter Synthesis Using Concept of Generalized-Immittance Converter", Electronic Circuits and Systems, Vol. 1, pp. 207-216, Nov. 1977.
31. Antoniou, A., "Realization of Gyration Using Operational Amplifiers and Their Use in RC-Active-Network Synthesis", Proc. IEE, Vol. 116, pp. 1838-1850, 1969.
32. Antoniou, A., "Novel RC-Active Network Synthesis Using Generalized-Immittance Converters", IEEE Trans. on Circuit Theory, Vol. CT-17, pp. 212-217, 1970.
33. Bruton, L.T., "Biquadratic Sections Using Generalized Impedance Converters", The Radio and Electronic Engineer, Vol. 41, pp. 510-512, Nov. 1971.
34. Mikhael, W.B. and Bhattacharyya, B.B., "New Minimal Capacitor Low-Sensitivity RC-Active Synthesis Procedure", Electronic Letters, Vol. 7, pp 694-696, Nov. 1971.

35. Bhattacharyya, B.B., Mikhael, W.B. and Antoniou, A., "Design of RC-Active Networks Using Generalized-Immittance Converters", Journal of The Franklin Institute, Vol. 297, pp. 45-58, Jan. 1974.
36. Fliege, W., "A New Class of Second-Order RC-Active Filters with Two Operational Amplifiers", Nachrichtentech. z., Vol. 26, pp. 279-282, 1973.
37. Balabanian, N., Network Synthesis, Prentice-Hall Book Co., 1958.
38. Weinberg, L., Network Analysis and Synthesis, McGraw-Hill Book Co., 1962.
39. Saal, R., The Design of Filters Using the Catalogue of Normalized Low-Pass Filters, Telefunken AG, Backnang, 1966.
40. Golden, R.M. and Kaiser, J.F., "Design of Wide-Band Sampled-Data Filters", Bell System Tech. J., Vol. 43, pp. 1533-1546, July 1964.
41. Golden, R.M., "Digital Filter Synthesis by Sampled-Data Transformation", IEEE Trans. on Audio and Electroacoust., Vol. AU-16, pp. 321-329. Sept. 1968.
42. Antoniou, A., "Design of Elliptic Digital Filters: Prescribed Specifications", Proc. IEE, Vol. 124, pp. 341-344, April 1977.
43. Antoniou, A., Digital Filters: Analysis and Design, McGraw-Hill Book Co. (in press).
44. Jackson, L.B., "On the Interaction of Roundoff Noise and Dynamic Range in Digital Filters", Bell Syst. Tech. J., Vol. 49, pp. 159-184, Feb. 1970.

45. Jackson, L.B., "Roundoff-Noise Analysis for Fixed-Point Digital Filters Realized in Cascade or Parallel Form", IEEE Trans. Audio Electroacoust., Vol. AU-18, pp. 107-122, June 1970.
46. Thyagarajan, K.S. and Sanchez-Sinencio, E., "A Systematic Procedure for Scaling Wave Digital Filters", Proc. IEEE, Vol. 66, pp. 512-513, April 1978.
47. Fettweis, A. and Meerkötter, K., "Suppression of Parasitic Oscillations in Wave Digital Filters", IEEE Trans. on Circuits and Systems, Vol. CAS-22, pp. 239-246, Mar. 1975.
48. Schwarz, R.J. and Friedland, B., Linear Systems, McGraw-Hill Book Co., 1965.
49. Fettweis, A., "A General Theorem for Signal-Flow Networks, with Applications", Archiv fur Elektronik und Ubertragungstechnik, Vol. 25, pp. 557-561, 1971.
50. Seviara, R.E. and Sablatash, M., "A Tellegen's Theorem for Digital Filters", IEEE Trans. on Circuit Theory, Vol. CT-18, pp. 201-203, Jan. 1971.
51. Knowles, J.B. and Olcayto, E.M., "Coefficient Accuracy and Digital Filter Response", IEEE Trans. on Circuit Theory, Vol. CT-15, pp. 31-41, Mar. 1968.
52. Renner, K. and Gupta, S.C., "On the Design of Wave Digital Filters with Low Sensitivity Properties", IEEE Trans. on Circuit Theory, Vol. CT-20, No.5, pp. 555-567, Sept. 1973.

53. Liu, B., Digital Filters and the Fast Fourier Transform, Halsted Press, 1975.
54. Jackson, L.B., "Roundoff Noise Bounds Derived from Coefficient Sensitivities for Digital Filters", IEEE Trans. on Circuits and Systems, Vol. CAS-23, pp. 481-485, Aug. 1976.
55. Oppenheim, A.V. and Weinstein, C.J., "Effects of Finite Register Length in Digital Filtering and the Fast Fourier Transform", Proc. IEEE, Vol. 60, pp. 957-976, Aug. 1972.
56. Agarwal, R.C. and Burrus, S., "New Recursive Digital Filter Structures having Very Low Sensitivity and Roundoff Noise", IEEE Trans. on Circuits and Systems, Vol. CAS-22, pp. 921-927, Dec. 1975.
57. Jackson, L.B., Lindgren, A.G. and Kim, Y., "Synthesis of State-Space Digital Filters with Low Roundoff Noise and Coefficient Sensitivity", Proc. 1977 IEEE Intern. Symp. on Circuits and Systems, pp. 41-44.
58. Bruton, L.T., "Low-Sensitivity Digital Ladder Filters", IEEE Trans. on Circuits and Systems, Vol. CAS-22, pp. 168-176, Mar. 1975.
59. Avenhaus, E., "On the Design of Digital Filters with Coefficients of Limited Word-Length", IEEE Trans. on Audio and Electroacoust., Vol. AU-20, pp. 206-212, Aug. 1972.
60. Crochiere, R.E., "A New Statistical Approach to the Coefficient Word-Length Problem for Digital Filters", IEEE Trans. on Circuits and Systems, Vol. CAS-22, pp. 190-196, Mar. 1975.

61. Fettweis, A., "Pseudopassivity, Sensitivity, and Stability of Wave Digital Filters", IEEE Trans. on Circuit Theory, Vol. CT-19, pp. 668 673, Nov. 1972.
62. Avenhaus, E., "A Proposal to Find Suitable Canonical Structures for the Implementation of Digital Filters with Small Coefficient Wordlength", Nachrichtentech. z., Vol. 25, pp. 377-382, Aug. 1972.
63. Liu, B., "Effect of Finite Word Length on the Accuracy of Digital Filters", IEEE Trans. on Circuit Theory, Vol. CT-18, pp. 670-677, Nov. 1971.